

**Phosphorylation – dependent Regulation of the Tumor
Suppressor TRIM3**

by

Ellen Hukkelhoven

A Dissertation

Presented to the Faculty of the Louis V. Gerstner, Jr.

Graduate School of Biomedical Sciences,

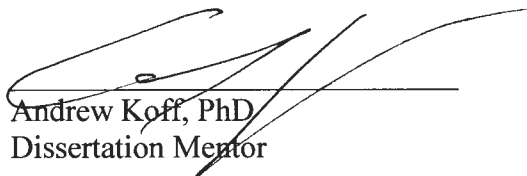
Memorial Sloan-Kettering Cancer Center

in Partial Fulfillment of the Requirements for the Degree of

Doctor of Philosophy

New York, NY

December, 2012


Andrew Koff, PhD
Dissertation Mentor

12/19/2012
Date

Copyright © 2012 by Ellen Hukkelhoven

All rights reserved

DEDICATION

This thesis is dedicated to my wonderful Mom and Dad. My Dad's personal passion for science and medicine, and my mother's incredible energy for planning and perfection together instilled the enthusiasm and practical drive necessary to complete this dissertation.

And if it wasn't for my father's endless drive towards efficiency - identifying the "critical part" in every household process from baking New Year's waffles to doing the dishes - I would never have squeezed so many experiments into a single day.

Thank you for always believing in me.

ABSTRACT

At a median survival of 14 months, glioblastoma multiforme (GBM) is practically incurable. Recent genome-wide sequencing efforts underscore the immense heterogeneity of these tumors. It has been hoped that these studies will reshape current classification schemes and by identifying key players in gliomagenesis will impact on therapeutic modalities. This thesis focuses on the regulation of TRIM3, a potentially important new player in this disease.

TRIM3 protein expression is reduced in approximately 20-40% of human GBM. Reducing expression of TRIM3 in mice increases the frequency and accelerates the development of proneural glioma in mice, indicating that it is a tumor suppressor. The orthologs in flies and worms regulate the asymmetric divisions of stem cells and loss of these gene products leads to an increase in the number of stem and progenitor cells. TRIM3 and its orthologs suppress growth through at least three different mechanisms including ubiquitination of myc, ubiquitination of p21, or through the miRISC complex. Additionally, TRIM3 may also have a role in vesicular transport. I set out to determine if protein interactions and phosphorylation could affect the growth suppressive activity of TRIM3.

Using a combination of molecular, cellular, and proteomic approaches, I identified a cluster of seven phosphorylation sites located between the NHL domain and the ABP domain of TRIM3. These were phosphorylated in a growth-dependent manner. Mutation of these sites to alanine increased the growth-suppressive activity, whereas mutation to

the phosphomimetic amino acid aspartate decreased growth suppressive activity. Therefore, phosphorylation inhibits the growth suppressive activity of TRIM3

I next set out to identify the kinases that could phosphorylate these sites. Using a combination of biochemical, bioinformatic, and proteomic approaches I identified a number of kinases that interact with TRIM3. Some of them bound to the NHL domain and others to the RBCC domain. These kinases phosphorylate TRIM3 in a growth dependent manner. One of these, CDK16 was needed for the proliferation of a PDGF-driven glial cell line. My work begins to define a regulatory circuit between CDK16, TRIM3 and growth suppression, and suggests a promise for CDK16 targeted therapy in proneural glioma.

ACKNOWLEDGMENTS

“WHAT is the question??” That very phrase somewhat famously identifies Andrew Koff throughout the Sloan-Kettering graduate school. Andy approaches experimental design, science communication and critical data evaluation first and foremost by asking this question. It represents the way he thinks, and the way he has taught me to think. To me, it was the start of my journey in the Koff lab.

I want to thank Andy for shaping over 1000 days of my life. (When I first joined the lab, Andy promised that if I worked hard, I would graduate in 1000 days. Every 1.5 weeks, I should have a meaningful piece of data that represents 1% of my thesis. It’s actually been 1,036 days - less than 5% error, not bad). At times he has been everything from a thesis advisor and boss, to a father-figure and friend. He has challenged me to think like a world-class scientist – critically and efficiently. And to be passionate about the little victories. At times we clashed about using new technologies in the lab. But ultimately a thorough cost-benefit analysis, along with hard data, always brought us to the same page. These lessons and countless more will stay with me forever.

I will sincerely miss the multi-hour philosophizing sessions in the lab. We covered everything from antibodies and exciting biotech to boyfriends, wives and presents. And of course I’ll miss our bi-weekly, absurdly long and productive meetings to discuss data. Andy was with me every step of the way, and his enthusiasm was contagious.

Andy was also open-minded and let me pursue my own passions, both in and out of the lab. He granted me the time to help biotech companies around NYC through InSITE. And we even adopted some business terms to describe our labwork (presentations, for

example, became “pitches”). For this flexibility, and for understanding and supporting me when following my passion would inevitably lead me out of the lab, I am truly grateful.

And then there’s the lab – Radhika, Nancy, David, Marta, Daniel, Yuhui and Aimee. Radhika, my bay mate, has been through it all with me. Thank you for so many helpful scientific discussions, and countless decidedly unscientific ones. Nancy, thank you for your endless patience, and for cloning literally hundreds of plasmids. I had two fantastic students – Marty and Marta. Marty defined an entire summer. Not only was he smart and ambitious, forcing me to think through the logic behind every experiment (thank you for your help with the TRIM3 associated kinase assay), he was also a joy to be around. He entertained us all with his endless teasing and dry sense of humor. And Marta, I cannot imagine having a better student and lab colleague than you. Thank you for starting the CDK16 work, for your countless insights lunches and energy. Andy is incredibly lucky to have you in his lab. You brought the lab to life with your laugh.

My committee members – Eric Holland and Xuejun Jiang. Thank you for your wisdom and suggestions. Our conversations were always helpful, and inspired me to look in new directions. Also, a special thanks to Eric for inviting me to watch brain surgery, and for not noticing when I almost fainted.

The mass spectrometry core here at Sloan Kettering, especially Hediye Erdjument-Bromage, was extremely helpful with all mass spectrometry experiments. Thank you for all the troubleshooting and your patience.

The graduate school and my grad school friends and classmates. Ken and the office made everything possible. Thank you for shaping the graduate school from the very beginning. Jenny, Nick and Bill, a special thank you for the wonderful times and the memories.

And of course my friends!! NYC would not have been the same without you. Thanks for listening to me when grad school was hard, and for trying to understand when I was excited about data and major milestones. Sloan, you are my life partner. Thank you for supporting me through absolutely everything the last seven years, and for always encouraging me to have perspective. Becca, your inability to stop bouncing has inspired me to be more spontaneous and flexible. Alex (Bisi), for sharing enthusiasm for both science and business. You're one of the smartest people I know. Carter, thank you for pushing me to keep an open mind, to pursue new passions, and to never accept anything less than the best from myself and those around me.

Finally, Mom, Dad and Irene – I love you! I couldn't have done this without your loving support.

TABLE OF CONTENTS

LIST OF FIGURES AND TABLES	XI
LIST OF ABBREVIATIONS.....	XII
CHAPTER 1	1
Introduction.....	1
<i>I. Glioblastoma Multiforme</i>	<i>1</i>
<i>II. TRIM3 is a tumor suppressor in glioma</i>	<i>3</i>
<i>III. The TRIM Family</i>	<i>4</i>
<i>IV. TRIM-NHL proteins in neuronal differentiation and stem cell renewal</i>	<i>7</i>
1. Mammalian TRIM-NHL proteins.....	7
2. Non-mammalian TRIM-NHL proteins	8
3. TRIM3 Functions.....	10
<i>V. Regulation of tumor suppressors by phosphorylation</i>	<i>13</i>
<i>VI. Scope of Thesis.....</i>	<i>19</i>
CHAPTER 2	20
Methods.....	20
<i>I. Cell Culture, transfection and infection</i>	<i>20</i>
<i>II. Immunoblot, phos-tag and immunoprecipitation.....</i>	<i>21</i>
<i>III. Recombinant proteins</i>	<i>21</i>
<i>IV. EdU incorporation assay</i>	<i>22</i>
<i>V. TRIM3 associated kinase assay</i>	<i>22</i>
<i>VI. Kinase assays.....</i>	<i>22</i>
<i>VII. Phosphopeptide MS analysis</i>	<i>23</i>
Protein identification by nano-Liquid Chromatography coupled to tandem Mass Spectrometry (LC-MS/MS) analysis	23
CHAPTER 3	26
The growth suppressive activity of TRIM3 is regulated by phosphorylation.....	26
<i>I. Background.....</i>	<i>26</i>
<i>II. Results</i>	<i>28</i>
1. TRIM3 phosphorylation is complex and growth-regulated.....	28

3. The effect of TRIM3 S7 phosphorylation on growth	34
4. Hinge phosphorylation inhibits TRIM3 growth suppressive activity	37
III. Discussion.....	39
1. Summary	39
2. Interaction between S7 and Hinge region phosphorylation	39
3. Affect of phosphorylation on TRIM3 structure	40
CHAPTER 4	42
CDK16 phosphorylates TRIM3 and is required for glioma cell growth	42
I. Background.....	42
II. Results	44
1. TRIM3 is phosphorylated by CDKs in vitro.....	44
2. TRIM3 is phosphorylated in vitro by multiple kinases at the “hinge” region ..	48
3. Identification of CDK16 as a potential TRIM3 kinase.....	53
4. CDK16 can bind and phosphorylate TRIM3 at the hinge region	62
5. CDK16 depletion suppresses growth.....	66
III. Discussion.....	68
1. Summary.....	68
2. TRIM3 functions.....	68
3. CDK16 and TRIM3 in neuronal vesicular trafficking and as therapeutic targets	69
CHAPTER 5	72
Implications	72
REFERENCES	82
APPENDIX: TRIM3 INTERACTOME	92

LIST OF FIGURES AND TABLES

Figure 1. The structural classification of human tripartite motif (TRIM) subfamily (C-I to C-XI) is shown.....	6
Figure 2. Mammalian TRIM-NHL domain structures.....	12
Figure 3. TRIM3 is phosphorylated in a growth dependent manner.....	30
Figure 4. TRIM3 is multiply phosphorylated at the hinge and S7.....	32
Figure 5. Hinge region and S7 phosphorylation sites are conserved.....	33
Figure 6. Mutation of S7 to aspartate modestly increases TRIM3 growth suppressive activity.....	36
Figure 7. Hinge phosphorylation inhibits TRIM3 growth suppressive activity.....	38
Figure 8. Cyclin dependent kinases phosphorylate TRIM3 in vitro at hinge residues.....	46
Figure 9. CDK2 and CDK5 phosphorylate TRIM3 and not GST.....	47
Figure 10. TRIM3 is phosphorylated by growth-regulated kinases in vitro.....	50
Figure 11. Multiple growth regulated kinases phosphorylate TRIM3 in vitro.....	52
Figure 12. TRIM3 co-immunoprecipitated with a network of known TRIM3 interacting proteins.....	54
Figure 13. TRIM3 interacting proteins are primarily involved in growth and cell maintenance pathway.....	55
Table 1. Kinases associated with endogenous TRIM3 in YH/J12 cells.....	57
Figure 14. Top three kinase candidates co-immunoprecipitated with networks of known interacting proteins.....	59
Figure 15. Raf-1 Kinase does not phosphorylate TRIM3 in vitro.....	60
Figure 16. EGFR Kinase minimally phosphorylates TRIM3 in vitro.....	61
Figure 17. CDK16 binds to the N-terminus of TRIM3.....	63
Figure 18. CDK16 is a TRIM3 hinge kinase in vitro.....	65
Figure 19. CDK16 depletion decreases cell growth.....	67
Figure 20. The hinge region of TRIM3 is disordered.....	77

LIST OF ABBREVIATIONS

GBM – Glioblastoma multiforme

PDGF – Platelet-derived growth factor

EGFR – Epidermal growth factor receptor

NF1 – Neurofibromatosis-1

PTEN – Phosphatase and tensin homolog

TCGA – The cancer genome atlas

TRIM – Tripartite motif protein

PML – Promyelocytic leukemia protein

ABP – Actin binding protein motif

NFL – Neurofilament light chain

GKAP – Guanylate kinase associated protein

CDK – Cyclin dependent kinase

CIP – Calf intestinal phosphatase

FACS – Fluorescence-activated cell sorting

MAPK – Mitogen activated protein kinase

NSF - N-ethylmaleimide-sensitive fusion protein

NLS – Nuclear localization sequence

IDP – Intrinsically disordered protein

PTM – Post-translational modification

CHAPTER 1

INTRODUCTION

I. Glioblastoma Multiforme

Although Glioblastoma Multiforme (GBM) only occurs in about 3 out of every 100,000 people (CBTRUS, 2012), it is one of the deadliest cancers and represents an enormous unmet medical need. Current treatment strategies are largely ineffective; less than 5% of patients survive 5 years after diagnosis (CBTRUS, 2012). Part of the difficulty of treating patients with this disease stems from its complex nature. On both the genetic and the cellular level, there are many different kinds of gliomas. Although we are already able to stratify gliomas into several subclasses with different behaviors and prognoses, standard first-line clinical treatment is uniform: surgical resection, radiation and temozolomide. This presents a great opportunity for improvement. Understanding the key differences between subtypes of this disease may allow us to develop targeted, personalized therapy strategies.

Revolutions in sequencing, microarray and mass spectrometry technologies have driven down the cost of genome and proteome-wide analyses, allowing these relatively unbiased approaches to be used to discover new pathways and players in this disease. The well-established signaling pathways in gliomagenesis are the upregulation of PDGF and EGFR signaling, and the loss of tumor suppressors INK4a/ARF, p53 and PTEN. Recent large-scale genomic studies such as The Cancer Genome Atlas both confirmed these known pathogenic signaling pathways and uncovered the importance of several lesser-known genes. Newly discovered alterations include neurofibromatosis 1 (NF1) (TCGA, 2008) and isocitrate dehydrogenase 1 (IDH1) (Parsons et al, 2008). This new data is beginning to clarify the genetic heterogeneity of the glioma landscape.

The current WHO glioma classification scheme is primarily dependent on histology-based grading, differentiation status, patient age, and 1p and 19q deletion status (Louis et al, 2007; Vitucci et al, 2011). Gene expression profiling has shown that there is significant heterogeneity within the classically defined subtypes, and it can be a better predictor of survival than histological grade or age (Freije et al, 2004; Gravendeel et al, 2009; Liang et al, 2005; Vitucci et al, 2011). In an attempt to glean practical utility from this wealth of molecular data, researchers have performed clustering studies on both genomic and proteomic datasets and produced more nuanced classification schemes.

Although there is no clear consensus for the best way to stratify glioma subclasses based on gene expression profiling, patterns are beginning to arise. For example, clustering of the TCGA dataset identified four subtypes: proneural, neural, mesenchymal and classical

(Verhaak et al, 2010). These subtypes have significant overlap with those identified in previous studies (Chen et al, 2012; Vitucci et al, 2011). The classical subtype often exhibited EGFR amplification, and the mesenchymal subtype had PTEN, P53 and NF1 mutations (Verhaak et al, 2010). The proneural class correlated with chronic PDGF signaling (Verhaak et al, 2010), a characteristic of several similar classes identified in other studies (Brennan et al, 2009; Gravendeel et al, 2009; Vitucci et al, 2011). Mouse modeling underscores the importance of PDGF signaling in this subtype; targeted overexpression of PDGF in nestin-expressing cells faithfully recapitulates many aspects of this disease (Dai et al, 2001). Nevertheless, these newly defined subgroups are still heterogeneous, indicating that there may be other important alterations not specific to a certain class (Chen et al, 2012; Vitucci et al, 2011).

Genomic approaches have proven invaluable for hypothesis generation, and have guided clinicians and scientists designing new classification schemes. However, to parse out and understand the regulatory networks that impact the true drivers of this complex disease, genomics must be combined with traditional molecular biology and state-of-the-art mouse modeling.

II. TRIM3 is a tumor suppressor in glioma

Recent genome-wide efforts have identified another player in gliomagenesis. TRIM3 maps to the chromosomal region 11p15.5, which is lost in about 20% of brain tumors (Boulay et al, 2009). In addition, approximately 15% of tumors in the TCGA data set exhibited loss of heterozygosity or homozygous deletion at the TRIM3 locus (Liu et al,

2012; TCGA, 2008). However, TRIM3 protein expression may be reduced more frequently, as TRIM3 protein levels were low or undetectable in 7 out of 11 fresh surgical glioma resections with intact 11p15.5 loci. The physiological relevance of this genomic and expression data was confirmed in a PDGF-driven mouse model of glioma, where TRIM3 depletion led to increased tumor formation (Liu et al, 2012). However, loss of TRIM3 expression is not unique to the PDGF driven class of gliomas, and therefore may be its own classification marker. Altogether, the data strongly support a tumor suppressive role for TRIM3 in gliomas.

III. The TRIM Family

TRIM family members are defined by a highly conserved tripartite motif (TRIM) consisting of a ring finger domain, one or two B-boxes, and a coiled-coil region (Reymond et al, 2001). The spatial organization of these domains is well conserved, suggesting that proper orientation and cooperation may be key to their function. The nature of the variable C-terminus divides the TRIM family into several subclasses (Fig. 1). TRIM family members are involved in a multitude of processes including cell growth and tumorigenesis (Bodine et al, 2001; Hatakeyama, 2011), differentiation and development (Wulczyn et al, 2011), apoptosis (Horn et al, 2004; Shyu et al, 2003), viral response and innate immunity (Nisole et al, 2005; Ozato et al, 2008; Uchil et al, 2008), and vesicular transport (Yan et al, 2005). Many TRIM family members have ubiquitination activity, and the presence of the RING domain has led some to suggest that the entire family could be E3 ubiquitin ligases (for review see (Bernardi et al, 2008; Meroni & Diez-Roux, 2005).

The oncogenic and tumor suppressive mechanisms of the TRIM family vary widely and are often context dependent. Some TRIM family members are involved in translocation resulting in oncogenic fusion proteins. One notable example is TRIM19, more commonly known as promyelocytic leukemia protein (PML). It fuses with retinoic acid receptor- α to form the PML-RAR α fusion protein found in 99% of acute promyelocytic leukemia patients (Bernardi et al, 2008). Several TRIM proteins, including PML, TRIM13, TRIM24, TRIM28 and TRIM29, can affect carcinogenesis through p53 regulation at either the transcriptional or post-translational level. In addition, a number of TRIM proteins control the growth and differentiation of stem and progenitor cells. For a comprehensive review of the oncogenic functions of TRIM proteins, see (Hatakeyama, 2011).

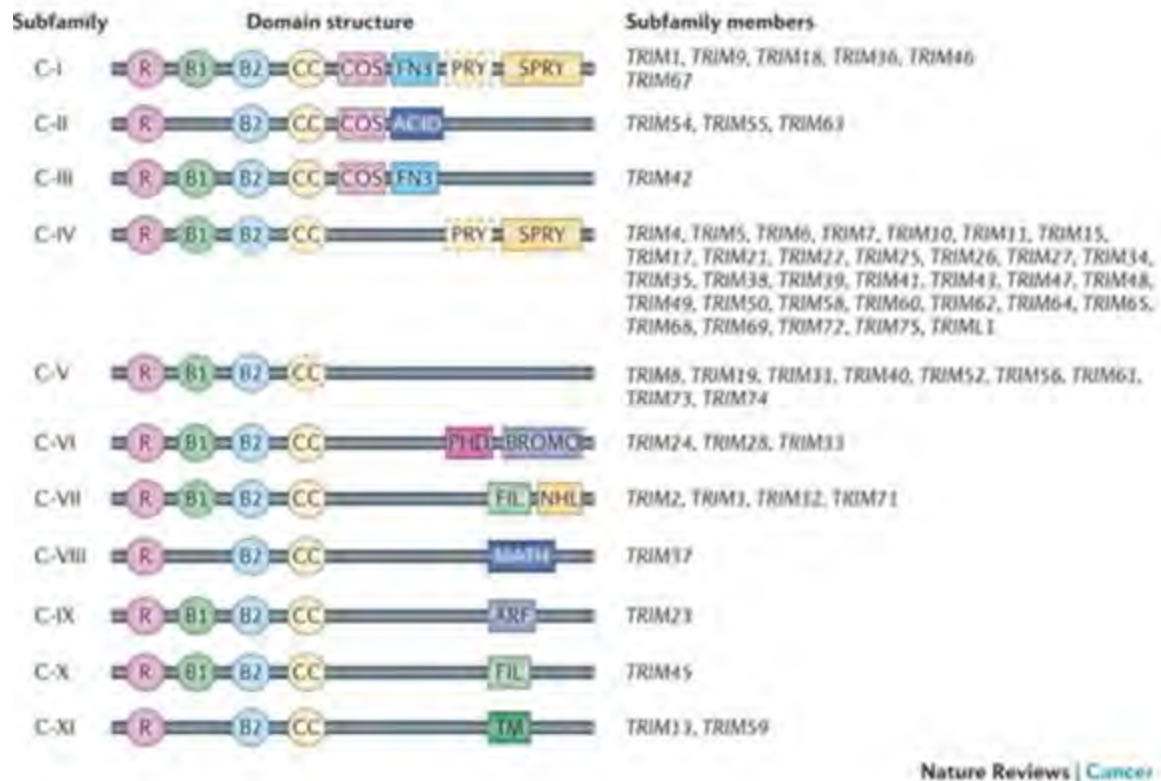


Figure 1: The structural classification of human tripartite motif (TRIM) subfamily (C-I to C-XI) is shown. Almost all TRIM proteins have a RING-finger domain (R), one or two B-box domains (B) and a coiled-coil domain (CC). Some members of the subfamily lack one or more amino-terminal domains (shown as dashed outline domains). ACID, acid-rich region; ARF, ADP-ribosylation factor family domain; BROMO, bromodomain; COS, cos-box; FIL, filamin-type I G domain; FN3, fibronectin type III repeat; MATH, meprin and TRAF-homology domain; NHL, NCL1, HT2A and LIN41 domain; PHD, PHD domain; PRY, PRY domain; SPRY, SPRY domain; TM, transmembrane region; Ub, ubiquitin.

Adapted by permission from Macmillan Publishers Ltd:
 Nature Reviews Cancer, 11(11):792-804, copyright 2011.
<http://www.nature.com/nrc/journal/v11/n11/full/nrc3139.html>

IV. TRIM-NHL proteins in neuronal differentiation and stem cell renewal

The ~70-member TRIM family can be subdivided into several classes based on the structure of their C-terminal functional domains (Fig. 1). TRIM3 is part of an evolutionarily conserved subfamily including TRIM2, TRIM32, and TRIM71 (Sardiello et al, 2008). These proteins are characterized by an actin binding (ABP)/filamin motif and/or a series of NHL repeats. TRIM32 has been the most extensively studied, and its mutation is associated with muscular dystrophies. Note that with the exception of TRIM3 and brat, TRIM-NHL proteins have not been directly implicated in tumor suppression. However, a broad look at the TRIM-NHL proteins in a variety of species uncovers common roles in neuronal differentiation and stem cell renewal. Both differentiation and cell growth are deregulated during tumorigenesis. Therefore, the roles of TRIM-NHL proteins in these processes are briefly discussed in the next two sections (reviewed in (Wulczyn et al, 2011)).

1. Mammalian TRIM-NHL proteins

All four mammalian TRIM-NHL proteins are expressed in the brain, where they have important roles in neurite outgrowth and stem cell renewal. TRIM2 regulates neuronal cytoskeleton dynamics through neurofilament light chain (NFL) ubiquitination (Balastik et al, 2008; Khazaei et al, 2011), and TRIM3 is required for neurite extension in the rat neuronal cell line PC12 (El-Husseini & Vincent, 1999). Occasional asymmetric inheritance of TRIM32 in neural progenitor cells favors cell cycle exit and neuronal cell fate, perhaps through miRNA regulation and ubiquitination of MYC (Schwamborn et al, 2009). Furthermore, mice deficient for TRIM32 have altered axon morphology (Kudryashova et al, 2009). TRIM71 plays a key role during development in zebrafish and

mouse models. It is required for neural tube closure and facilitates the self-renewal of pluripotent stem cells, perhaps through association with Argonaute2 and miRNA mediated repression of the cyclin-dependent-kinase inhibitor p21^{CIP1/WAF1} (Chang et al, 2012; Lin et al, 2007; Maller Schulman et al, 2008). Altogether, it is clear that TRIM-NHL proteins play key roles during neurogenesis through both ubiquitination and interaction with miRNA regulatory proteins. Whether they promote or repress progenitor cell renewal is not always clear and may be context dependent.

2. Non-mammalian TRIM-NHL proteins

The importance of TRIM-NHL proteins in progenitor cell differentiation and self-renewal is well conserved through flies, worms and mollusks (Bae et al, 2001; Kohlmaier & Edgar, 2008; van Diepen et al, 2005). L-TRIM knockdown inhibits neurite outgrowth in mollusks (van Diepen et al, 2005). In *C. elegans*, disruption of each of the five TRIM-NHL proteins results in a range of embryonic polarity defects (Hyenne et al, 2008). Interestingly, NHL2 may play an opposing role to other TRIM-NHL proteins such as LIN41. Loss of NHL2 led to stem cell maturation and partially rescued a lin-41 mutant (Hammell et al, 2009). Like some of the mammalian TRIM-NHL proteins, NHL2 may function through miRNA pathway modulation. It associates and cooperates with components of the miRISC complex to repress target gene expression (Hammell et al, 2009).

TRIM-NHL proteins have been most extensively studied in flies, where brat and mei-P26 have well-characterized roles in establishing cell polarity and regulating daughter cell

fate. Brat and mei-P26 both promote differentiation of progenitor cells in different *Drosophila* stem cell niches. Mutation of mei-P26 results in cystocyte tumors in the ovarian stem cell niche, where mei-P26 normally inhibits miRNAs during cyst differentiation (Caussinus & Gonzalez, 2005). Brat (brain tumor) was named after its mutant phenotype, as *brat* mutant flies form tumor-like tissue with close to 100% penetrance (Caussinus & Gonzalez, 2005; Loop et al, 2004). Brat plays a key role in neuroblast differentiation. In the neural stem cell niche, a large neuroblast cell divides asymmetrically, sequestering brat in a secondary neuroblast termed a transit amplifying cell. This cell self-renews rapidly and divides asymmetrically, producing a ganglion mother cell which gives rise to two neurons. Mutation of *brat* results in overproliferation of uncommitted transit amplifying cells in the neuroblast stem cell niche (Betschinger et al, 2006; Bowman et al, 2008; Kohlmaier & Edgar, 2008; Lee et al, 2006; Reichert, 2011).

How brat promotes differentiation is not entirely clear. Brat inhibits general protein translation, which may prevent cell growth and support differentiation. Brat also posttranscriptionally inhibits dMYC, which could lead to suppression of growth related processes (Betschinger et al, 2006; Bowman et al, 2008). Interestingly, mutations in the NHL domain of *brat* are sufficient for fly tumorigenesis, suggesting that this domain might be critical for tumor suppression (Arama et al, 2000). This domain has been crystallized and resembles a WD40 beta-propeller blade, a structure known to mediate protein-protein interactions (Edwards et al, 2003). Disruption of these protein interactions is therefore likely to lead to tumor-like overgrowth.

3. TRIM3 Functions

Of the mammalian TRIM-NHL proteins, only TRIM3 has been clearly implicated in the control of cell proliferation and tumorigenesis. Like many of its family members, it has a N-terminal tripartite motif, followed by an ABP/filamin domain. A ~40 amino acid unstructured linker region (“hinge”) connects the filamin domain to the 6 NHL repeats, which likely form a 6-bladed beta-propeller (Fig. 2). TRIM3 is highly expressed in the brain (El-Husseini & Vincent, 1999), and maps to 11p15.5, a region commonly deleted in many tumor types, including brain tumors (Boulay et al, 2009; El-Husseini et al, 2001). TRIM3 knockout mice are viable and do not display any gross or histological abnormalities (Cheung et al, 2010). Although these mice have not been crossed to any other tumor models, work from our lab using shRNA to deplete TRIM3 levels in a PDGF-driven model for glioma increased tumor incidence (Liu et al, 2012). How TRIM3 exerts its proliferative control is still unclear, but may be related to its function in several processes. Therefore, a short review of known TRIM3 activities, interactions and functions is provided below.

Several reports have implicated TRIM3 in vesicular trafficking (El-Husseini et al, 2000; El-Husseini & Vincent, 1999; Mosesson et al, 2009; Yan et al, 2005). TRIM3 was first described as a myosin V interacting protein (El-Husseini & Vincent, 1999). The TRIM3 WD40-like beta propeller domain binds to the C-terminal tail of myosin V, a region of myosin V usually involved in cargo transport. Shortly thereafter, the same group reported that TRIM3 interacts with alpha-actinin-4, another protein that can associate with the actin cytoskeleton (El-Husseini et al, 2000). This data was tied together when Yan et al.

identified a 'CART' complex containing all three proteins and the endosome-associated protein hrs. The CART complex is necessary for efficient transferrin receptor recycling (Yan et al, 2005). Another group linked TRIM3 to EGFR sorting through interaction with Lst2. Intriguingly, the ability of Lst2 to bind endosomes and direct EGFR trafficking is regulated by ubiquitination, although TRIM3 did not appear to be the ubiquitin ligase (Mosesson et al, 2009). Most recently, Cheung et al. correlated GABA_AR γ 2 activity and protein expression with TRIM3 presence and suggested that TRIM3 may regulate GABA_AR intracellular trafficking (Cheung et al, 2010). Further work needs to be done to understand the specific role TRIM3 plays in receptor recycling – which receptors are involved, how it exerts its control and in which cellular contexts.

TRIM3 also regulates neuron morphology. Overexpression of a TRIM3 mutant lacking the beta-propeller domain, a presumptive dominant negative mutant, inhibited neurite outgrowth in PC12 cells (El-Husseini & Vincent, 1999). Expression of this dominant-negative mutant, as well as TRIM3 depletion by RNAi in hippocampal neurons resulted in enlarged dendritic spine heads. In these spine heads, TRIM3 ubiquitinates the postsynaptic scaffold protein GKAP, thereby modulating synaptic strength (Hung et al, 2010). Whether the roles of TRIM3 in receptor trafficking or neurons are important for tumor suppression is unclear.

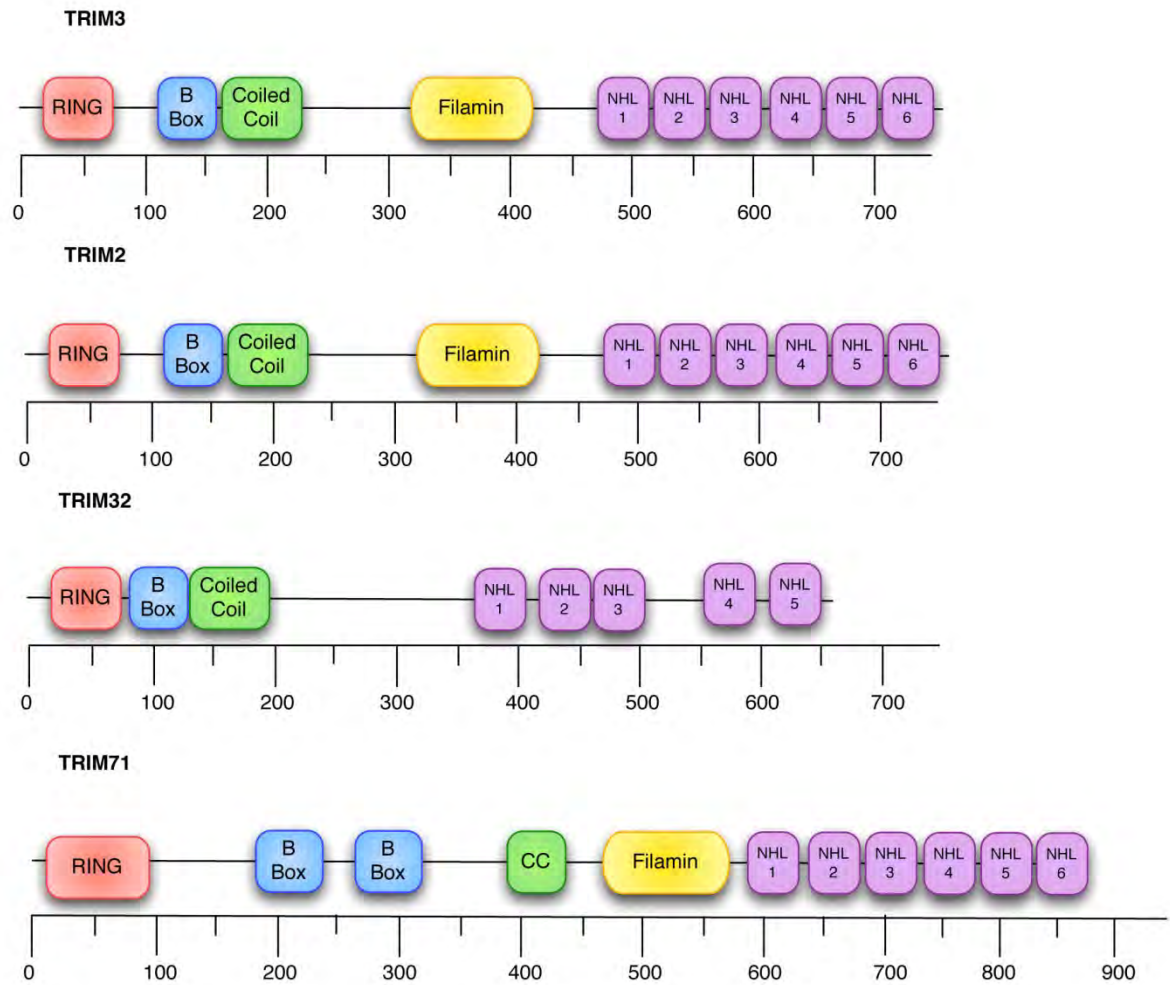


Figure 2: Mammalian TRIM-NHL domain structures. The four mammalian TRIM-NHL proteins and their domains boundaries as catalogued in the Uniprot database. The scale on the bottom indicates amino acid number. Note the conserved order of the tripartite motif and the NHL repeats.

Recently, our lab has discovered a novel function of TRIM3 that may account for some of its tumor suppressive qualities. In PDGF-driven gliomas, where expression of p21 is associated with cellular growth, TRIM3 ubiquitinates and promotes the degradation of newly translated p21 (Liu et al, 2012; Raheja et al, 2012). This prevents p21 from stabilizing cyclin D1-cdk4 complexes, reducing cell proliferation and tumor growth in mice. However, even mice lacking p21 form tumors when TRIM3 is depleted, suggesting that other pathways are also important for TRIM3 tumor suppressive function.

V. Regulation of tumor suppressors by phosphorylation

I wanted to understand how the tumor suppressive activity of TRIM3 is inactivated such that p21 can accumulate to promote cell growth. Some studies in our lab indicated that p21 bound to cyclin D1-cdk4 complexes is protected from TRIM3 binding (Liu et al, 2012). This suggests that in growing cells, where cyclin-cdk complexes are prevalent, p21 binds these complexes and enters the nucleus. In this scenario, p21 is sequestered away from cytosolic TRIM3, thereby indirectly inactivating the tumor suppressive activity of TRIM3. However, it is also possible that TRIM3 itself is regulated in some fashion, especially since some of the TRIM3 tumor suppressive activity is p21-independent.

The regulation of tumor suppressors that are directly implicated in cell cycle control or indirectly by modulating key cell cycle regulators occurs at two levels: the level of protein accumulation (including transcriptional, translational and post-translational mechanisms) and the level of post-translational modifications (including

phosphorylation, ubiquitination and methylation). I quickly discovered that the protein levels of TRIM3 were not regulated in a growth-dependent manner in glial cells (see Results), and therefore turned towards post-translational modifications. The most common of these is phosphorylation. In this section I will focus on how phosphorylation can regulate tumor suppressive activity.

Tumor suppressors can be modulated by single and/or multi-site phosphorylation events. Often both single and multi-site phosphorylation changes the structure of the tumor suppressor. Structural alterations, in turn, can directly affect the biochemical activity of the protein (such as kinase or ubiquitination activity), affect the ability to interact with other proteins, and/or change the localization of the protein. These mechanisms are not mutually exclusive, and a few examples of each will be described below.

Multisite phosphorylation presents the opportunity for incredibly complex regulation of protein function. Therefore, it is not surprising that many tumor suppressors are multiply phosphorylated in their regulatory domains. The more phosphorylation sites there are, the greater number of possible phosphoforms, which may have distinct functions within the cell. Many phosphoforms may be present at the same time – kinases and phosphatases can act in concert to, in theory, create an unlimited number of stable phosphoforms (Thomson & Gunawardena, 2009). Regulation of these phosphoforms provides flexibility for the cell in responding to various upstream signals and stresses.

One example of such a tumor suppressor is p53, which is mutated in over 50% of human

cancers (Toledo & Wahl, 2006). Known as the “guardian of the genome”, p53 directs the cellular response to stress signals such as DNA damage primarily by regulating the transcription of genes involved in processes ranging from DNA repair to senescence (Kruse & Gu, 2009). As a central signaling conduit, it is not surprising that p53 is carefully regulated. Levels are quite low in growing cells, but in stressed cells, p53 is stabilized and activated by several mechanisms, including post-translational modifications, especially phosphorylation (Dai & Gu, 2010). Most of the phosphorylation sites reside in the regulatory domains at the N and C termini, and at steady state, most of them are unphosphorylated (Bode & Dong, 2004). However, conditions of cellular stress can quickly induce the phosphorylation of many of these sites, stabilizing the protein and directing it to various functions (some discussed below).

Another multiply-phosphorylated tumor suppressor is retinoblastoma protein (Rb). Multisite phosphorylation of Rb by CDKs leads to its inactivation and the release of E2F transcription factors that drive the cell cycle forward (Poznic, 2009). Although rarely mutated in cancer, Rb is often inactivated by alterations in its regulators, particularly the CDKs and p16/INK4a (Poznic, 2009). It has at least 16 phosphorylation sites, many in unstructured regions of the protein. Recent structural studies have shown that phosphorylation at some of these sites results in specific changes in the structure of Rb, which in turn change its affinity for E2F transcription factors through distinct mechanisms (Burke et al, 2012; Heilmann & Dyson, 2012). Since Rb can interact with ~200 proteins, it has been suggested that these individual changes in structure could direct the complexes with which it interacts, and thereby the functions it can perform

(Heilmann & Dyson, 2012).

There are several common themes of regulation by multi-site phosphorylation. The first theme is promiscuity - multiple kinases can phosphorylate multiple sites, and multiple sites can be phosphorylated by multiple kinases. P53, for example, has multiple phosphorylation sites at the N-terminus that can be phosphorylated by several kinases (see (Bode & Dong, 2004) for a list of p53 kinases and their phosphorylation sites). S15 can be phosphorylated by at least seven kinases, including ATM, ERKs and p38 kinases (Toledo & Wahl, 2006). A single kinase can also phosphorylate multiple sites. For example, p38 kinases can phosphorylate multiple sites on p53, including S15, S33, S46 and S392. Similar promiscuity has been found for the Rb (Poznic, 2009) and the mTOR regulator raptor (Foster et al, 2010). This flexibility allows the cell to regulate these proteins through multiple upstream pathways.

The second theme is redundancy and fine-tuning. A single phosphorylation event often does not affect function measurably, however multiple phosphorylation events together can regulate activity dramatically. S15 and S20 phosphorylation of p53, for instance, reduce its affinity for HDM2, an E3 ubiquitin ligase that marks p53 for degradation. While single point mutations of S15 or S20 in p53 knock-in mice barely affect p53 stability (S18 and S23 in mouse p53), double-mutants are more severely compromised (Chao et al, 2006; Sluss et al, 2004; Toledo & Wahl, 2006; Wu et al, 2002). This suggests that there is some redundancy, or “fail-safe” mechanism in the way that p53 is regulated by phosphorylation.

Multi-site phosphorylation has been particularly important in cell cycle control, where it can result in switch-like behavior. In yeast, degradation of the Cdk1 inhibitor Sic1 (p27 is the human homolog) is regulated by multiple multi-site phosphorylation cascades that carefully control protein docking and thereby the G1/S transition (Koivomagi et al, 2011). The same is true for Rb – a single phosphorylation event doesn't abolish E2F binding, but multiple phosphorylation events by various cyclin-cdk complexes act in concert to ultimately release E2F (Brown et al, 1999; Burke et al, 2012).

In some instances, however, a single phosphorylation event can change the activity of a tumor suppressor. One example is tyrosine phosphorylation of the inhibitory α_3 -helix of the tumor suppressors p27 and p21. By affecting the ability of the α_3 -helix to bind in the ATP-binding pocket of CDKs, this single phosphorylation event may determine whether p27 and p21 inhibit or stabilize cyclin-cdk complexes (Grimmler et al, 2007). This modification has been shown to affect tumor development in a mouse model of gliomagenesis (Hukkelhoven et al, 2012).

Phosphorylation of tumor suppressors can also determine their cellular localization, which can have profound effects on tumorigenesis. Among other mechanisms, the localization of p27 is regulated by phosphorylation of S10, a residue within the nuclear localization signal (NLS) (Chu et al, 2008; Connor et al, 2003). p27 that is phosphorylated at S10 preferentially binds to the CRM1 exportin, thereby inducing its nuclear export. Cytoplasmic p27 can interact with cytoplasmic proteins such as the

GTPase RhoA, and is associated with poor prognosis in tumors in mice and humans (Besson et al, 2008; Serres et al, 2011). Phosphorylation can also promote nuclear localization. For example, the nuclear accumulation of p53 is enhanced by DNA-damage-induced phosphorylation of S15, a residue in one of its nuclear export signals (Zhang & Xiong, 2001).

In some instances, changing protein complexes can directly affect the degradation and/or stabilization of tumor suppressors. As mentioned above, the interaction of p53 with the E3 ubiquitin ligase HDM2 is inhibited by phosphorylation at S15 and S20, thereby stabilizing the protein (reviewed in (Toledo & Wahl, 2006)). Similarly, the control of p27 degradation by two different ubiquitin ligase complexes is partially regulated by specific phosphorylation events. While KPC1 interacts with and ubiquitinates unphosphorylated p27 in the G1 phase of the cell cycle, SCF^{SKP2} specifically recognizes and ubiquitinates p27 that is phosphorylated at T187 in the S and G2 phases (Follis et al, 2012; Tsvetkov et al, 1999).

As detailed above, phosphorylation can regulate the activity of tumor suppressors through a wide variety of mechanisms, ranging from changes in complex formation to changes in subcellular localization. Many of these mechanisms are cell-context dependent. It is hoped that understanding these mechanisms in detail will help guide the development of therapeutic strategies aimed at modulating their activity.

VI. Scope of Thesis

With the above mechanisms in mind, I wanted to understand how TRIM3 growth-suppressive activity was regulated. After determining that protein levels are unchanged in growing and non-growing PDGF-driven glial cells, I decided to focus on post-translational modifications. In this thesis I combined state-of-the-art mass spectrometry approaches with traditional biochemical and cell biology to uncover a novel regulatory circuit in gliomagenesis. I found that TRIM3 can be multiply phosphorylated in a region adjacent to the beta-propeller WD40 domain. Furthermore, if phosphorylation is prevented in this region by mutating these sites to alanine, the growth suppressive activities of TRIM3 are enhanced. Together this suggests that TRIM3 activity can be regulated by phosphorylation in cycling cells. I then sought to identify the kinases that can phosphorylate this region of TRIM3, and find that multiple N and C-terminally associated kinases can phosphorylate this hinge region. I identified CDK16 (PCTAIRE-1), a growth-regulated cytoplasmic kinase also involved in vesicular trafficking and neural differentiation, as a TRIM3 kinase and thereby define a novel CDK16-TRIM3 regulatory circuit.

CHAPTER 2 METHODS

I. Cell Culture, transfection and infection

YH/J12 cells are PDGF-transformed primary glial cells described previously (Liu et al, 2007). T98G and 293T cells were purchased from ATCC. All cell lines were cultured in DMEM containing 10% heat-inactivated fetal calf serum and 2mM glutamine. 293T cells were transfected using standard calcium phosphate methods. T98G cells were transfected using lipofectamine 2000 (Invitrogen) as per the manufacturer's instructions.

To generate stable cell lines expressing lentiviral shRNA against CDK16, T98G cells were selected with 1 μ g/mL puromycin 72 hours after infection. Myc-TRIM3 vector was described previously (Raheja et al, 2012). Deletion and point mutation constructs were generated by site-directed mutagenesis.

II. Immunoblot, phos-tag and immunoprecipitation

Cell extracts were prepared in 'Buffer B' containing 50mM HEPES-KOH, pH 7.5, 150mM NaCl, 1mM EDTA, 2.5mM EGTA, 1mM DTT, 0.1% Tween-20, 10% glycerol, 80mM β -glycerophosphate, 1mM NaF, 0.1mM Na-orthovanadate, 1 μ g/mL leupeptin, aproteinin and soybean trypsin inhibitor, and 1mM PMSF.

Immunoblot and immunoprecipitation was performed as described previously (Liu et al, 2007). We used the following antibodies: TRIM3 (mouse IP and immunoblot: Santa Cruz sc-136363, human IP and immunoblot: Lifespan LS-B2870, IP for mass spectrometry: BD 610760 and Bethyl A301-209A), myc (Santa Cruz sc-40), Cyclin A (Santa Cruz sc-751), CDK16 (Santa Cruz, sc-174), and tubulin (Santa Cruz).

Phosphorylated TRIM3 species were resolved using 8% acrylamide gels containing 75 mM Phos-tag reagent (Wako Pure Chemical Industries) and 75 mM $MnCl_2$, prepared and run according to the manufacturer's instructions (phos-tag.com). Prior to transfer, gels were soaked in transfer buffer with 1 mM EDTA for 30 min, and then in transfer buffer without EDTA for 10 min.

III. Recombinant proteins

GST-tagged TRIM3 was generated in *E.coli* using the GST Gene Fusion System and pGEX expression plasmids (Amersham Biosciences).

IV. EdU incorporation assay

Click-iT EdU Flow Cytometry assay kits were purchased from Invitrogen. Cells were pulsed with 10uM EdU for 90 mins 48 hours post transfection, and then processed as per the manufacturer's instructions.

V. TRIM3 associated kinase assay

YH/J12 cells were lysed in HKM buffer (20mM HEPES-KOH pH 7.5, 5m M KCl, 0.5mM MgCl₂, 100mM NaCl, 2mM PMSF, 0.5mM DTT). Recombinant GST-TRIM3 was incubated in 200-800ng lysate for 1 hour on ice. 20uL of glutathione-agarose (Sigma) and 300uL Buffer B (described above) were added and rotated overnight at 4°C. Beads were washed 2 times in Buffer B, and 3 times in kinase buffer without ATP (20mM Tris pH 7.5, 7.5mM MgCl₂, 1mM DTT), and subsequently resuspended in kinase buffer with 0.3mM ATP and [γ -³²P]ATP. Reactions were terminated after 30mins at 30°C with the addition of 4X SDS Sample Buffer and heating to 95C for 5 mins. Samples were resolved by SDS-PAGE, stained with CBB, and kinase activity was detected by autoradiography and phosphorimager. Quantitation was done with ImageGauge software.

VI. Kinase assays

CDK2-Cyclin A, CDK5-p35, active EGFR, active Raf-1 and all p38MAPKs (MAPK11, 12 and 13) were purchased from Millipore. Kinases were incubated for 30 mins at 30°C in the manufacturer's recommended kinase buffer supplemented with 0.5ug substrate (recombinant TRIM3, Histone H1 or MBP) and [γ -³²P]ATP. Recombinant human CDK16 was purchased from Creative Biomart and kinase reactions were performed as

per the manufacturer's instructions. All quantitation was performed using a phosphorimager and ImageGauge software.

VII. Phosphopeptide MS analysis

Endogenous TRIM3 was immunopurified from 20mg of protein extract with a mixture of TRIM3 antibodies (30ug each of Santa Cruz sc-136363, Life Span LS-B2870 and BD 610760). The immune-purified material was resolved by SDS-PAGE, stained with CBB for 15 mins, and the visible TRIM3 band was excised and digested with trypsin. Nano-LC-MS/MS analysis was done as outlined below, with additional variable modification of serine, threonine and tyrosine phosphorylation used in database searches.

Protein identification by nano-Liquid Chromatography coupled to tandem Mass Spectrometry (LC-MS/MS) analysis

Endogenous TRIM3-containing protein complexes were immunopurified from 30mg of YH/J12 protein extract on a 1mL α TRIM3 affinity column. This column was generated by cross-linking 200ug of antibody to protein A sepharose (Sigma) with dimethylpimelidate as described previously (Raheja et al, 2012). One half of the column was eluted using 0.1M triethylamine pH 11.5, the other half with 0.2M glycine pH 2.2. TCA protein precipitation was performed to purify and concentrate protein mixtures into a single, 3-mm wide "stack" by electrophoresing through an SDS 'stacking gel' until entering the 'separation gel', followed by brief staining with Coomassie Blue and excision of the stacked protein gel bands. *In situ* trypsin digestion of polypeptides in each gel slice was performed as described (Sebastiaan Winkler et al, 2002). The tryptic peptides were purified using a 2- μ l bed volume of Poros 50 R2 (Applied Biosystems,

CA) reversed-phase beads packed in Eppendorf gel-loading tips (Erdjument-Bromage et al, 1998). The purified peptides were diluted to 0.1% formic acid and then subjected to nano-liquid chromatography coupled to tandem mass spectrometry (nanoLC-MS/MS) analysis as follows. Peptide mixtures (in 20 μ l) were loaded onto a trapping guard column (0.3 x 5mm Acclaim PepMap 100 C18 cartridge from LC Packings, Sunnyvale, CA) using an Eksigent nano MDLC system (Eksigent Technologies, Inc. Dublin, CA) at a flow rate of 20 μ l/min. After washing, the flow was reversed through the guard column and the peptides eluted with a 5-45% acetonitrile gradient over 85 min at a flow rate of 200 nl/min, onto and over a 75-micron x 15-cm fused silica capillary PepMap 100 C18 column (LC Packings, Sunnyvale, CA). The eluent was directed to a 75-micron (with 10-micron orifice) fused silica nano-electrospray needle (New Objective, Woburn, MA). The electrospray ionization needle was set at 1800 V. A linear ion quadrupole trap-Orbitrap hybrid analyzer (LTQ-Orbitrap, ThermoFisher, San Jose, CA) was operated in automatic, data-dependent MS/MS acquisition mode with one MS full scan (450-2000 m/z) in the Orbitrap analyzer at 60,000 mass resolution and up to five concurrent MS/MS scans in the LTQ for the five most intense peaks selected from each survey scan. Survey scans were acquired in profile mode and MS/MS scans were acquired in centroid mode. The collision energy was automatically adjusted in accordance with the experimental mass (m/z) value of the precursor ions selected for MS/MS. Minimum ion intensity of 2000 counts was required to trigger an MS/MS spectrum; dynamic exclusion duration was set at 60 s.

Initial protein/peptide identifications from the LC-MS/MS data were performed using the Mascot search engine (Matrix Science, version 2.3.02;

www.matrixscience.com) with the rodent segment of Uniprot protein database (25,897 sequences; European Bioinformatics Institute, Swiss Institute of Bioinformatics and Protein Information Resource). The search parameters were as follows: (i) two missed cleavage tryptic sites were allowed; (ii) precursor ion mass tolerance = 10 ppm; (iii) fragment ion mass tolerance = 0.8Da; and (iv) variable protein modifications were allowed for methionine oxidation, cysteine acrylamide derivatization and protein N-terminal acetylation. MudPit scoring was typically applied using significance threshold score $p < 0.01$. Decoy database search was always activated and, in general, for merged LS-MS/MS analysis of a gel lane with $p < 0.01$, false discovery rate averaged around 1%.

Scaffold (Proteome Software Inc., Portland, OR), version 3.5.1 was used to further validate and cross-tabulate the tandem mass spectrometry (MS/MS) based peptide and protein identifications. Protein and peptide probability was set at 95% with a minimum peptide requirement of 1.

CHAPTER 3

THE GROWTH SUPPRESSIVE ACTIVITY OF TRIM3 IS REGULATED BY PHOSPHORYLATION

I. Background

TRIM3 is a novel tumor suppressor in gliomas. One or two copies of the TRIM3 gene are lost in 15-20% of human glioblastoma multiforme, and protein expression may be reduced in an even greater number (Boulay et al, 2009; Liu et al, 2012). The mechanism for TRIM3 tumor suppression in glioma is still unclear, but may be related to its ability to ubiquitinate and promote the degradation of the cell cycle regulator p21^{WAF1/CIP1}. TRIM3 and its family members have multiple other roles and activities, and what regulates switching between these activities is an open question.

TRIM (tripartite motif) proteins are divided into several sub-families based on the

structure of their C-terminus. TRIM3 and three other TRIMs (TRIM2, TRIM32 and TRIM71) have C-terminal NHL repeats, which together compose a WD40-like beta-propeller domain (Sardiello et al, 2008). This TRIM-NHL sub-family is conserved throughout flies (*brat* and *mei-P26*), worms (NHL-2) and mollusks (L-TRIM) and members play key roles in neuronal stem cell maintenance and tumor suppression. It is not entirely clear how TRIM-NHL proteins participate in these processes, but correlative evidence suggests that ubiquitination activity and miRNA regulation may be involved (Hammell et al, 2009; Kohlmaier & Edgar, 2008; Lee et al, 2006; Reichert, 2011).

The most is known about a *Drosophila* TRIM-NHL family member, brain tumor (*brat*). In *Drosophila* neural progenitor cells, *brat* promotes differentiation (Betschinger et al, 2006; Lee et al, 2006). *Brat* mutant secondary neuroblasts cannot differentiate, and *brat* mutant flies form tumor-like growths in the brain at nearly 100% penetrance (Causinus & Gonzalez, 2005; Loop et al, 2004). Interestingly, mutations in the beta-propeller domain of *brat* are sufficient for fly tumorigenesis, suggesting that this domain might be critical for tumor suppression by *brat* (Arama et al, 2000).

Mammalian TRIM3 has not been extensively characterized, but like *brat*, it can regulate cell growth of various stem and progenitor cells, and reducing its expression can cooperate with overexpression of PDGF to drive gliomagenesis (Liu et al, 2012). Unlike *brat* and other TRIM-NHL family members, TRIM3 has not been found to regulate the miRNA pathway (Hammell et al, 2009; Lin et al, 2007; Maller Schulman et al, 2008; Schwamborn et al, 2009; Wulczyn et al, 2011).

Understanding the regulation of tumor suppressors is of utmost importance. I wanted to understand how upstream growth signals could inactivate TRIM3 growth-inhibitory activity, thereby permitting cell growth. Other tumor suppressors such as Rb, p27 and p53 are regulated at the transcriptional level, by post-translational modification, and by changes in protein interactions. Therefore, I asked whether TRIM3 was regulated by similar mechanisms. In this chapter I focus on the growth dependent regulation of TRIM3 by the most common post-translational modification – phosphorylation. In the next chapter I look broadly at TRIM3 protein interactions and ultimately suggest a kinase that may be phosphorylating TRIM3.

II. Results

1. TRIM3 phosphorylation is complex and growth-regulated

I set out to understand the mechanism by which cells control TRIM3 activity. Because I was interested in its role in glioma, I focused my work on glial cell lines. YH/J12 is a spontaneously immortalized PDGF expressing cell line derived from the infection of nestin-tva transgenic whole brain cell cultures with the avian retrovirus RCAS expressing the PDGF oncogene. These cells can be growth arrested by treatment with PTK787, a PDGFR inhibitor. I found that TRIM3 is expressed at equal levels in growing and arrested cells (Fig. 3A), suggesting that TRIM3 protein expression is not regulated in a cell growth-dependent manner.

To determine whether TRIM3 was regulated by post-translational modifications, I mixed phos-tag into our gels. Phos-tag is a cationic compound that retards the mobility of phosphorylated proteins. The migration of endogenous TRIM3 from growing cells was complex (Fig. 3B-C). The complexity of this pattern was reduced when we treated lysates with calf-intestinal phosphatase (Fig. 3B), suggesting that TRIM3 was phosphorylated in growing lysates. The migration of TRIM3 from PTK787 treated cells was simple and comparable to the CIP treated lysates from growing cells (Fig. 3C). Together, these data suggest that TRIM3 phosphorylation is regulated in a growth-dependent manner.

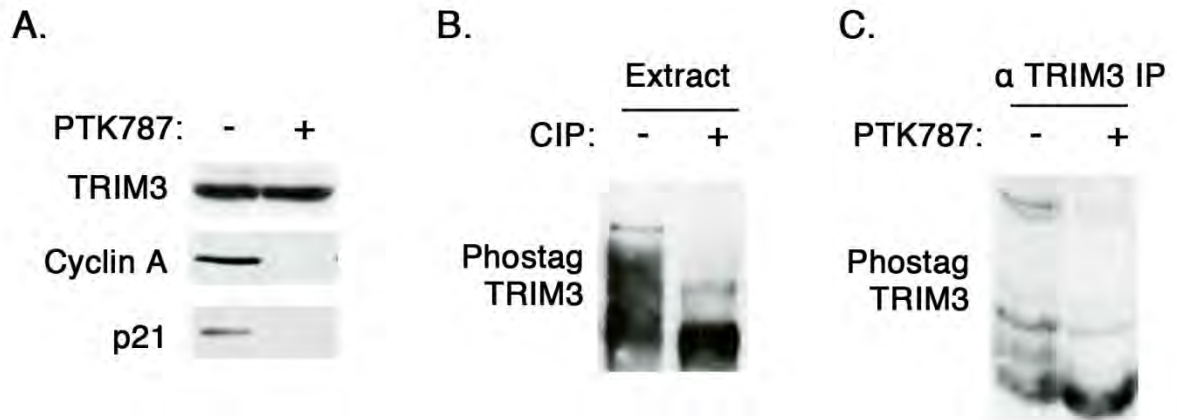


Figure 3: TRIM3 is phosphorylated in a growth dependent manner. (A) TRIM3 is expressed in growing and arrested cells. YH/J12 glial cells were treated with 20 μM PTK787 for 48 hours. Lysates were prepared and the amount of TRIM3, p21 and Cyclin A was determined by immunoblot. (B) TRIM3 is phosphorylated in growing cells. Endogenous TRIM3 was immunoprecipitated from growing YH/J12 lysates with anti-TRIM3 antibody and treated with Calf Intestinal Phosphatase (CIP). Immunoprecipitated protein was resolved by phos-tag SDS-PAGE, followed by anti-TRIM3 immunoblot. (C) TRIM3 phosphorylation decreases after PTK787 treatment. Lysates were treated as in (A) and resolved by phos-tag SDS-PAGE followed by immunoblot with anti-TRIM3 antibody.

2. TRIM3 is multiply phosphorylated at the hinge region and at S7

The complex migration pattern in cycling cells suggested the possibility that TRIM3 was highly phosphorylated. I set out to identify TRIM3 phosphorylation sites by using mass spectrometry to identify the specific site, and then I attempted to validate individual sites by resolving overexpressed mutants by phos-tag SDS-PAGE. I immunoprecipitated endogenous TRIM3 from two different PDGF-driven glioma cell lines (YH/J12 and T98G) and a rat neuronal cell line (PC-12) by LC-MS/MS, and found 80 dalton peak shifts consistent with phosphorylation at S7 and S427 (Fig 4A). However, mutation of these two sites to alanine only modestly reduced the complex pattern of migration through phos-tag gels (Fig 4B), suggesting there might be other phosphorylation sites.

A series of shotgun phosphoproteomic mass spectrometry studies cataloged in the PhosphoSitePlus Database indicated that TRIM3 might be phosphorylated at multiple sites between the WD40 and filamin domains (“hinge” region) (Hornbeck et al). These sites are well conserved throughout mammals (Fig 5). The MS coverage of this region was quite poor (Fig 4A – yellow bars). Thus I mutated all potential sites to alanine or aspartic acid and looked at the effect on TRIM3 migration (Hinge A and Hinge D mutants). Both mutants migrated as a doublet. Further mutation of S7 to alanine reduced the migration of TRIM3 to a single band, suggesting that TRIM3 is phosphorylated at both S7 and in the hinge region of TRIM3 *in vivo*.

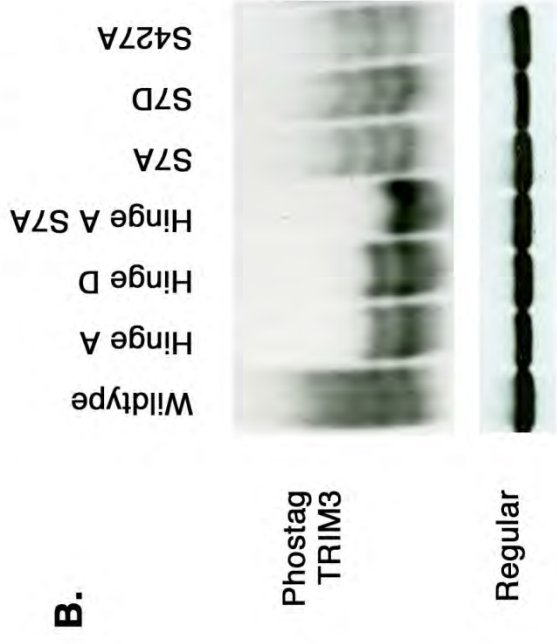
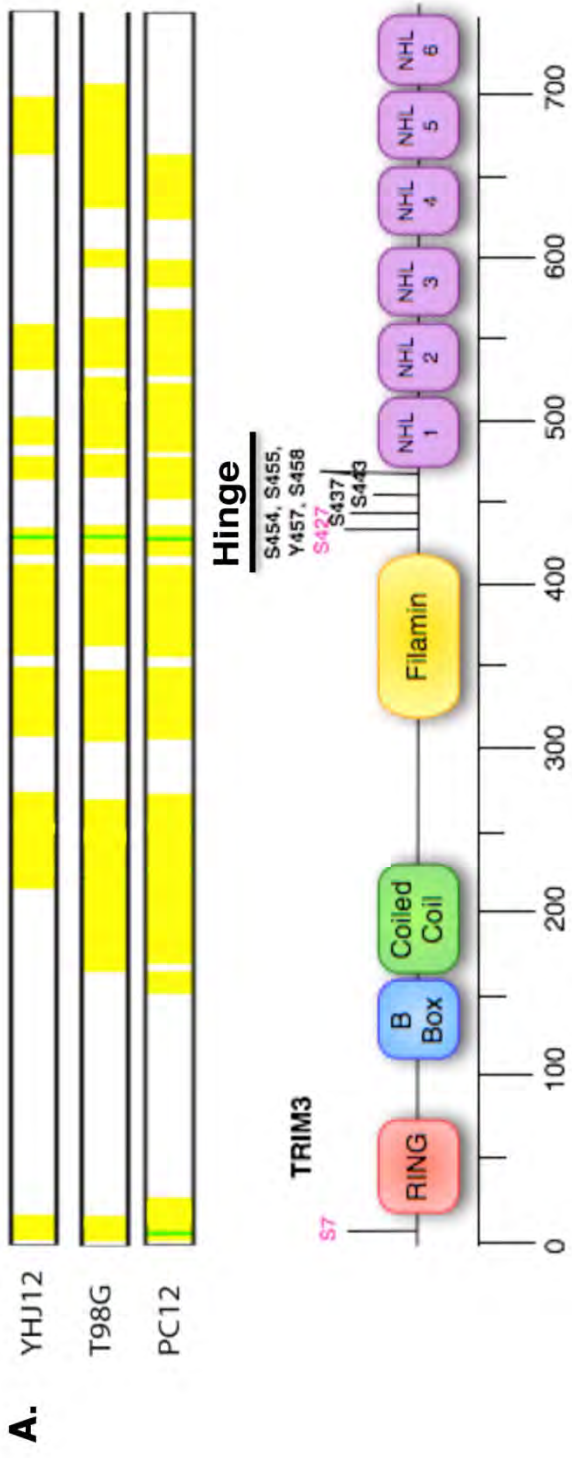


Figure 4: TRIM3 is multiply phosphorylated at the hinge and S7. (A) TRIM3 phosphorylation sites. Sites found in our MS analysis (pink – S7 and S427) and sites found in PhosphoSitePlus database (black). The yellow bars indicate mass spectrometry coverage in each sample. Endogenous TRIM3 was immunoprecipitated from 20mg YH/J12, T98G and PC12 extracts. Products were resolved by SDS-PAGE and stained briefly with CBB. TRIM3 bands were excised and digested with trypsin prior to LC-MS/MS analysis. **(B)** TRIM3 is phosphorylated at the hinge and S7. Myc-TRIM3 mutants were expressed in 293T cells. Cells were harvested after 48 hours and lysates were resolved by phos-tag SDS-PAGE (top panel) and regular SDS-PAGE (lower panel) followed by immunoblot with anti-myc antibody.

Homo sapiens TRIM3 2 AKRED SPGPEVQPMDD--KQF
Mus musculus TRIM3 2 AKRED SPGPEVQPMDD--KQF
Rattus norvegicus TRIM3 2 AKRED SPGPEVQPMDD--KQF
Bos taurus TRIM3 2 AKRED SPGPEVQPMDD--KQF
Canis familiaris TRIM3 2 AKRED SPGPEVQPMDD--KQF
Danio rerio BRAT 38 DLHSQNGQVLEHQPCLE
Drosophila melanogaster BRAT181 ACKSKCSDAVAKCFE--CQS'

Homo sapiens TRIM3 425 P--P SPDDVKRRVKSPGGPGSHVRQKAVRRPSSMYST 459
Mus musculus TRIM3 425 P--P SPDDVKRRVKSPGGPGSHVRQKAVRRPSSMYST 459
Rattus norvegicus TRIM3 425 P--P SPDDVKRRVKSPGGPGSHVRQKAVRRPSSMYST 459
Bos taurus TRIM3 425 P--P SPDDVKRRVKSPGGPGSHVRQKAVRRPSSMYST 459
Canis familiaris TRIM3 425 P--P SPDDVKRRVKSPGGPGSHVRQKAVRRPSSMYST 459
Danio rerio BRAT 492 P-VLEKRMCDVRWEVRDSTLEFITQLTVALDNSGFV 527
Drosophila melanogaster BRAT 702 SGVSGSSAVADAFASLSAVGGSVVSGAGAGGSTVSE 738

Figure 5: Hinge region and S7 phosphorylation sites are conserved. Alignment of the hinge region and S7 TRIM3 phosphorylation sites (purple) with homologs in the indicated species. CLUSTALW software was used for the alignment.

3. The effect of TRIM3 S7 phosphorylation on growth

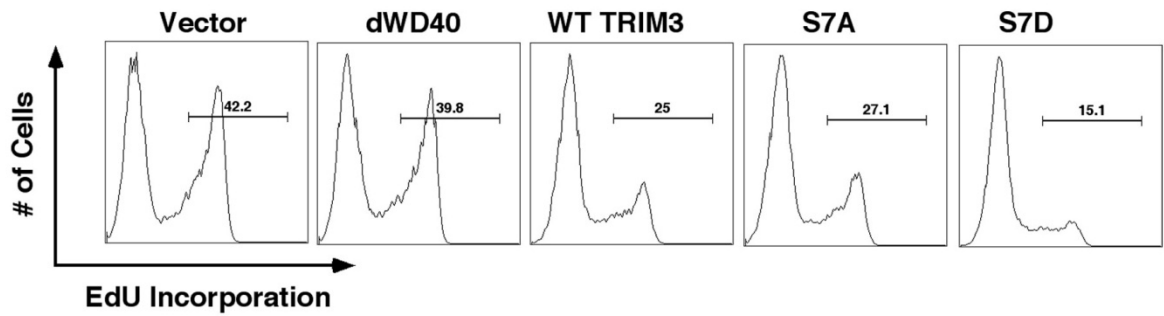
Is phosphorylation of TRIM3 associated with its activity as a growth suppressor? TRIM3 can be expressed in cells and will inhibit cell proliferation as measured by BrdU incorporation or FACS. Reducing TRIM3 levels is associated with increased proliferation (Raheja et al, 2012). Since the complex migration of TRIM3 was reduced in PTK787 treated cells (Fig. 3B), I wondered whether phosphorylation would eliminate TRIM3-mediated growth suppression.

Thus I co-transfected cells with various TRIM3 mutants and GFP, and measured S-phase by EdU incorporation and flow cytometry. To distinguish transfected from untransfected cells, I gated on the top 30% of GFP-expressing cells. Approximately half of the cells expressing wild type TRIM3 fail to incorporate EdU (Fig 6A-B). These cells accumulate in the G1 phase of the cell cycle (Raheja et al, 2012). As expected from our previous work and studies in *Drosophila* (Arama et al, 2000), the mutant lacking the WD40 domain (Δ WD40) was inactive and cells expressing it incorporate the same amount of EdU as vector transduced cells or untransfected cells.

Of the phosphorylation sites, I first tested S7. Mutation of S7 in addition to the hinge region clearly reduced the migration of TRIM3 through phos-tag gels, suggesting it is heavily phosphorylated (Fig. 4B). However mutation of this site to alanine and the phosphomimetic aspartate did not significantly affect the growth suppressive activity of TRIM3. Cells transduced with TRIM3 S7A and S7D mutants incorporated only a slightly

different amount of EdU compared to cells transduced with wild type TRIM3 (Fig. 6A-B). Albeit insignificant, this change trended towards a reduction in the growth suppressive activity of TRIM3 S7A, and an increase in TRIM3 S7D. This is consistent with a model where phosphorylation of S7 enhances TRIM3 activity. Because this change was very small, and also inconsistent with my data indicating that TRIM3 is phosphorylated in growing cells, I did not pursue this phosphorylation site further.

A.



B.

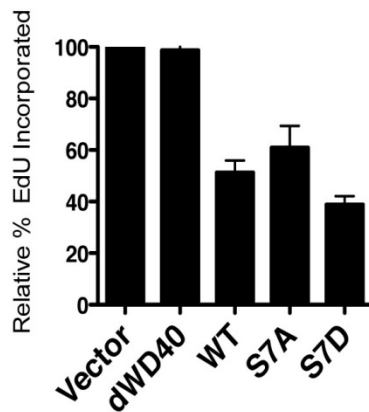


Figure 6: Mutation of S7 to aspartate modestly increases TRIM3 growth suppressive activity. (A) 293T cells were co-transfected with TRIM3 mutants and GFP. After 48 hours, cells were treated with 10mM EdU for 90 mins, fixed, stained with anti-EdU antibody and analyzed by flow cytometry. Plots were gated on the top 30% of GFP-expressing cells. EdU incorporation is log scale, number of cells is linear. (B) Average of three independent experiments. Error bars are SEM.

4. Hinge phosphorylation inhibits TRIM3 growth suppressive activity

Next I turned to the hinge region phosphorylation sites of TRIM3 and asked whether phosphorylation of these sites might affect the growth suppressive activity of TRIM3. I expressed the Hinge A and Hinge D mutants in cells and measured S-phase cells by EdU incorporation and flow cytometry. Cells expressing the TRIM3 Hinge A mutant incorporated approximately 2-fold less EdU compared to wild type TRIM3 (Fig. 7A-B). This unphosphorylated mutant was more growth suppressive than TRIM3. This is consistent with my previous finding that the phosphorylation of TRIM3 is reduced in non-growing cells. In addition, cells expressing the phosphomimetic Hinge D incorporated 3-fold more EdU than the Hinge A mutant (Fig. 7A-B). Note that all mutants were expressed at similar levels (Fig. 7C). Together, these data imply that phosphorylation at hinge residues reduces the growth suppressive activity of TRIM3 (Fig. 7D).

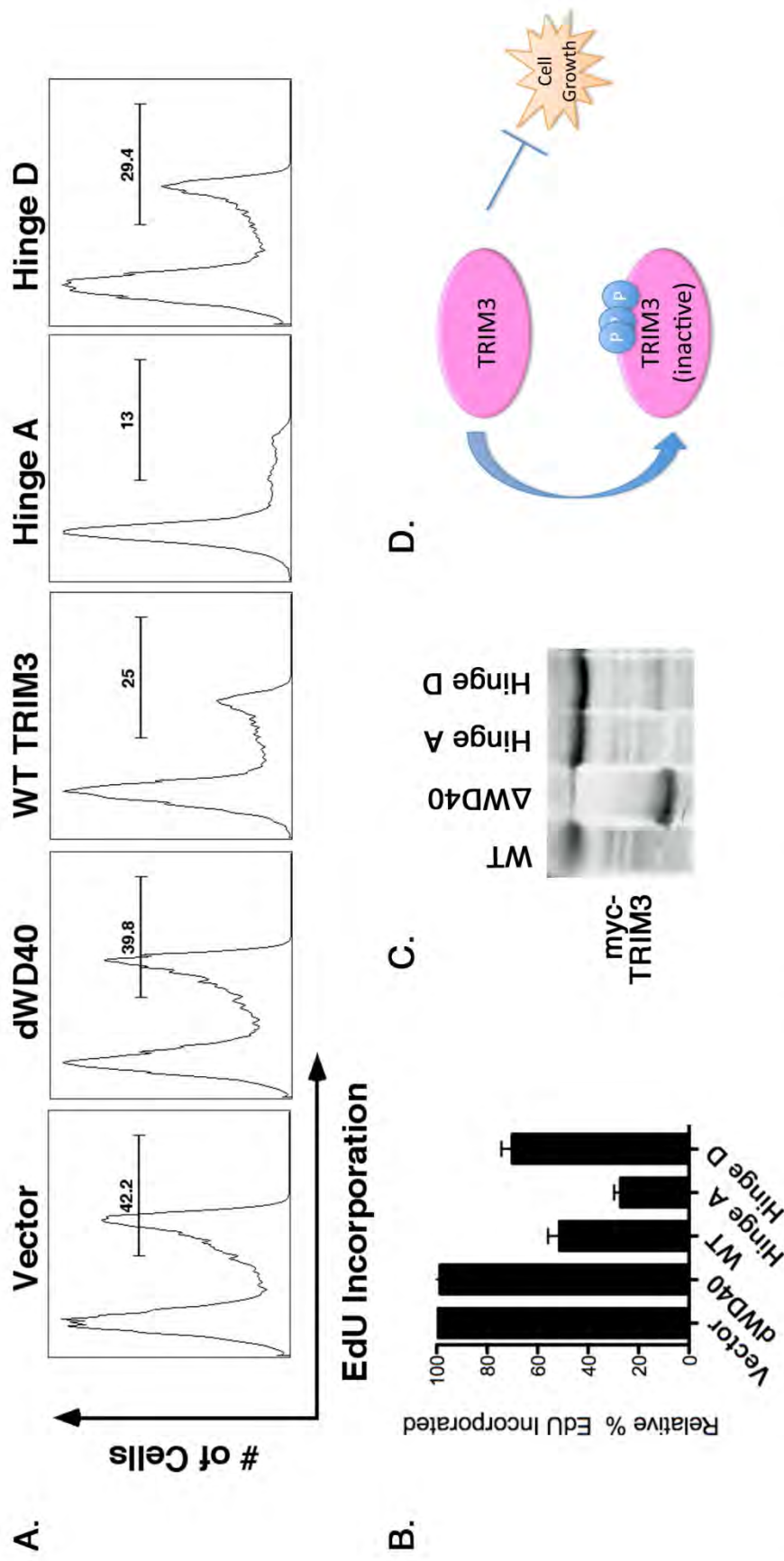


Figure 7: Hinge phosphorylation inhibits TRIM3 growth suppressive activity. (A) Mutation of all hinge phosphorylation sites to alanine increases TRIM3 activity. 293T cells were co-transfected with TRIM3 mutants and GFP. After 48 hours, cells were treated with 10mM EdU for 90 mins, fixed, stained with anti-EdU antibody and analyzed by flow cytometry. Plots were gated on the top 30% of GFP-expressing cells. EdU is log scale, number of cells is linear. **(B)** Average of three independent experiments. Error bars are SEM. **(C)** TRIM3 mutants are expressed at equal levels. Lysates were made from half the cells in **(A)** prior to fixation. These were immunoblotted with an anti-myc antibody. **(D)** Model. Phosphorylation inhibits TRIM3.

III. Discussion

1. Summary

In this chapter, I set out to understand how the growth suppressive activity of TRIM3 is regulated. I show for the first time that TRIM3 is phosphorylated at multiple sites in the hinge region, and at S7 near the N-terminus. I find that phosphorylation at the hinge region is decreased in PTK787 arrested cells, and modulates the growth suppressive activity of TRIM3. Specifically, mutating these sites to the unphosphorylatable amino acid alanine increases the growth suppressive activity of TRIM3, whereas mutation to the phosphomimetic aspartate decreases activity. Altogether, this data supports a model in which growth-regulated, multi-site phosphorylation inhibits the growth suppressive activity of TRIM3.

2. Interaction between S7 and Hinge region phosphorylation

The effects of hinge region and S7 phosphorylation on the growth suppressive activity of TRIM3 trend in opposite directions. Where hinge phosphorylation is inhibitory, S7 phosphorylation mildly activates TRIM3. It is possible that these sites are interdependent, and this leads to a few interesting models of TRIM3 regulation. For example, phosphorylation at S7 could inhibit phosphorylation of the hinge region, perhaps through modulating the ability of hinge kinases to bind to TRIM3, thereby indirectly increasing growth suppressive activity. Conversely, the lack of S7 phosphorylation could be permissive to hinge phosphorylation. In addition, hinge phosphorylation could inhibit phosphorylation at S7. These types of interdependent mechanisms have been reported for

other proteins, including p53 (Bode & Dong, 2004; Dai & Gu, 2010; Dumaz et al, 1999), the mTOR regulator raptor (Foster et al, 2010) and the cell cycle regulator Wee1 (Watanabe et al, 2005).

As a preliminary test of the interdependence of these TRIM3 phosphorylation events, I transfected cells with all combinations of Hinge A/D and S7 A/D mutants and resolved the phosphorylated proteins by SDS-PAGE. There was no discernable difference between A and D mutants (Fig. 4B and data not shown), suggesting that phosphorylation of these regions was independent.

If these phosphorylation events are independent, the question remains which is dominant for its effect on TRIM3 growth suppressive activity. The effect of hinge region phosphorylation overall is greater than the effect of S7 phosphorylation, but that does not conclusively show that hinge phosphorylation is dominant. Growth suppression assays with all combinations of Hinge A/D and S7 A/D mutants could begin to shed light on this question. Preliminary data indicates that mutation of the hinge region still dictates overall TRIM3 activity, and therefore S7 likely only plays a minimal role (data not shown).

3. Affect of phosphorylation on TRIM3 structure

Given the role of p21 and evidence that p21 ubiquitination may be needed for tumor suppressive activity, how does phosphorylation affect the growth suppressive activity of TRIM3? From a structural standpoint, the introduction of negative charge through multi-

site phosphorylation at the TRIM3 hinge region could affect the folding of this region. This, in turn, could alter the orientation of the beta-propeller domain in relation to the ring, b-box and coiled-coil domains. Indeed, I-TASSER (Roy et al) structure prediction comparing wildtype TRIM3 to Hinge D indicated that the addition of negative charge to this region changed TRIM3 conformation in all five predicted models. In addition, mutation of S412 to alanine, a residue immediately adjacent to the hinge region, eliminated the 80kDa breakdown product otherwise present during purification. I mapped the breakpoint of this product to the hinge region using mass spectrometry. Altogether, this suggests that slight modifications in or near the TRIM3 hinge region may affect overall TRIM3 folding.

There is some precedence for this type of mechanism in other growth-regulated proteins. One example is the p68 subunit of DNA polymerase primase. Like TRIM3, this protein is multiply phosphorylated by a cyclin-dependent kinase (Cyclin A-cdk2), and this phosphorylation affects the activity of the entire globular primase complex (Ott et al, 2002; Voitenleitner et al, 1999). Although no direct link has been established between the structure of this complex and phosphorylation, it is likely that these clustered sites act in concert, gradually decreasing polymerase primase activity during S phase as DNA replication finishes, perhaps by changing the orientation of the globular domains (Ott et al, 2002; Zhou et al, 2012). It is possible that TRIM3 structure is regulated in a similar manner. How structure could affect TRIM3 function in the context of a cell, however, is much more complex. This is further discussed in Chapter 5.

CHAPTER 4

CDK16 PHOSPHORYLATES TRIM3 AND IS REQUIRED FOR GLIOMA CELL GROWTH

I. Background

As discussed in the introduction, many tumor suppressors are tightly regulated by complex phosphorylation events. The kinases that regulate these tumor suppressors are of utmost importance. A more complete understanding of the regulatory circuits controlling the activity of several tumor suppressors including Rb and p53 has led to the development of therapeutic strategies targeting the kinases that phosphorylate them. For example, part of the rationale for targeting cyclin dependent kinase-4 (CDK4) is its central role in inactivating the tumor suppressor Rb by phosphorylation (Lapenna &

Giordano, 2009). Much work needs to be done to fully understand the impact of these inhibitors on cell signaling and tumorigenesis.

Multisite phosphorylation of tumor suppressors is often redundant and complex, with multiple kinases able to phosphorylate a single site, and a single kinase phosphorylating multiple sites. As mentioned in the introduction, p53 is primarily phosphorylated at its C and N-terminal regulatory regions, and many of these sites are phosphorylated by multiple kinases. S15, for example, can be phosphorylated by at least seven kinases, including ATM, ERKs and p38 kinases (Bode & Dong, 2004; Kruse & Gu, 2009).

The previous chapter established that phosphorylation of the hinge region of TRIM3 inhibits its growth suppressive activity. I also demonstrated that this phosphorylation is regulated by cell growth in a mouse glioma cell line. Phos-tag gel analysis of endogenous TRIM3 further suggests that there are multiple phosphoforms of TRIM3 present in the cell at any one moment. Therefore, like many other phosphorylated tumor suppressors, it is possible that a complex network of kinases and phosphatases dictates TRIM3 phosphorylation. This chapter focuses on identifying some of these growth-regulated kinases that can directly phosphorylate TRIM3.

II. Results

1. *TRIM3 is phosphorylated by CDKs in vitro*

Having identified a cluster of TRIM3 phosphorylation sites that affect TRIM3 activity, I next sought to determine which kinases might phosphorylate TRIM3 and inactivate its growth suppressive activity. To accomplish this, I first used two different kinase prediction software programs, and asked whether the predicted kinases can phosphorylate TRIM3 *in vitro*.

The programs use fundamentally different algorithms to make predictions. The first of these algorithms, NetworkIN, combines consensus motifs with network context (i.e. cellular localization, temporal and cell-type specific expression, co-localization by protein interactions, etc) to predict *in vivo* kinase-substrate relationships (Linding et al, 2007). The second, Group-based Prediction System 2.0, compares a putative phosphorylation site with over 3000 known phosphorylation site-kinase pairs and assigns a similarity score for each. The average similarity score yields the final prediction score for each kinase. This algorithm assumes that kinases in the same group or family identify substrates with similar motifs (Xue et al, 2008).

Both NetworkIN and Group-based Prediction System 2.0 predicted that p38MAPKs and CDKs could phosphorylate TRIM3 at hinge residues, particularly S427 and S437. Note that these sites have the well-established S-P consensus motif for CDKs and MAPKs. To determine which of these kinases, if any, could phosphorylate TRIM3 *in vitro*, I used equal specific activities of the top predicted recombinant P38MAPKs and CDK kinases –

CDK2, CDK5, MAPK11, MAPK12 and MAPK13 - to phosphorylate recombinant TRIM3 *in vitro*. Of the kinases tested, CDK2 and CDK5 had the most TRIM3-directed kinase activity *in vitro* (Fig 8A), suggesting that these could be possible TRIM3 kinases *in vivo*.

It is possible that the CDKs are phosphorylating the GST moiety attached to the recombinant TRIM3 used in this system. To rule out this possibility, I performed the TRIM3 kinase assay with CDK2 and CDK5 as usual, and subsequently cleaved the GST tag from the recombinant TRIM3 with thrombin over a timecourse. GST is approximately 27kDa, and TRIM3 is 81kDa. Therefore, thrombin cleavage results in a mobility shift from 108kDa to 81kDa. I resolved the phosphorylated, thrombin-cleaved reaction products by SDS-PAGE, and measured phosphorylation by autoradiography. Note that the 81kDa moiety is phosphorylated, indicating that TRIM3, and not the GST region of TRIM3, is phosphorylated by CDK2 and CDK5 *in vitro* (Fig. 9). Altogether, these data demonstrate that CDK2 and CDK5 can phosphorylate TRIM3.

However, since there are multiple hinge phosphorylation sites, these data do not definitively show that CDKs have a higher propensity to phosphorylate a single site on TRIM3 than MAPKs. It is possible that this system is not sensitive enough to detect a single phosphorylation event of one amino acid, and that the CDKs simply phosphorylate more sites. In order to compare the relative contribution of two S-P motif sites, S427 and S7, to overall TRIM3 phosphorylation by CDK2, I used recombinant TRIM3 S7A, TRIM3 S427A and the double mutant in the kinase assay. The hinge residue S427 largely

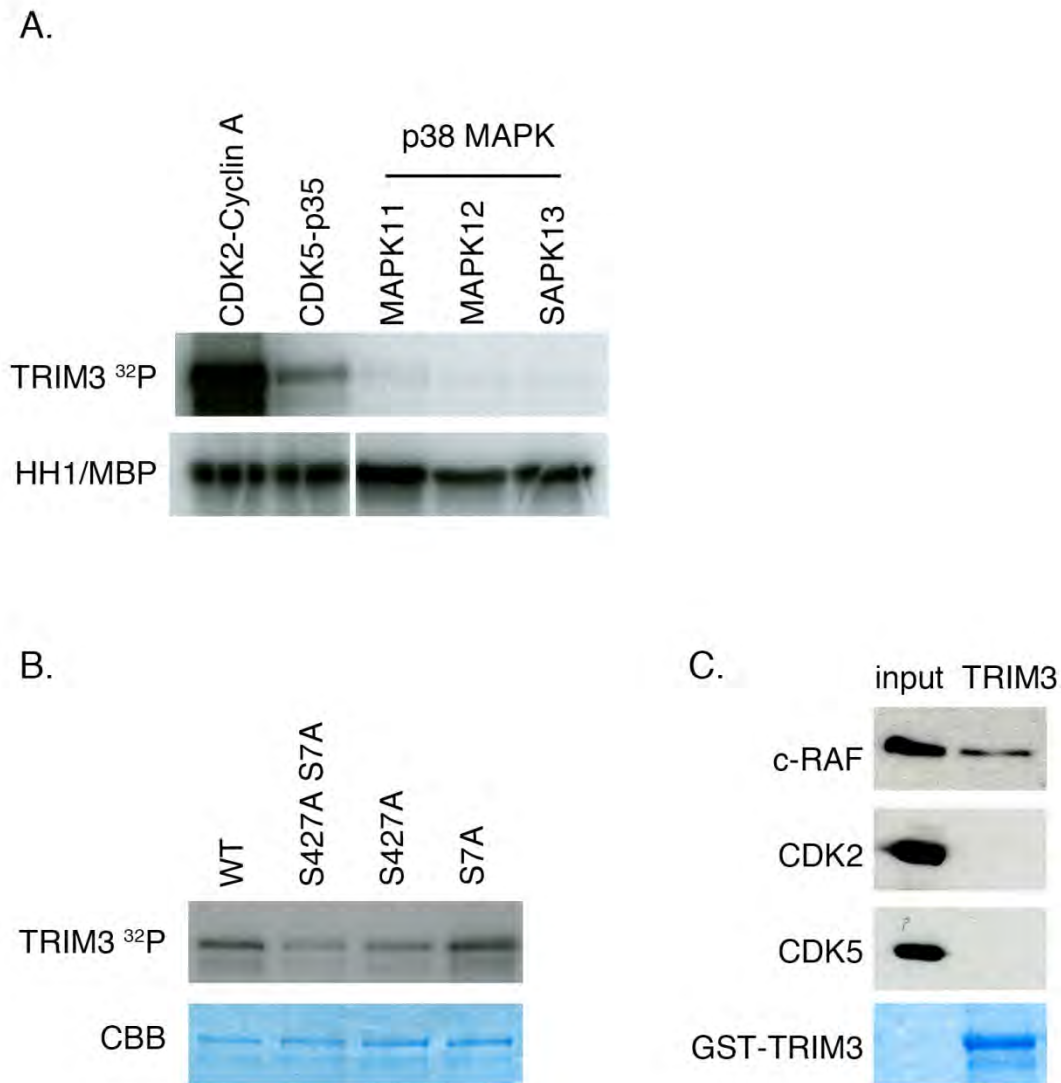


Figure 8: Cyclin dependent kinases phosphorylate TRIM3 in vitro at hinge residues. (A) CDK2 and CDK5 phosphorylate recombinant TRIM3. Equal activities of recombinant kinases were used to phosphorylate 2ug of GST-TRIM3 in the presence of $[\gamma\text{-}^{32}\text{P}]\text{ATP}$ in vitro for 1 hour. Reaction products were resolved by SDS-PAGE, and phosphorylation was detected by autoradiography. (B) CDK2 phosphorylates TRIM3 at hinge residue S427 in vitro. Kinase assay using the indicated TRIM3 mutants. (C) No detectable association between GST-TRIM3 and CDK2 or CDK5, but some association with Raf-1. GST-TRIM3 was incubated in YH/J12 cell lysates with GLT-sepharose overnight. Associated proteins were re-purified, resolved on SDS-PAGE and immunoblotted with anti-CDK2 or anti-CDK5 antibody.

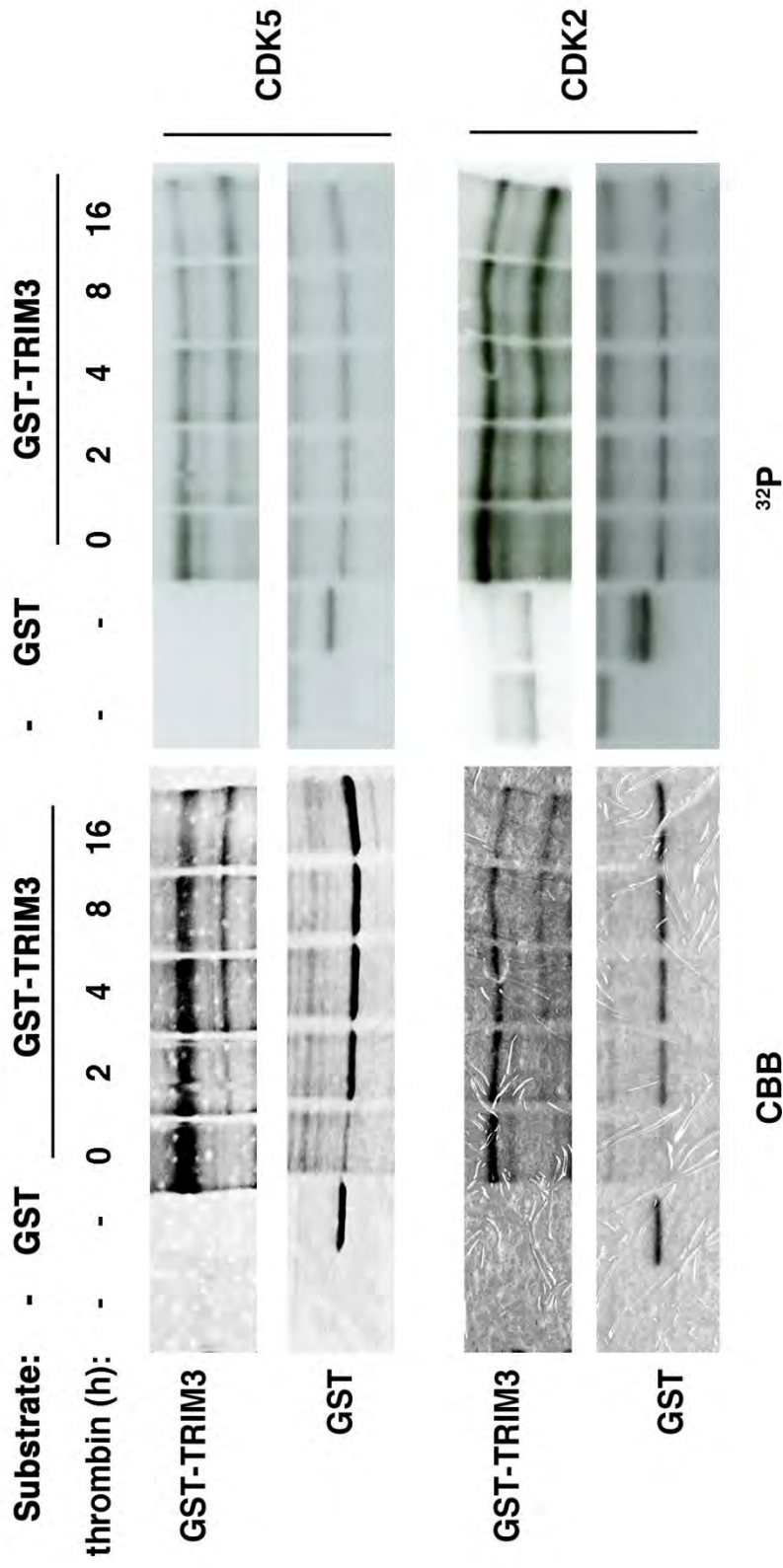


Figure 9: CDK2 and CDK5 phosphorylate TRIM3 and not GST. 2ug of GST-TRIM3 was incubated with recombinant CDK2 or CDK5 in the presence of [γ -³²P]ATP in vitro for 1 hour. Thrombin (or buffer) was subsequently added for the indicated time period at room temperature (0-16 hours), and reactions were stopped with the addition of 4X sample buffer. Reactions products were resolved by SDS-PAGE, and phosphorylation was detected by autoradiography. CBB images are included to show TRIM3 cleavage. Note the appearance of a faster migrating band after thrombin treatment.

2. TRIM3 is phosphorylated in vitro by multiple kinases at the “hinge” region

I wanted to complement my *in silico* approach with an approach that would help me identify kinases in extracts. Therefore, I developed a biochemical assay to measure TRIM3-directed kinase activity present in extracts. In this assay, GST-TRIM3 was incubated with lysates and re-purified with interacting proteins on glutathione beads. Subsequently, the reaction was incubated in kinase buffer supplemented with [γ -³²P]ATP, and occasionally an additional substrate was added. Phosphorylation of TRIM3 and/or the additional substrate was detected by autoradiography (Fig. 10A).

Under these conditions, kinase(s) present in lysates were able to bind and phosphorylate TRIM3 (Fig. 10B). Phosphorylation was dependent on the inclusion of lysates and GST-TRIM3. Subsequent mutagenesis studies (Fig. 11B), as well as the CDK2 and CDK5 thrombin cleavage experiments (Fig. 9) together suggest that the TRIM3 portion of the fusion protein, and not GST, was phosphorylated in this assay. In order for a kinase to phosphorylate TRIM3 in this assay, two requirements must be met: (1) the kinase must be able to bind to the “bait” TRIM3 in the first incubation, and (2) the kinase must be able to phosphorylate sites present on the “bait” TRIM3 and/or any subsequent substrates added to the reaction. Importantly, phosphorylation was dependent on the presence of bait TRIM3; even if substrate TRIM3 was added after the binding reaction, no phosphorylation was detected. Finally, to ensure that TRIM3-directed kinases were not binding to the GST portion of the fusion protein, GST was used as bait and TRIM3 as substrate. Again, no phosphorylation was detected, indicating that kinases bind and phosphorylate TRIM3 specifically in this assay.

In Chapter 3 I showed that TRIM3 phosphorylation is growth dependent. Therefore, I asked whether the activity of TRIM3 directed kinases in this assay was also growth-dependent. I performed the TRIM3 associated kinase assay with PTK787 treated lysates and with growing lysates and, as expected, found that there was more TRIM3 directed kinase activity present in the growing extracts (Fig. 10C). Together, these data support the use of the TRIM3 associated kinase assay in evaluating TRIM3-directed kinases.

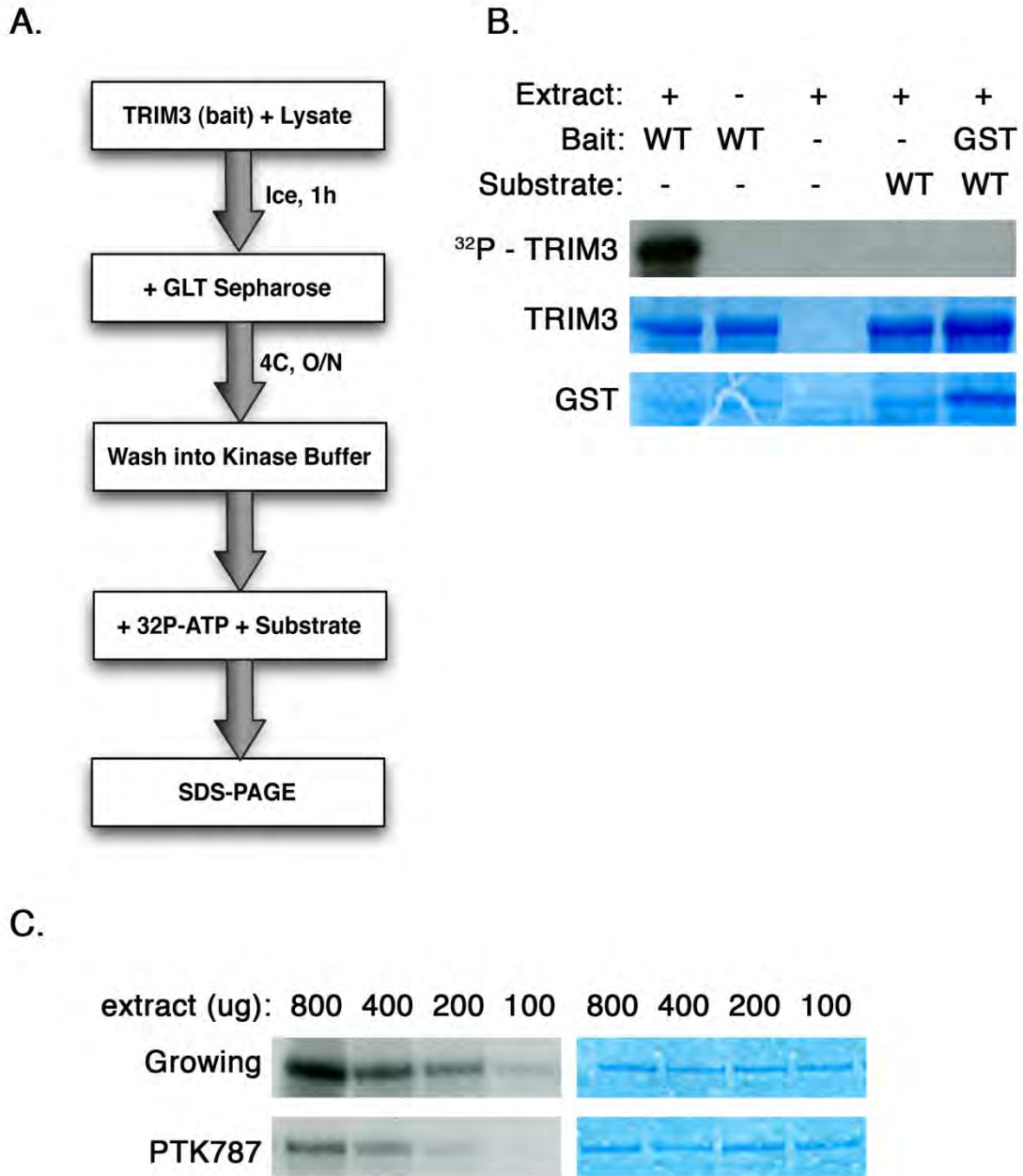


Figure 10: TRIM3 is phosphorylated by growth-regulated kinases in vitro. (A) TRIM3 associated kinase assay schematic. Briefly, recombinant TRIM3 is incubated in lysates, repurified and phosphorylated by associated kinases. Phosphorylation was detected by autoradiography. (B) Kinases specifically bind and phosphorylate recombinant TRIM3 in vitro. TRIM3 associated kinase assay with the indicated bait and substrates (controls). (C) TRIM3 associated kinase activity is growth regulated. TRIM3 associated kinase assay was performed with growing and not growing lysates.

To confirm that these kinases phosphorylate the hinge region, I generated a set of N-terminal and C-terminal deletion mutants with and without the hinge region (N, NH, C, HC – Fig. 11A). I used N-terminal and C-terminal mutants since I knew activity in this assay depended on both protein binding and the availability of phosphorylation sites. Therefore, this assay not only measured the ability of TRIM3 to be phosphorylated, but also the binding requirements of TRIM3-directed kinases. Interestingly, only mutants with the hinge region intact were phosphorylated (NH and HC, Fig. 11B). Simply removing this 60 amino acid region was sufficient to eliminate any detectable phosphorylation. This suggests that kinases bound to the N- and C-terminal halves of TRIM3 all target the hinge region for phosphorylation under these conditions.

Are kinase(s) associated with the N and C mutants, but simply unable to phosphorylate these mutants due to the lack of hinge-region phosphorylation sites? Or is the hinge region required for kinase binding? To distinguish between these possibilities, I “baited” kinases with the C and N mutants during the binding reaction, and subsequently provided NH or CH as substrates. Phosphorylation was detected whenever a substrate with a hinge region was present, independent of the presence of the hinge region during the binding reaction. Altogether, this data suggests that the hinge region is not required for binding of N-terminal and C-terminal TRIM3 kinases, and establishes that there are both N and C-terminal TRIM3 kinases (Fig. 11B).

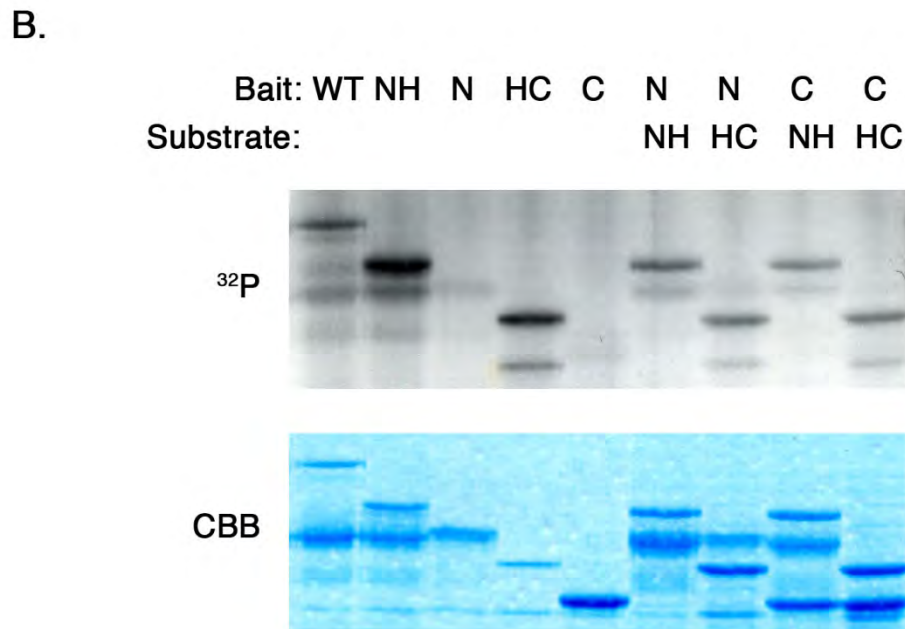
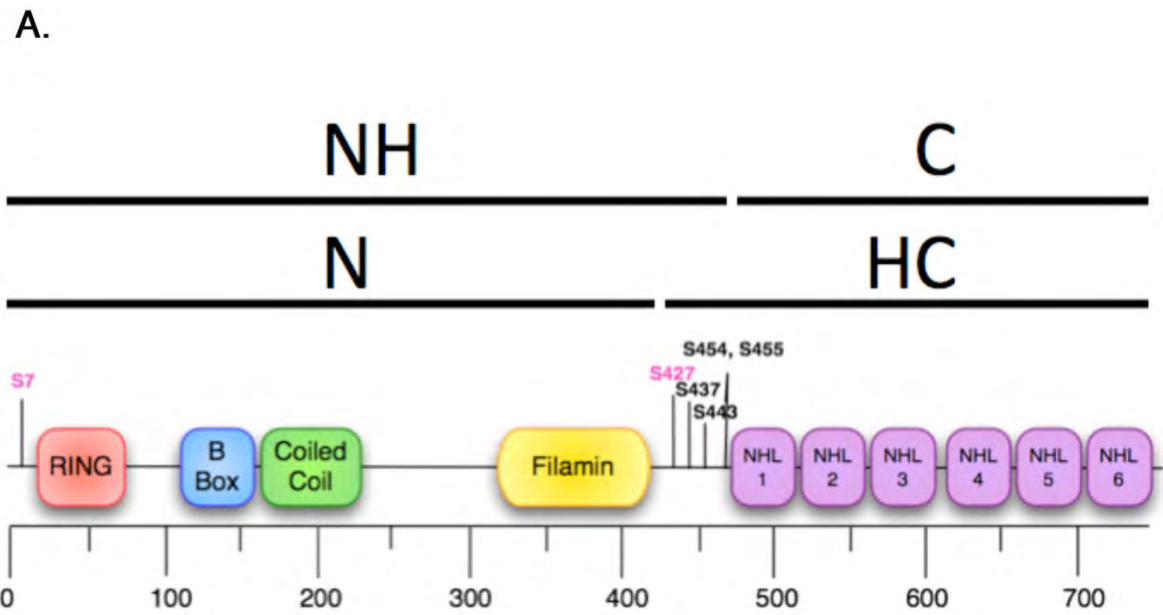


Figure 11: Multiple growth regulated kinases phosphorylate TRIM3 in vitro. (A) Schematic of TRIM3 mutants. **(B)** Kinases bind the N and C terminus of TRIM3, and phosphorylate the hinge region. TRIM3 associated kinase assay with the indicated baits and substrates.

3. Identification of CDK16 as a potential TRIM3 kinase

To specifically identify candidate kinases that can bind and phosphorylate TRIM3, I immunoprecipitated TRIM3 from growing and PTK787 treated YH/J12 extracts and identified the endogenous interacting proteins by LC-MS/MS. Three independent experiments using two different TRIM3 antibodies identified a 306-member TRIM3-interactome (Appendix). Importantly, I identified TRIM3 itself in each of these experiments.

To further validate this study, I looked for previously identified TRIM3 interacting proteins. I found two such proteins, Myosin-Va and α -actinin-4, as well as a network of known α -actinin-4 and Myosin-Va interactors (Fig 12). As expected, I also identified over 20 proteins involved in protein trafficking. Ontological analysis of the entire TRIM3 interactome revealed that these proteins are primarily involved in cellular growth and proliferation as well as cellular assembly, organization and maintenance (Fig 13). This is consistent with the known role of TRIM3 and its homologs as a regulator of growth and differentiation in the brain.

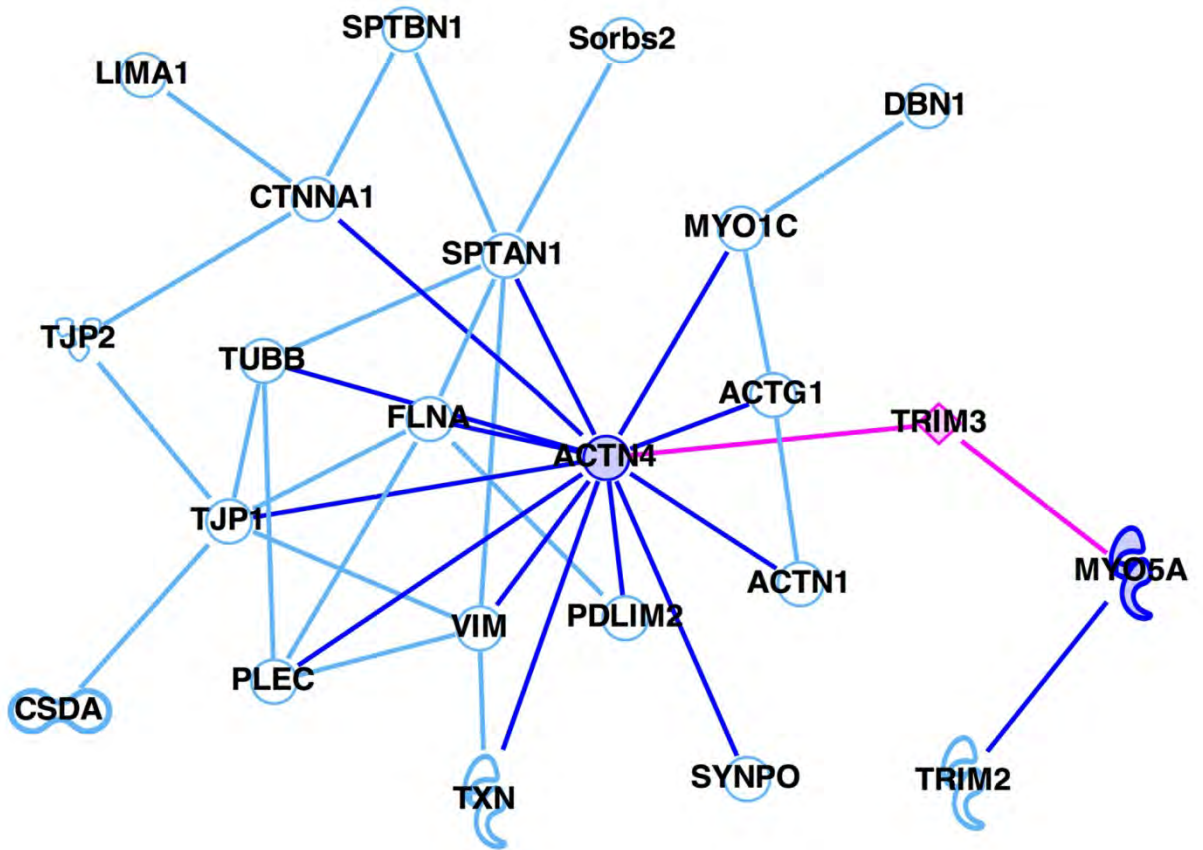


Figure 12: TRIM3 co-immunoprecipitated with a network of known TRIM3 interacting proteins. Ingenuity Pathway Analysis software was used to identify known TRIM3 interacting proteins from the 306-member TRIM3 interactome. The pathway was started by manually adding TRIM3, and then using the grow function to query the interactome for previously documented protein-protein interactions. In this figure we iterated this process three times to generate a network of interacting proteins from our dataset.

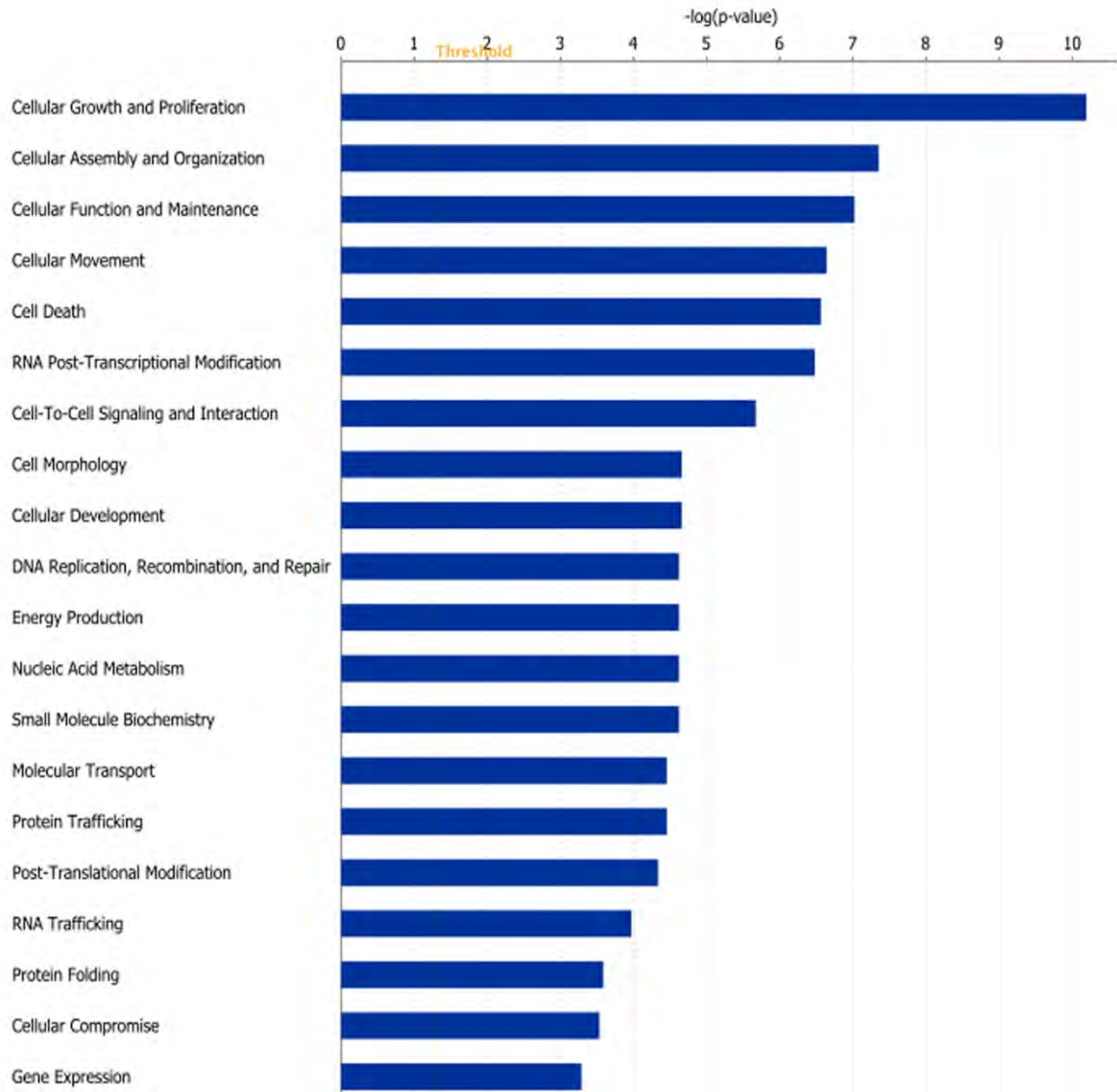


Figure 13: TRIM3 interacting proteins are primarily involved in growth and cell maintenance pathways. Ingenuity Pathway Analysis was used to determine the molecular and cellular functions of the proteins that co-immunoprecipitate with TRIM3. The threshold was set at $p < .05$.

As I was primarily interested in identifying TRIM3 kinases, I turned to this protein class. Out of all the TRIM3 interacting proteins, I found nine kinases (Table 1). I used three criteria to prioritize these kinases: (1) presence of known kinase consensus sites on TRIM3, such as a serine followed by a proline (S-P sites) for cyclin-dependent kinases (2) cytoplasmic localization (3) known involvement in growth regulation or other TRIM3 functions. Interestingly, one of the kinases was a cytoplasmic CDK known to be involved in protein trafficking – CDK16 (PCTAIRE1). Because so little is known about CDK16 and its substrates, kinase prediction softwares (NetworkIN and GPS 2.0) could not predict CDK16 as a TRIM3 kinase – it is not currently listed in the databases these programs use. However, the structure of CDK16 is similar to CDK2 (Mikolcevic et al, 2012a), and I had already shown that CDK2 can phosphorylate TRIM3 *in vitro* (Fig. 8). Although CDK16 was clearly the top hit, I also examined RAF-1 and EGFR more closely.

Table 1: Kinases associated with endogenous TRIM3 in YH/J12 cells

Kinase	Function / interest	Consensus Sequence (# residues)	Implicated in Growth	Cytoplasm	Tested?
CDK16 (PCTAIRE1)	Part of CDK family; activated by CDK5; phosphorylates NSF (involved in vesicular transport)	+++ (3)	+	+	YES (+)
RAF-1 (C-Raf)	Downstream of Ras GTPases, MAP3K; phosphorylates MEK1 and MEK2	+(1)	+	+	YES (-)
EGFR	Tyrosine kinase that sets off signaling cascades to stimulate growth	+(1)	+	+	YES (+)
AXL	Signals from ECM to cytoplasm through GAS6; cell proliferation, migration, differentiation	-	+	+	
ATR	Required for cell cycle arrest after DNA damage; Phosphorylates CHK1, RAD17, RAD9 and BRCA1	-	+	-	
CLK2	Phosphorylates spliceosomal complex; regulates alternative splicing	-	+	-	
TJP2	Necessary for tight junction formation	?	-	+	
PKM2	Involved in glycolysis as a pyruvate kinase	-	+	+	
ALDH18A1	Mutation causes neurodegeneration; involved in biosynthesis of amino acids	-	+	-	

To begin to validate these kinases, I used protein interaction network analysis to look for other proteins known to bind the top three kinases in the TRIM3 interactome. I found several for CDK16 (Fig 14A), RAF-1 (Fig 14B), and EGFR (Fig 14C). Next I performed *in vitro* kinase assays with recombinant protein to determine whether the kinases could phosphorylate TRIM3. Although RAF-1 can bind to TRIM3 (Fig 8C), we were unable to phosphorylate recombinant TRIM3 with active RAF-1 *in vitro* (Fig 15). In addition, although EGFR is well characterized in glioma and therefore an attractive candidate, there is only one tyrosine residue in the hinge region, and it is minimally phosphorylated *in vitro* (Fig 16). In contrast to RAF-1 and EGFR, CDK16 seemed quite attractive for the following reasons:

- (1) CDK16 can bind and phosphorylate TRIM3 (see below)
- (2) CDK2 and CDK5 can phosphorylate TRIM3 (Fig. 8A), and CDK16 is structurally similar to CDK2 (Mikolcevic et al, 2012a)
- (3) CDK16 and TRIM3 are both implicated in endosome sorting and growth regulation (Liu et al, 2006; Mokalled et al; Palmer et al, 2005)

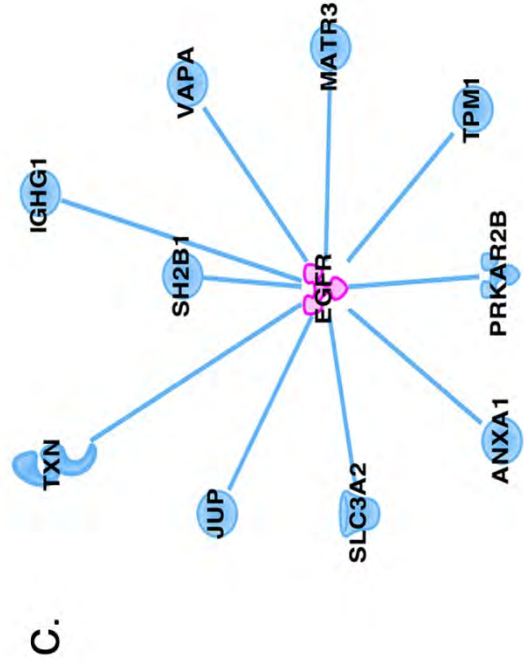
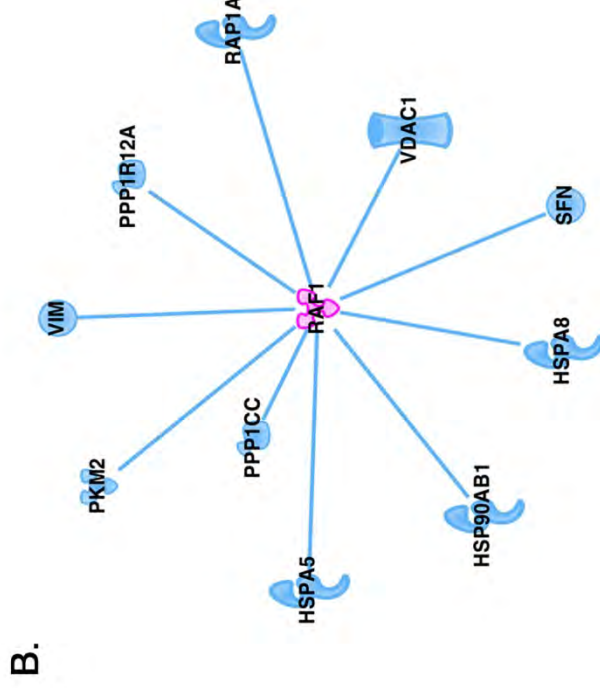
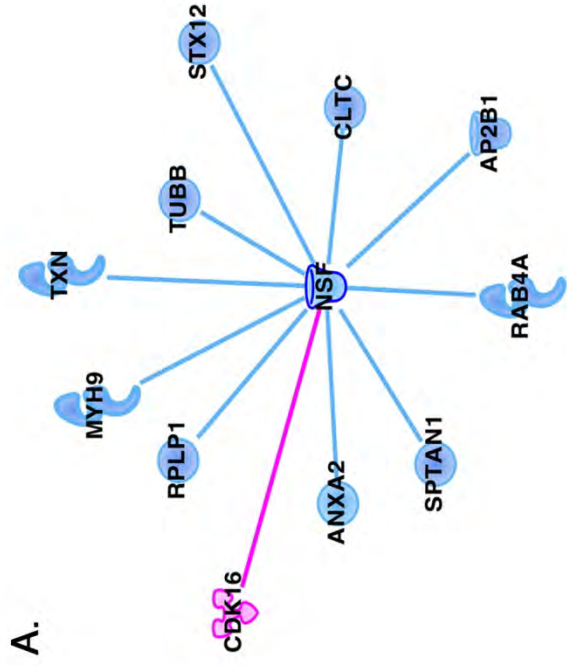


Figure 14: Top three kinase candidates co-immunoprecipitated with networks of known interacting proteins. Each pathway was started by manually adding (A) CDK16 (B) RAF-1 (C) EGFR to the Ingenuity Pathway Analysis map. The grow function was then used to query the list of TRIM3 co-immunoprecipitating proteins for known protein-protein interactions.

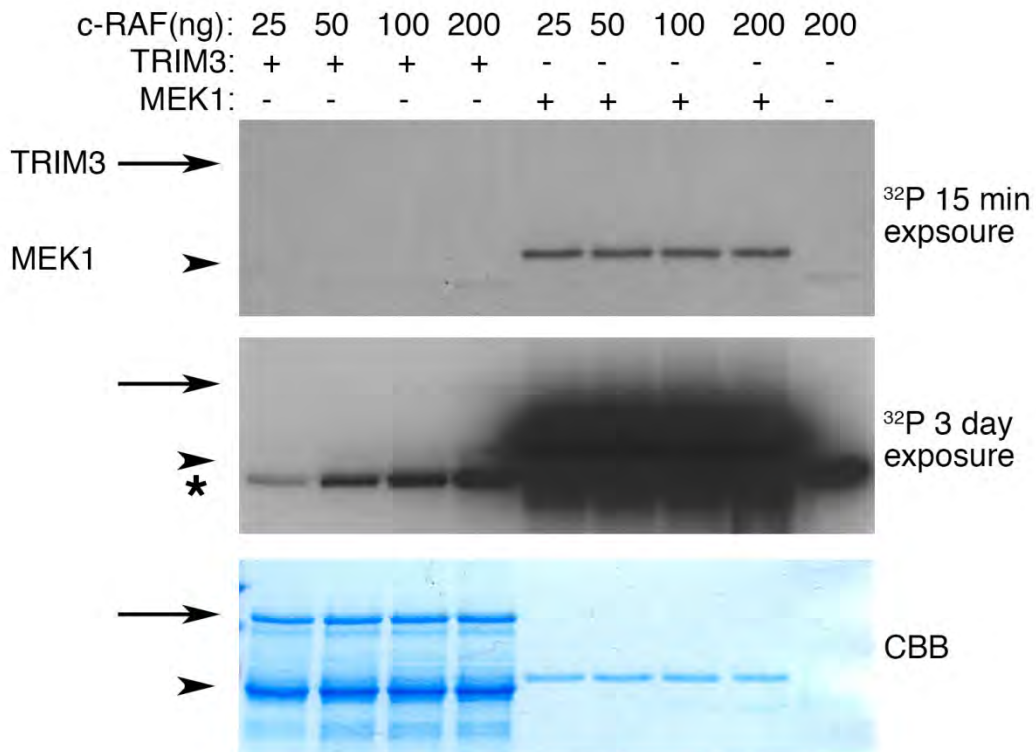


Figure 15: Raf-1 Kinase does not phosphorylate TRIM3 in vitro. Recombinant Raf-1 was titrated with recombinant GST-TRIM3 in a kinase assay for 30 mins at 30°C. Note strong MEK1 phosphorylation as a positive control (arrow heads). TRIM3 phosphorylation (arrow) is undetectable by autoradiography even on a long 3-day exposure (middle panel). Note c-Raf autophosphorylation on the longer exposure in all lanes, even when no substrate is added (*).

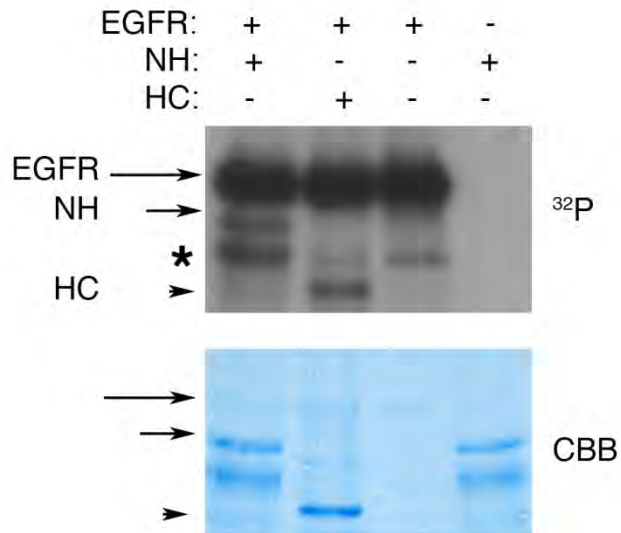
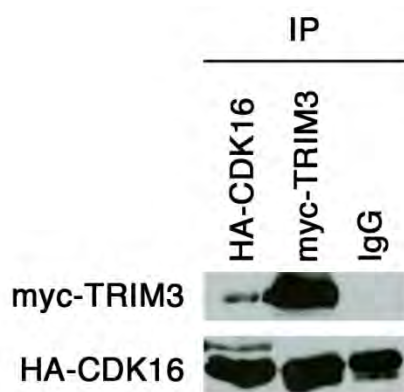


Figure 16: EGFR Kinase minimally phosphorylates TRIM3 in vitro. Recombinant EGFR kinase was incubated with NH and HC TRIM3 mutants in a kinase assay for 30 mins at 30°C and phosphorylation was detected by autoradiography. Since full length TRIM3 phosphorylation was obscured by EGFR autophosphorylation, we used NH and HC mutants instead. EGFR autophosphorylation (long arrow), NH (medium arrow), HC (arrowhead), non-specific band (*).

4. CDK16 can bind and phosphorylate TRIM3 at the hinge region

I closely examined the ability of CDK16 to bind TRIM3 *in vitro* and *in vivo*. To confirm that CDK16 can bind to TRIM3 in a cellular context, I expressed myc-TRIM3 and HA-CDK16 in 293T cells and co-immunoprecipitated the proteins (Fig. 17A). I next mapped the CDK16 binding region to the N-terminus of TRIM3 using recombinant TRIM3 NH and HC mutants (Fig. 17B). Note that I was unable to find CDK16 associated with the C-terminus of TRIM3, and since there are C-terminally associated TRIM3 kinases (Fig. 11), there must be additional kinases that also phosphorylate this region. This could be an avenue for future research.

A.



B.

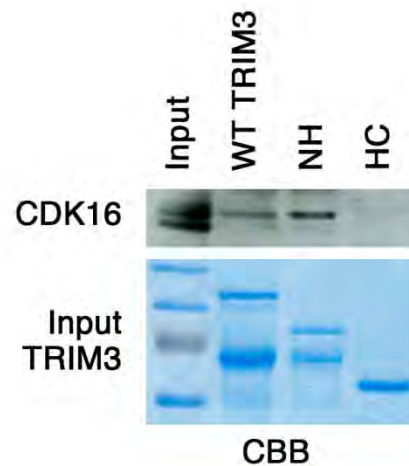


Figure 17: CDK16 binds to the N-terminus of TRIM3. (A) TRIM3 and CDK16 can associate in cells. HA-CDK16 and myc-TRIM3 were co-transfected into 293T cells. Lysates were prepared after 48 hours and co-immunoprecipitated with anti-CDK16 antibody. Associated proteins were immunoblotted as indicated. (B) CDK16 specifically binds to the N-terminal half of TRIM3 (NH mutant). GST-TRIM3 mutants were incubated in YH/J12 cell lysates with GLT-sepharose overnight. Associated proteins were re-purified, resolved on SDS-PAGE and immunoblotted with an anti-CDK16 antibody.

To establish that CDK16 can phosphorylate TRIM3, I performed kinase assays using both endogenous and recombinant CDK16. First, I immunoprecipitated endogenous CDK16 from YH/J12 lysates and asked whether these complexes could phosphorylate recombinant TRIM3. Indeed, I was able to detect phosphorylation (Fig. 18A). To confirm that CDK16 directly phosphorylates TRIM3, I used an entirely recombinant system. Recombinant CDK16 phosphorylated TRIM3 in a dose dependent manner (Fig. 18B), and was unable to phosphorylate the Hinge A mutant (Fig. 18C). Together, these data indicate that CDK16 is an N-terminally associated kinase that can phosphorylate the hinge region of TRIM3, a region important for its growth suppressive activity.

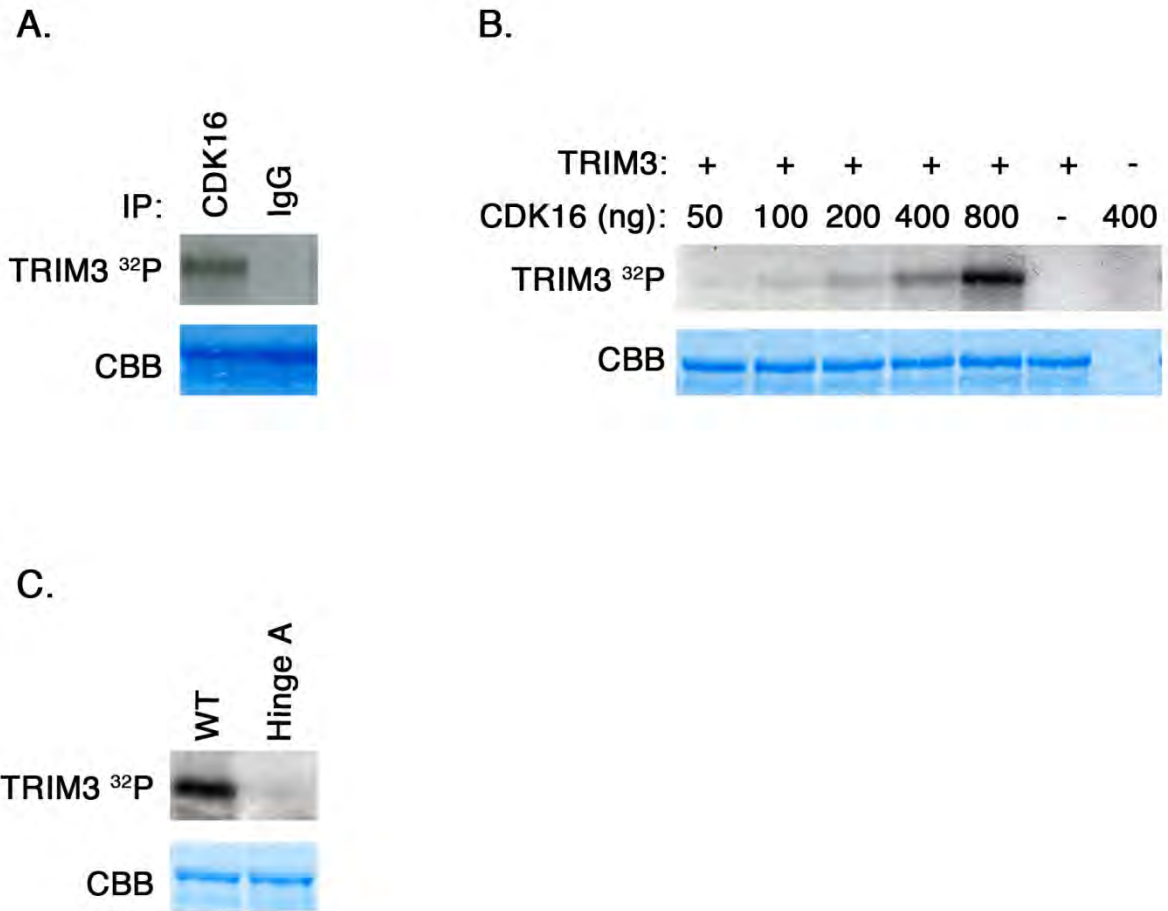


Figure 18: CDK16 is a TRIM3 hinge kinase in vitro. (A) Endogenous CDK16 can phosphorylate GST-TRIM3 in vitro. YH/J12 lysates were immunoprecipitated with an anti-CDK16 antibody and incubated with GST-TRIM3 and [γ -³²P]ATP for 30 mins at 37°C. Sample buffer was added to stop the reaction, and phosphorylation detected by autoradiography. (B) Recombinant CDK16 phosphorylates GST-TRIM3 in a dose-dependent manner in vitro. Recombinant CDK16 and GST-TRIM3 were incubated with [γ -³²P]ATP for 1h at 30C. Phosphorylation was detected by autoradiography. (C) Recombinant CDK16 phosphorylates GST-TRIM3 at the hinge region in vitro. Recombinant CDK16 and wildtype or Hinge A TRIM3 were incubated with [γ -³²P]ATP for 1h at 30C. Phosphorylation was detected by autoradiography.

5. CDK16 depletion suppresses growth

To further establish CDK16 as a biologically relevant TRIM3 kinase, I probed the relationship between CDK16 and growth suppression in cells. I generated two stable T98G cell lines harboring an shRNA against CDK16 (Fig. 19A). Compared to a stable T98G cell line harboring scrambled shRNA, shCDK16 cell lines incorporated 30-45% less EdU (Fig. 19B). This is consistent with the growth promoting role for CDK16.

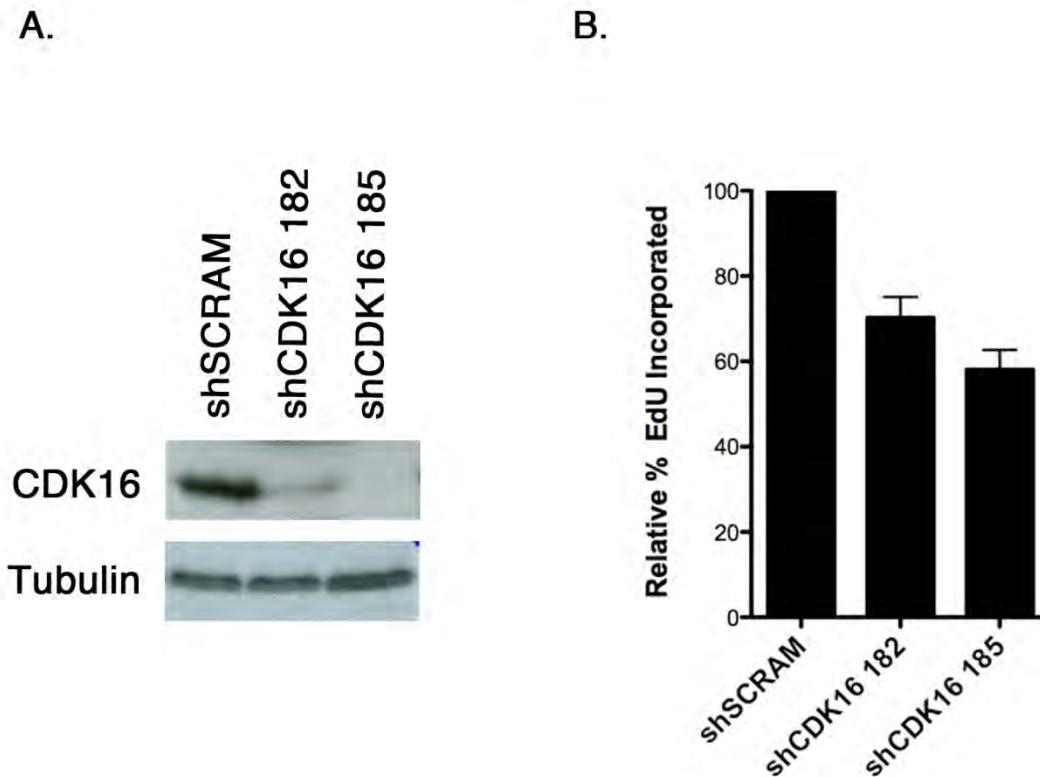


Figure 19: CDK16 depletion decreases cell growth. (A) Endogenous CDK16 levels are reduced in two stable T98G cell lines harboring shRNA against CDK16. Immunoblot of the indicated cell lysates using anti-CDK16 antibody. **(B)** CDK16 depletion decreases cell growth. The cell lines from (A) were pulse-labeled with EdU for 90mins, fixed, stained for EdU and analyzed by flow cytometry. EdU incorporation was normalized to shSCRAM. Error bars represent the SEM of three independent experiments.

III. Discussion

1. Summary

In this chapter I demonstrated that TRIM3 can be phosphorylated by N- and C-terminally associated kinases at its hinge region. By defining the TRIM3 interactome in a mouse glioma cell line, I identified one such kinase, CDK16, and showed that it is able to bind and phosphorylate the hinge region of TRIM3 specifically *in vitro*. Furthermore, as is expected for an inhibitory kinase, depletion of CDK16 reduced the growth of a human glioma cell line. Altogether, this establishes the regulation of a TRIM-NHL protein by phosphorylation, and suggests a growth-promoting role for CDK16 in gliomagenesis.

2. TRIM3 functions

Although there are less than 10 studies published on TRIM3, it has already been assigned roles in at least three different cellular processes. First, TRIM3 is involved in cellular trafficking. Interaction with the CART complex is necessary for this role, although it is possible TRIM3 affects trafficking through other mechanisms as well. Second, TRIM3 is a growth and tumor suppressor, partially through its ability to ubiquitinate the cell-cycle regulator p21. Finally, there is some evidence that TRIM3 is necessary for neuronal outgrowth and morphology, and it may play a role in differentiation. Biochemically the RING domain and the ubiquitination activity of TRIM3 are necessary for its roles in growth suppression and neuronal outgrowth.

Interestingly, unlike other TRIM-NHL family members, a RING independent role for TRIM3 in translational or miRNA regulation has not been noted. Whether this indicates

that TRIM3 has unique functionality, or this type of role has simply not been uncovered is currently unclear. Nevertheless, the TRIM3 interactome I identified by IP-mass spectrometry does not contain any miRISC or miRNA regulatory components. This suggests that perhaps TRIM3 is not involved in miRNA regulation.

3. CDK16 and TRIM3 in neuronal vesicular trafficking and as therapeutic targets

For the first time, this study suggests that targeting CDK16 (PCTAIRE1) in gliomas may be an effective therapeutic strategy. CDK16 depletion in T98G cells slows the growth of these cells, possibly by reducing TRIM3 phosphorylation and thereby increasing the growth suppressive activity of TRIM3. No CDK16-specific inhibitors exist, but as it is a kinase, developing such an inhibitor should be possible. Furthermore, CDK16 is involved in similar processes as TRIM3 and therefore may also play a role in tumorigenesis.

Although it is part of the cyclin-dependent kinase family, little is known about CDK16 and its related family members PCTAIRE2 and PCTAIRE3. It is a ubiquitously expressed serine/threonine kinase, and activity peaks during the S and G2 phases of the cell cycle (Charrasse et al, 1999). Unlike other members of the cdk family, CDK16 does not require another subunit for activity (Graeser et al, 2002), although recently one group has identified a membrane-associated protein, cyclin Y, that may activate CDK16 in the testis (Mikolcevic et al, 2012b). A conditional CDK16 knockout allele revealed that although CDK16 is not required for normal development, it is critical for spermatogenesis (Mikolcevic et al, 2012b). Like some TRIM-NHL family members, CDK16 is inherited asymmetrically during development (specifically, during

spermatogenesis), although whether this also occurs in neuron development is unknown (Besset et al, 1999; Rhee & Wolgemuth, 1995).

No relationship has been previously suggested between CDK16 and TRIM3. However, both play key roles in neurogenesis, possibly through the regulation of vesicular trafficking. A study of CDK16-like kinases in various species suggests that CDK16 may have evolved along with the nervous system, as only eumetazoa have CDK16 homologs (with the exception of insects such as *Drosophila*) (Mikolcevic et al, 2012a). This underscores the importance of CDK16 in neurons. Furthermore, CDK16 is necessary for neurite outgrowth and migration, perhaps by indirectly modulating actin polymerization (Fu et al; Mokalled et al). Note that TRIM3 is also necessary for neurite outgrowth and interacts with the actin cytoskeleton through alpha-actinin-4 and the CART complex.

It is possible that the roles of TRIM3 and CDK16 in neuron development are related to their roles in vesicular trafficking. The CDK16 *c.elegans* homolog PCT-1 is crucial in the directed trafficking of synaptic vesicles and proteins to axons (Ou et al, 2010), and mammalian CDK16 interacts with the COPII complex to direct secretory cargo transport (Palmer et al, 2005). In addition, CDK16 phosphorylates N-ethylmaleimide-sensitive fusion protein (NSF), a component of the SNAP-SNARE complex that is essential for membrane trafficking and fusion (Liu et al, 2006). Although TRIM3 has not been directly implicated in these complexes, it is known to localize to vesicles and direct vesicular trafficking through the CART complex. Intriguingly, the mass spectrometry TRIM3-

interactome contains several proteins known to interact with these complexes including NSF itself and COPB2, suggesting that CDK16 might regulate TRIM3 in these processes.

There are several lines of evidence that point towards functional interactions between CDK16 and TRIM3, and thereby may implicate CDK16 in tumor development. (1) This thesis found that CDK16 can phosphorylate TRIM3 at residues that regulate its growth suppressive activity. (2) Both proteins are involved in neuronal development and vesicular trafficking. (3) CDK16 and TRIM3 interact with the same or similar proteins important in these processes. (4) Depletion of CDK16 in T98G cells reduces growth. Despite this evidence, the potential role of CDK16 in tumor development will need to be verified in mouse models. Both CDK16 and TRIM3 knockout mice have recently been established (Cheung et al, 2010; Mikolcevic et al, 2012b), so there is a great opportunity to study the effect of these genes on tumorigenesis *in vivo*, both individually and cooperatively. The TRIM3 knockout mouse did not spontaneously develop tumors, yet shRNA depletion of TRIM3 accelerated tumor development in a PDGF-driven glioma mouse model (Liu et al, 2012). Therefore it may be necessary to cross these mice into various tumor models to truly understand the role of CDK16 and TRIM3 in tumorigenesis.

CHAPTER 5 IMPLICATIONS

I. Overview

In this thesis, I demonstrate for the first time that the growth suppressive activity of a TRIM-NHL family member is regulated by phosphorylation. In particular, I find that the growth inhibitory activity of TRIM3 is inhibited by growth-dependent multi-site phosphorylation. Multiple kinases can bind and phosphorylate TRIM3, and I focused on one of these, CDK16. I identify CDK16 as a novel TRIM3 interacting kinase that can phosphorylate it at the key sites important for activity. In a PDGF-driven glial cell line, CDK16 depletion decreases cell growth. Altogether, TRIM3 is a novel CDK16 substrate, and TRIM3 phosphorylation by CDK16 may inhibit its growth suppressive activity.

II. TRIM3 growth-regulated multi-site phosphorylation in a cellular context

How phosphorylation inhibits TRIM3 growth suppressive activity is still an open question. Perhaps it changes the structure of TRIM3 (see Discussion of Chapter 3), or perhaps phosphorylation marks TRIM3 for another function in the cell (see Introduction and Chapter 4 discussion for other TRIM3 functions). Phosphorylation is a common regulatory mechanism, and speculating on its potential effects yields a few interesting insights.

There are three ways that phosphorylation could switch TRIM3 function in a cellular context. Phosphorylation could affect (1) complex assembly (2) cellular localization or (3) directly affect activity such as ubiquitination. These mechanisms are not mutually exclusive, and distinct mechanisms could be important for different phosphorylation sites. Each will be discussed briefly below.

Phosphorylation could be specifically recognized by TRIM3 binding proteins, and thereby shift TRIM3 complex assembly. The nature of the TRIM3-containing complex could determine the process in which it functions. For example, phosphorylated TRIM3 could preferentially associate with the CART complex, thereby sequestering it away from p21 and/or other functions. To test this I overexpressed Hinge A and WT TRIM3 and co-immunoprecipitated alpha-actinin-4 and Myosin Va. I was not able to detect a difference in association (data not shown). Of course this does not rule out the possibility of variable

complex assembly, as overexpression could lead to forced binding, and phosphorylation could affect binding of other interacting proteins.

Phosphorylation could also affect TRIM3 cellular localization, thereby limiting the pool of available interacting proteins and TRIM3 function. In fact, there is some evidence that compartmentalization is important for the function of the entire TRIM family (Reymond et al, 2001). Intriguingly, one group reported two putative nuclear localization sequences (NLS) in the hinge region - one immediately adjacent to S437 and another encompassing S454, S455, Y457 and S458 (van Diepen et al, 2005). However, treating T98G cells overexpressing TRIM3 with the CRM1 nuclear export inhibitor did not result in significant TRIM3 nuclear accumulation (data not shown). As TRIM3 has no known nuclear functions, this NLS is still merely speculative.

Finally, phosphorylation could directly change TRIM3 activity, such as ubiquitination. This seems especially likely if phosphorylation affects the overall conformation of TRIM3 (See Discussion of Chapter 3). For example, p21 binds to the C-terminal WD40 domain of TRIM3, and may also require an intact filamin domain to bind (Raheja et al, 2012). However, ubiquitination activity requires the N-terminal ring domain. Therefore, orientation of these domains to each other could be critical for efficient E3 ligase activity.

Overall, which of these mechanisms account for the effect of phosphorylation on TRIM3 growth suppression is still unclear. It is also likely that TRIM3 growth suppression is regulated by additional mechanisms, such as the accessibility of downstream targets. For

example, the ubiquitination of p21 by TRIM3 accounts for at least some of its tumor suppressive activity (Liu et al, 2012; Raheja et al, 2012). Binding of p21 to cyclin D1-CDK4 stabilizes the complex and sequesters p21 away from TRIM3. Therefore, in this pathway, TRIM3 may simply not always be able to access p21 directly. Given the multiple functions of TRIM3 in the cell, as well as the evidence in this thesis that multiple kinases phosphorylate TRIM3, I favor a combination of mechanisms, some of which may be context-dependent.

III. The hinge region is intrinsically disordered

The regulation of disordered regions of proteins by phosphorylation is extremely common. Intriguingly, two independent algorithms that predict intrinsically disordered protein regions (FoldIndex and IUPred) specifically score the hinge region of TRIM3 as unstructured ((Dosztanyi et al, 2005; Prilusky et al, 2005), Fig. 20). Note that this disordered region entirely encompasses the seven hinge phosphorylation sites discussed in this thesis. All the mechanisms mentioned above, from structural changes between globular domains to changes in protein localization, are especially common for proteins with phosphorylation sites at disordered regions. A short discussion of intrinsically disordered proteins and parallel mechanisms is therefore provided below.

Intrinsically disordered proteins (IDPs) or proteins with large unstructured regions compose at least one-third of all eukaryotic proteins. They are evolutionarily advantageous, and less common in prokaryotes, possibly because of the greater need to regulate signaling in eukaryotes (Dunker et al, 2000; Dunker et al, 2008). Several

characteristics make disordered regions perfectly suited for the coordination of signaling within the cell. They are (1) flexible, (2) largely solvent exposed and therefore available for protein-protein interactions and post-translational modifications, and (3) able to fold and unfold upon post-translational modification, thereby mediating signaling.

IDP functional importance is underscored by their tight regulation and deregulation in disease, especially cancer (Uversky et al, 2009). Overall, on a proteome-wide level, the activity and protein levels of IDPs are more tightly regulated than structured proteins (Gsponer et al, 2008). This could be because deregulation of disordered proteins is often related to human disease. Strikingly, cancer-associated and signaling proteins are significantly enriched in unstructured regions as compared to all eukaryotic proteins (Iakoucheva et al, 2002).

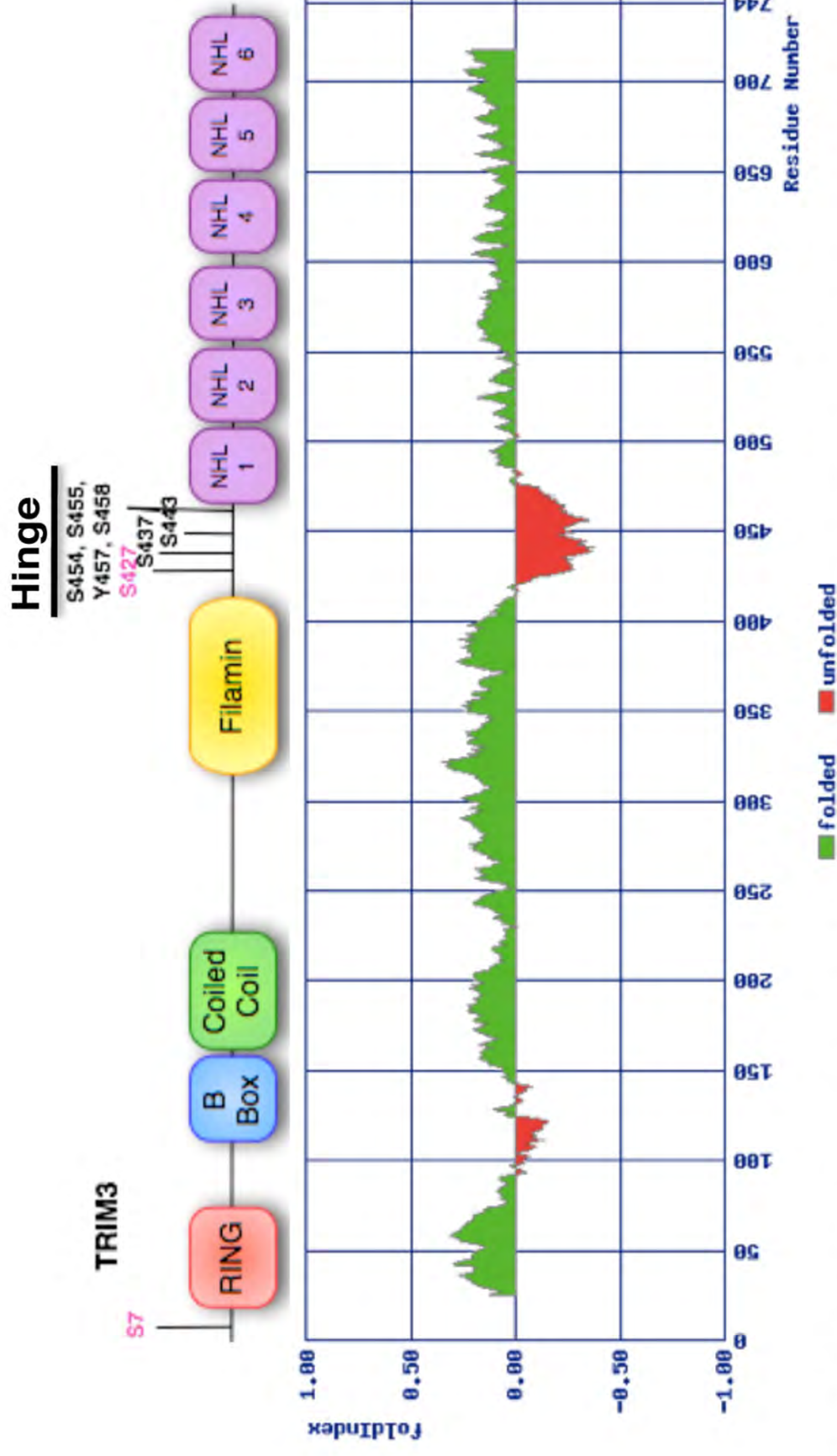


Figure 20: The hinge region of TRIM3 is disordered. FoldIndex was used to predict the disorder of TRIM3 (Prilusky et al, 2005). The FoldIndex score is plotted. Positive scores (green) indicate structured regions of the protein, and negative scores (red) indicate unstructured regions of the protein. A diagram of TRIM3 domain structure is aligned above the plot.

The regulation of IDPs is often achieved through post-translational modification. Some evidence suggests that phosphorylation may even occur predominantly in intrinsically disordered protein regions (Iakoucheva et al, 2004). This is definitely the case for TRIM3, where all seven phosphorylation sites studied in this thesis are located in the disordered region of the protein. One study found a significant preference for unstructured kinase substrates - 51% of all kinase substrates were classified as unstructured, whereas only 19% were highly structured (even though each category contained roughly equal numbers of proteins) (Gsponer et al, 2008). This is not surprising, as disordered segments are readily exposed to solvent and available to mediate protein-protein interactions with both kinases as well as proteins that interact specifically with phosphorylated sites.

Furthermore, it is common for PTM sites to be clustered within disordered regions. This is exactly the pattern that this thesis describes for TRIM3, with seven phosphorylation sites a mere 30 residues apart in the unstructured “hinge” region. Another well-studied example is p27; phosphorylation and ubiquitination of this highly unstructured protein alter its function, localization and activities under different cellular conditions, while its unstructured nature facilitates promiscuous binding to various cyclin-cdk complexes (reviewed in (Follis et al, 2012)). Whether individual TRIM3 phosphorylation sites are regulated and specifically affect TRIM3 function in such a way remains an open question.

IDPs are on average substrates of twice as many kinases as structured proteins (Gsponer et al, 2008). This is consistent with data in this thesis indicating that TRIM3 can be phosphorylated by multiple kinases. Although this thesis focused on one kinase, the TRIM3 associated kinase assay as well as the kinases found by mass spectrometry in the TRIM3 interactome together demonstrate that multiple kinases can bind to both the N- and C- terminus of TRIM3 and phosphorylate residues in the unstructured hinge region. In addition, kinases that regulate disordered proteins are often cell-cycle, growth or stress-regulated (Gsponer et al, 2008). It is possible that growth and stress signals regulate the activity of these kinases upstream, thereby altering TRIM3 phosphorylation state and function. Whether the hinge phosphorylation sites act in concert or each modulate specific interactions or localization signals is still unclear.

Pairing flexible regions with modular protein domains can empower proteins to act as signaling conduits. One well-studied example of such a protein is p53. P53 is a modular protein, with structured DNA binding and tetramerization domains, but disordered regulatory elements at the C- and N-terminus (Ayed et al, 2001; Joerger & Fersht, 2010). The unstructured nature of these ends facilitates promiscuous binding and thereby the plethora of p53 functions ranging from transcriptional regulation to apoptosis to DNA repair. Switching between these functions is largely mediated by post-translational modification. Here again the unstructured elements contain the majority of sites for posttranslational modification and bind to the proteins that regulate p53 function, localization and degradation (Bode & Dong, 2004).

It is tempting to speculate that TRIM3 function is regulated in a similar way. The flexible, solvent-exposed hinge region is the ideal receptor for this type of regulation. It is ready to bind and receive signals from multiple kinases, activated by different signaling cascades upstream. Some of these, such as CDK16, are growth regulated. This clustered multi-site phosphorylation could then affect TRIM3 structure, complex association, localization and/or ubiquitination activity. This model places the TRIM3 hinge at the center of activity, a pattern seen throughout eukaryotes for cancer-associated proteins with disordered regions.

IV. Relevance to TRIM-NHL family, and TRIMs at large

What regulates the ability to switch from one function to another is an open question for this entire class of TRIM-NHL proteins. This class of proteins can act as E3 ubiquitin ligases and/or translation repressors through the miRNA pathway in a multitude of processes including differentiation, cell growth suppression, vesicular trafficking and apoptosis. This thesis is the first to study post-translational modifications of any TRIM-NHL family member.

Two lines of evidence suggest that multi-site phosphorylation may be a common regulatory element for this family. (1) The unstructured nature of the region immediately N-terminal of the beta-propeller domain is a conserved element throughout much of the TRIM-NHL family. (2) Proteome-wide mass spectrometry studies have found phosphorylation sites in this same region for several members of this family. In particular, the PhosphoSitePlus database lists similar multi-site phosphorylation adjacent

to the NHL domains for both TRIM2 and TRIM32 (Hornbeck et al). In addition, a phosphoproteomic mass spectrometry study of *Drosophila* found Brat phosphorylation in this region (Bodenmiller et al, 2008). The same is true for the N-terminal S7 residue - There are seven additional TRIM family members in the PhosphoSitePlus database with phosphorylation sites near the N-terminus, and the function of these sites has never been elucidated (TRIM2, TRIM19 (PML), TRIM29, TRIM32, TRIM35, TRIM56) (Hornbeck et al). Of course it is intriguing to speculate that the function of these sites is conserved, and that this thesis has begun to uncover a regulatory mechanism that is relevant for this entire class of proteins. However, whether these phosphorylation events affect protein function at all, and in which way, will require further biochemical and cell biological studies.

REFERENCES

- Arama E, Dickman D, Kimchie Z, Shearn A, Lev Z (2000) Mutations in the beta-propeller domain of the Drosophila brain tumor (brat) protein induce neoplasm in the larval brain. *Oncogene* **19**(33): 3706-3716
- Ayed A, Mulder FA, Yi GS, Lu Y, Kay LE, Arrowsmith CH (2001) Latent and active p53 are identical in conformation. *Nat Struct Biol* **8**(9): 756-760
- Bae DS, Cho SB, Kim YJ, Whang JD, Song SY, Park CS, Kim DS, Lee JH (2001) Aberrant expression of cyclin D1 is associated with poor prognosis in early stage cervical cancer of the uterus. *Gynecol Oncol* **81**(3): 341-347
- Balastik M, Ferraguti F, Pires-da Silva A, Lee TH, Alvarez-Bolado G, Lu KP, Gruss P (2008) Deficiency in ubiquitin ligase TRIM2 causes accumulation of neurofilament light chain and neurodegeneration. *Proc Natl Acad Sci USA* **105**(33): 12016-12021
- Bernardi R, Papa A, Pandolfi PP (2008) Regulation of apoptosis by PML and the PML-NBs. *Oncogene* **27**(48): 6299-6312
- Besset V, Rhee K, Wolgemuth DJ (1999) The cellular distribution and kinase activity of the Cdk family member Pctaire1 in the adult mouse brain and testis suggest functions in differentiation. *Cell Growth Differ* **10**(3): 173-181
- Besson A, Dowdy SF, Roberts JM (2008) CDK inhibitors: cell cycle regulators and beyond. *Dev Cell* **14**(2): 159-169
- Betschinger J, Mechtler K, Knoblich JA (2006) Asymmetric segregation of the tumor suppressor brat regulates self-renewal in Drosophila neural stem cells. *Cell* **124**(6): 1241-1253
- Bode AM, Dong Z (2004) Post-translational modification of p53 in tumorigenesis. *Nat Rev Cancer* **4**(10): 793-805
- Bodenmiller B, Campbell D, Gerrits B, Lam H, Jovanovic M, Picotti P, Schlapbach R, Aebersold R (2008) PhosphoPep--a database of protein phosphorylation sites in model organisms. *Nat Biotechnol* **26**(12): 1339-1340
- Bodine SC, Latres E, Baumhueter S, Lai VK, Nunez L, Clarke BA, Poueymirou WT, Panaro FJ, Na E, Dharmarajan K, Pan ZQ, Valenzuela DM, DeChiara TM, Stitt TN, Yancopoulos GD, Glass DJ (2001) Identification of ubiquitin ligases required for skeletal muscle atrophy. *Science* **294**(5547): 1704-1708
- Boulay J-L, Stiefel U, Taylor E, Dolder B, Merlo A, Hirth F (2009) Loss of heterozygosity of TRIM3 in malignant gliomas. *BMC Cancer* **9**: 71

- Bowman SK, Rolland V, Betschinger J, Kinsey KA, Emery G, Knoblich JA (2008) The tumor suppressors Brat and Numb regulate transit-amplifying neuroblast lineages in *Drosophila*. *Dev Cell* **14**(4): 535-546
- Brennan C, Momota H, Hambardzumyan D, Ozawa T, Tandon A, Pedraza A, Holland E (2009) Glioblastoma subclasses can be defined by activity among signal transduction pathways and associated genomic alterations. *PLoS One* **4**(11): e7752
- Brown VD, Phillips RA, Gallie BL (1999) Cumulative effect of phosphorylation of pRB on regulation of E2F activity. *Mol Cell Biol* **19**(5): 3246-3256
- Burke JR, Hura GL, Rubin SM (2012) Structures of inactive retinoblastoma protein reveal multiple mechanisms for cell cycle control. *Genes Dev* **26**(11): 1156-1166
- Caussinus E, Gonzalez C (2005) Induction of tumor growth by altered stem-cell asymmetric division in *Drosophila melanogaster*. *Nat Genet* **37**(10): 1125-1129
- CBTRUS. (2012) CBTRUS Statistical Report: Primary Brain and Central Nervous System Tumors Diagnosed in the United States in 2004-2008 (March 23, 2012 Revision). Central Brain Tumor Registry of the United States.
- Chang HM, Martinez NJ, Thornton JE, Hagan JP, Nguyen KD, Gregory RI (2012) Trim71 cooperates with microRNAs to repress Cdkn1a expression and promote embryonic stem cell proliferation. *Nat Commun* **3**: 923
- Chao C, Herr D, Chun J, Xu Y (2006) Ser18 and 23 phosphorylation is required for p53-dependent apoptosis and tumor suppression. *EMBO J* **25**(11): 2615-2622
- Charrasse S, Carena I, Hagmann J, Woods-Cook K, Ferrari S (1999) PCTAIRE-1: characterization, subcellular distribution, and cell cycle-dependent kinase activity. *Cell Growth Differ* **10**(9): 611-620
- Chen J, McKay RM, Parada LF (2012) Malignant glioma: lessons from genomics, mouse models, and stem cells. *Cell* **149**(1): 36-47
- Cheung CC, Yang C, Berger T, Zaugg K, Reilly P, Elia AJ, Wakeham A, You-Ten A, Chang N, Li L, Wan Q, Mak TW (2010) Identification of BERP (brain-expressed RING finger protein) as a p53 target gene that modulates seizure susceptibility through interacting with GABA(A) receptors. *Proc Natl Acad Sci U S A* **107**(26): 11883-11888
- Chu IM, Hengst L, Slingerland JM (2008) The Cdk inhibitor p27 in human cancer: prognostic potential and relevance to anticancer therapy. *Nat Rev Cancer* **8**(4): 253-267
- Connor MK, Kotchetkov R, Cariou S, Resch A, Lupetti R, Beniston RG, Melchior F, Hengst L, Slingerland JM (2003) CRM1/Ran-mediated nuclear export of p27(Kip1)

involves a nuclear export signal and links p27 export and proteolysis. *Mol Biol Cell* **14**(1): 201-213

Dai C, Celestino JC, Okada Y, Louis DN, Fuller GN, Holland EC (2001) PDGF autocrine stimulation dedifferentiates cultured astrocytes and induces oligodendrogliomas and oligoastrocytomas from neural progenitors and astrocytes in vivo. *Genes Dev* **15**(15): 1913-1925

Dai C, Gu W (2010) p53 post-translational modification: deregulated in tumorigenesis. *Trends Mol Med* **16**(11): 528-536

Dosztanyi Z, Csizmok V, Tompa P, Simon I (2005) IUPred: web server for the prediction of intrinsically unstructured regions of proteins based on estimated energy content. *Bioinformatics* **21**(16): 3433-3434

Dumaz N, Milne DM, Meek DW (1999) Protein kinase CK1 is a p53-threonine 18 kinase which requires prior phosphorylation of serine 15. *FEBS Lett* **463**(3): 312-316

Dunker AK, Obradovic Z, Romero P, Garner EC, Brown CJ (2000) Intrinsic protein disorder in complete genomes. *Genome Inform Ser Workshop Genome Inform* **11**: 161-171

Dunker AK, Oldfield CJ, Meng J, Romero P, Yang JY, Chen JW, Vacic V, Obradovic Z, Uversky VN (2008) The unfoldomics decade: an update on intrinsically disordered proteins. *BMC Genomics* **9 Suppl 2**: S1

Edwards TA, Wilkinson BD, Wharton RP, Aggarwal AK (2003) Model of the brain tumor-Pumilio translation repressor complex. *Genes Dev* **17**(20): 2508-2513

El-Husseini AE, Fretier P, Vincent SR (2001) Cloning and characterization of a gene (RNF22) encoding a novel brain expressed ring finger protein (BERP) that maps to human chromosome 11p15.5. *Genomics* **71**(3): 363-367

El-Husseini AE, Kwasnicka D, Yamada T, Hirohashi S, Vincent SR (2000) BERP, a novel ring finger protein, binds to alpha-actinin-4. *Biochem Biophys Res Commun* **267**(3): 906-911

El-Husseini AE, Vincent SR (1999) Cloning and characterization of a novel RING finger protein that interacts with class V myosins. *J Biol Chem* **274**(28): 19771-19777

Erdjument-Bromage H, Lui M, Lacomis L, Grewal A, Annan RS, McNulty DE, Carr SA, Tempst P (1998) Examination of micro-tip reversed-phase liquid chromatographic extraction of peptide pools for mass spectrometric analysis. *J Chromatogr A* **826**(2): 167-181

- Follis AV, Galea CA, Kriwacki RW (2012) Intrinsic protein flexibility in regulation of cell proliferation: advantages for signaling and opportunities for novel therapeutics. *Adv Exp Med Biol* **725**: 27-49
- Foster KG, Acosta-Jaquez HA, Romeo Y, Ekim B, Soliman GA, Carriere A, Roux PP, Ballif BA, Fingar DC (2010) Regulation of mTOR complex 1 (mTORC1) by raptor Ser863 and multisite phosphorylation. *J Biol Chem* **285**(1): 80-94
- Freije WA, Castro-Vargas FE, Fang Z, Horvath S, Cloughesy T, Liao LM, Mischel PS, Nelson SF (2004) Gene expression profiling of gliomas strongly predicts survival. *Cancer Res* **64**(18): 6503-6510
- Fu WY, Cheng K, Fu AK, Ip NY Cyclin-dependent kinase 5-dependent phosphorylation of Pctaire1 regulates dendrite development. *Neuroscience* **180**: 353-359
- Graeser R, Gannon J, Poon RY, Dubois T, Aitken A, Hunt T (2002) Regulation of the CDK-related protein kinase PCTAIRE-1 and its possible role in neurite outgrowth in Neuro-2A cells. *J Cell Sci* **115**(Pt 17): 3479-3490
- Gravendeel LA, Kouwenhoven MC, Gevaert O, de Rooi JJ, Stubbs AP, Duijm JE, Daemen A, Bleeker FE, Bralten LB, Kloosterhof NK, De Moor B, Eilers PH, van der Spek PJ, Kros JM, Sillevius Smitt PA, van den Bent MJ, French PJ (2009) Intrinsic gene expression profiles of gliomas are a better predictor of survival than histology. *Cancer Res* **69**(23): 9065-9072
- Grimmler M, Wang Y, Mund T, Cilensek Z, Keidel EM, Waddell MB, Jakel H, Kullmann M, Kriwacki RW, Hengst L (2007) Cdk-inhibitory activity and stability of p27Kip1 are directly regulated by oncogenic tyrosine kinases. *Cell* **128**(2): 269-280
- Gsponer J, Futschik ME, Teichmann SA, Babu MM (2008) Tight regulation of unstructured proteins: from transcript synthesis to protein degradation. *Science* **322**(5906): 1365-1368
- Hammell CM, Lubin I, Boag PR, Blackwell TK, Ambros V (2009) nhl-2 Modulates microRNA activity in *Caenorhabditis elegans*. *Cell* **136**(5): 926-938
- Hatakeyama S (2011) TRIM proteins and cancer. *Nat Rev Cancer* **11**(11): 792-804
- Heilmann AM, Dyson NJ (2012) Phosphorylation puts the pRb tumor suppressor into shape. *Genes Dev* **26**(11): 1128-1130
- Horn EJ, Albor A, Liu Y, El-Hizawi S, Vanderbeek GE, Babcock M, Bowden GT, Hennings H, Lozano G, Weinberg WC, Kulesz-Martin M (2004) RING protein Trim32 associated with skin carcinogenesis has anti-apoptotic and E3-ubiquitin ligase properties. *Carcinogenesis* **25**(2): 157-167

Hornbeck PV, Kornhauser JM, Tkachev S, Zhang B, Skrzypek E, Murray B, Latham V, Sullivan M PhosphoSitePlus: a comprehensive resource for investigating the structure and function of experimentally determined post-translational modifications in man and mouse. *Nucleic Acids Res* **40**(Database issue): D261-270

Hukkelhoven E, Liu Y, Yeh N, Ciznadija D, Blain SW, Koff A (2012) Tyrosine Phosphorylation of the p21 Cyclin-dependent Kinase Inhibitor Facilitates the Development of Proneural Glioma. *J Biol Chem* **287**(46): 38523-38530

Hung AY, Sung CC, Brito IL, Sheng M (2010) Degradation of postsynaptic scaffold GKAP and regulation of dendritic spine morphology by the TRIM3 ubiquitin ligase in rat hippocampal neurons. *PLoS One* **5**(3): e9842

Hyenne V, Desrosiers M, Labbe JC (2008) *C. elegans* Brat homologs regulate PAR protein-dependent polarity and asymmetric cell division. *Dev Biol* **321**(2): 368-378

Iakoucheva LM, Brown CJ, Lawson JD, Obradovic Z, Dunker AK (2002) Intrinsic disorder in cell-signaling and cancer-associated proteins. *J Mol Biol* **323**(3): 573-584

Iakoucheva LM, Radivojac P, Brown CJ, O'Connor TR, Sikes JG, Obradovic Z, Dunker AK (2004) The importance of intrinsic disorder for protein phosphorylation. *Nucleic Acids Res* **32**(3): 1037-1049

Joerger AC, Fersht AR (2010) The tumor suppressor p53: from structures to drug discovery. *Cold Spring Harb Perspect Biol* **2**(6): a000919

Khazaei MR, Bunk EC, Hillje AL, Jahn HM, Riegler EM, Knoblich JA, Young P, Schwamborn JC (2011) The E3-ubiquitin ligase TRIM2 regulates neuronal polarization. *J Neurochem* **117**(1): 29-37

Kohlmaier A, Edgar BA (2008) Proliferative control in *Drosophila* stem cells. *Curr Opin Cell Biol* **20**(6): 699-706

Koivomagi M, Valk E, Venta R, Iofik A, Lepiku M, Balog ER, Rubin SM, Morgan DO, Loog M (2011) Cascades of multisite phosphorylation control Sic1 destruction at the onset of S phase. *Nature* **480**(7375): 128-131

Kruse JP, Gu W (2009) Modes of p53 regulation. *Cell* **137**(4): 609-622

Kudryashova E, Wu J, Havton LA, Spencer MJ (2009) Deficiency of the E3 ubiquitin ligase TRIM32 in mice leads to a myopathy with a neurogenic component. *Hum Mol Genet* **18**(7): 1353-1367

Lapenna S, Giordano A (2009) Cell cycle kinases as therapeutic targets for cancer. *Nat Rev Drug Discov* **8**(7): 547-566

- Lee C-Y, Wilkinson BD, Siegrist SE, Wharton RP, Doe CQ (2006) Brat is a Miranda cargo protein that promotes neuronal differentiation and inhibits neuroblast self-renewal. *Dev Cell* **10**(4): 441-449
- Liang Y, Diehn M, Watson N, Bollen AW, Aldape KD, Nicholas MK, Lamborn KR, Berger MS, Botstein D, Brown PO, Israel MA (2005) Gene expression profiling reveals molecularly and clinically distinct subtypes of glioblastoma multiforme. *Proc Natl Acad Sci U S A* **102**(16): 5814-5819
- Lin YC, Hsieh LC, Kuo MW, Yu J, Kuo HH, Lo WL, Lin RJ, Yu AL, Li WH (2007) Human TRIM71 and its nematode homologue are targets of let-7 microRNA and its zebrafish orthologue is essential for development. *Mol Biol Evol* **24**(11): 2525-2534
- Linding R, Jensen LJ, Ostheimer GJ, van Vugt MA, Jorgensen C, Miron IM, Diella F, Colwill K, Taylor L, Elder K, Metalnikov P, Nguyen V, Pasculescu A, Jin J, Park JG, Samson LD, Woodgett JR, Russell RB, Bork P, Yaffe MB, Pawson T (2007) Systematic discovery of in vivo phosphorylation networks. *Cell* **129**(7): 1415-1426
- Liu Y, Cheng K, Gong K, Fu AK, Ip NY (2006) Pctaire1 phosphorylates N-ethylmaleimide-sensitive fusion protein: implications in the regulation of its hexamerization and exocytosis. *J Biol Chem* **281**(15): 9852-9858
- Liu Y, Raheja R, Yeh N, Ciznadija D, Pedraza A, Ozawa T, Hukkelhoven E, Erdjument-Bromage H, Tempst P, Gauthier N, Brennan C, Holland E, Koff A (2012) TRIM3, a tumor suppressor linked to regulation of p21Waf1/Cip1. *Oncogene* **In Press**
- Liu Y, Yeh N, Zhu X-H, Leversha M, Cordon-Cardo C, Ghossein R, Singh B, Holland E, Koff A (2007) Somatic cell type specific gene transfer reveals a tumor-promoting function for p21(Waf1/Cip1). *EMBO J* **26**(22): 4683-4693
- Loop T, Leemans R, Stiefel U, Hermida L, Egger B, Xie F, Primig M, Certa U, Fischbach K-F, Reichert H, Hirth F (2004) Transcriptional signature of an adult brain tumor in Drosophila. *BMC Genomics* **5**(1): 24
- Louis DN, Ohgaki H, Wiestler OD, Cavenee WK, Burger PC, Jouvet A, Scheithauer BW, Kleihues P (2007) The 2007 WHO classification of tumours of the central nervous system. *Acta Neuropathol* **114**(2): 97-109
- Maller Schulman BR, Liang X, Stahlhut C, DelConte C, Stefani G, Slack FJ (2008) The let-7 microRNA target gene, Mlin41/Trim71 is required for mouse embryonic survival and neural tube closure. *Cell Cycle* **7**(24): 3935-3942
- Meroni G, Diez-Roux G (2005) TRIM/RBCC, a novel class of 'single protein RING finger' E3 ubiquitin ligases. *Bioessays* **27**(11): 1147-1157

- Mikolcevic P, Rainer J, Geley S (2012a) Orphan kinases turn eccentric: A new class of cyclin Y-activated, membrane-targeted CDKs. *Cell Cycle* **11**(20): 3758-3768
- Mikolcevic P, Sigl R, Rauch V, Hess MW, Pfaller K, Barisic M, Pelliniemi LJ, Boesl M, Geley S (2012b) Cyclin-dependent kinase 16/PCTAIRE kinase 1 is activated by cyclin Y and is essential for spermatogenesis. *Mol Cell Biol* **32**(4): 868-879
- Mokalled MH, Johnson A, Kim Y, Oh J, Olson EN Myocardin-related transcription factors regulate the Cdk5/Pctaire1 kinase cascade to control neurite outgrowth, neuronal migration and brain development. *Development* **137**(14): 2365-2374
- Mosesson Y, Chetrit D, Schley L, Berghoff J, Ziv T, Carvalho S, Milanezi F, Admon A, Schmitt F, Ehrlich M, Yarden Y (2009) Monoubiquitylation regulates endosomal localization of Lst2, a negative regulator of EGF receptor signaling. *Dev Cell* **16**(5): 687-698
- Nisole S, Stoye JP, Saïb A (2005) TRIM family proteins: retroviral restriction and antiviral defence. *Nat Rev Microbiol* **3**(10): 799-808
- Ott RD, Rehfuess C, Podust VN, Clark JE, Fanning E (2002) Role of the p68 subunit of human DNA polymerase alpha-primase in simian virus 40 DNA replication. *Mol Cell Biol* **22**(16): 5669-5678
- Ou CY, Poon VY, Maeder CI, Watanabe S, Lehrman EK, Fu AK, Park M, Fu WY, Jorgensen EM, Ip NY, Shen K (2010) Two cyclin-dependent kinase pathways are essential for polarized trafficking of presynaptic components. *Cell* **141**(5): 846-858
- Ozato K, Shin DM, Chang TH, Morse HC, 3rd (2008) TRIM family proteins and their emerging roles in innate immunity. *Nat Rev Immunol* **8**(11): 849-860
- Palmer KJ, Konkel JE, Stephens DJ (2005) PCTAIRE protein kinases interact directly with the COPII complex and modulate secretory cargo transport. *J Cell Sci* **118**(Pt 17): 3839-3847
- Parsons DW, Jones S, Zhang X, Lin JC, Leary RJ, Angenendt P, Mankoo P, Carter H, Siu IM, Gallia GL, Olivi A, McLendon R, Rasheed BA, Keir S, Nikolskaya T, Nikolsky Y, Busam DA, Tekleab H, Diaz LA, Jr., Hartigan J, Smith DR, Strausberg RL, Marie SK, Shinjo SM, Yan H, Riggins GJ, Bigner DD, Karchin R, Papadopoulos N, Parmigiani G, Vogelstein B, Velculescu VE, Kinzler KW (2008) An integrated genomic analysis of human glioblastoma multiforme. *Science* **321**(5897): 1807-1812
- Poznic M (2009) Retinoblastoma protein: a central processing unit. *J Biosci* **34**(2): 305-312

- Prilusky J, Felder CE, Zeev-Ben-Mordehai T, Rydberg EH, Man O, Beckmann JS, Silman I, Sussman JL (2005) FoldIndex: a simple tool to predict whether a given protein sequence is intrinsically unfolded. *Bioinformatics* **21**(16): 3435-3438
- Raheja R, Liu Y, Hukkelhoven E, Yeh N, Koff A. (2012) TRIM3, an E3 ligase controlling p21 levels. Memorial Sloan Kettering Cancer Center.
- Reichert H (2011) Drosophila neural stem cells: cell cycle control of self-renewal, differentiation, and termination in brain development. *Results Probl Cell Differ* **53**: 529-546
- Reymond A, Meroni G, Fantozzi A, Merla G, Cairo S, Luzi L, Riganelli D, Zanaria E, Messali S, Cainarca S, Guffanti A, Minucci S, Pelicci PG, Ballabio A (2001) The tripartite motif family identifies cell compartments. *EMBO J* **20**(9): 2140-2151
- Rhee K, Wolgemuth DJ (1995) Cdk family genes are expressed not only in dividing but also in terminally differentiated mouse germ cells, suggesting their possible function during both cell division and differentiation. *Dev Dyn* **204**(4): 406-420
- Roy A, Kucukural A, Zhang Y I-TASSER: a unified platform for automated protein structure and function prediction. *Nat Protoc* **5**(4): 725-738
- Sardiello M, Cairo S, Fontanella B, Ballabio A, Meroni G (2008) Genomic analysis of the TRIM family reveals two groups of genes with distinct evolutionary properties. *BMC Evol Biol* **8**: 225
- Schwamborn JC, Berezikov E, Knoblich JA (2009) The TRIM-NHL protein TRIM32 activates microRNAs and prevents self-renewal in mouse neural progenitors. *Cell* **136**(5): 913-925
- Sebastian Winkler G, Lacomis L, Philip J, Erdjument-Bromage H, Svejstrup JQ, Tempst P (2002) Isolation and mass spectrometry of transcription factor complexes. *Methods* **26**(3): 260-269
- Serres MP, Zlotek-Zlotkiewicz E, Concha C, Gurian-West M, Daburon V, Roberts JM, Besson A (2011) Cytoplasmic p27 is oncogenic and cooperates with Ras both in vivo and in vitro. *Oncogene* **30**(25): 2846-2858
- Shyu H-W, Hsu S-H, Hsieh-Li H-M, Li H (2003) Forced expression of RNF36 induces cell apoptosis. *Exp Cell Res* **287**(2): 301-313
- Sluss HK, Armata H, Gallant J, Jones SN (2004) Phosphorylation of serine 18 regulates distinct p53 functions in mice. *Mol Cell Biol* **24**(3): 976-984
- TCGA (2008) Comprehensive genomic characterization defines human glioblastoma genes and core pathways. *Nature* **455**(7216): 1061-1068

Thomson M, Gunawardena J (2009) Unlimited multistability in multisite phosphorylation systems. *Nature* **460**(7252): 274-277

Toledo F, Wahl GM (2006) Regulating the p53 pathway: in vitro hypotheses, in vivo veritas. *Nat Rev Cancer* **6**(12): 909-923

Tsvetkov LM, Yeh KH, Lee SJ, Sun H, Zhang H (1999) p27(Kip1) ubiquitination and degradation is regulated by the SCF(Skp2) complex through phosphorylated Thr187 in p27. *Curr Biol* **9**(12): 661-664

Uchil PD, Quinlan BD, Chan W-T, Luna JM, Mothes W (2008) TRIM E3 ligases interfere with early and late stages of the retroviral life cycle. *PLoS Pathog* **4**(2): e16

Uversky VN, Oldfield CJ, Midic U, Xie H, Xue B, Vucetic S, Iakoucheva LM, Obradovic Z, Dunker AK (2009) Unfoldomics of human diseases: linking protein intrinsic disorder with diseases. *BMC Genomics* **10 Suppl 1**: S7

van Diepen MT, Spencer GE, van Minnen J, Gouwenberg Y, Bouwman J, Smit AB, van Kesteren RE (2005) The molluscan RING-finger protein L-TRIM is essential for neuronal outgrowth. *Mol Cell Neurosci* **29**(1): 74-81

Verhaak RG, Hoadley KA, Purdom E, Wang V, Qi Y, Wilkerson MD, Miller CR, Ding L, Golub T, Mesirov JP, Alexe G, Lawrence M, O'Kelly M, Tamayo P, Weir BA, Gabriel S, Winckler W, Gupta S, Jakkula L, Feiler HS, Hodgson JG, James CD, Sarkaria JN, Brennan C, Kahn A, Spellman PT, Wilson RK, Speed TP, Gray JW, Meyerson M, Getz G, Perou CM, Hayes DN (2010) Integrated genomic analysis identifies clinically relevant subtypes of glioblastoma characterized by abnormalities in PDGFRA, IDH1, EGFR, and NF1. *Cancer Cell* **17**(1): 98-110

Vitucci M, Hayes DN, Miller CR (2011) Gene expression profiling of gliomas: merging genomic and histopathological classification for personalised therapy. *Br J Cancer* **104**(4): 545-553

Voitenleitner C, Rehfuess C, Hilmes M, O'Rear L, Liao PC, Gage DA, Ott R, Nasheuer HP, Fanning E (1999) Cell cycle-dependent regulation of human DNA polymerase alpha-primase activity by phosphorylation. *Mol Cell Biol* **19**(1): 646-656

Watanabe N, Arai H, Iwasaki J, Shiina M, Ogata K, Hunter T, Osada H (2005) Cyclin-dependent kinase (CDK) phosphorylation destabilizes somatic Wee1 via multiple pathways. *Proc Natl Acad Sci U S A* **102**(33): 11663-11668

Wu Z, Earle J, Saito S, Anderson CW, Appella E, Xu Y (2002) Mutation of mouse p53 Ser23 and the response to DNA damage. *Mol Cell Biol* **22**(8): 2441-2449

Wulczyn FG, Cuevas E, Franzoni E, Rybak A (2011) miRNAs Need a Trim : Regulation of miRNA Activity by Trim-NHL Proteins. *Adv Exp Med Biol* **700**: 85-105

Xue Y, Ren J, Gao X, Jin C, Wen L, Yao X (2008) GPS 2.0, a tool to predict kinase-specific phosphorylation sites in hierarchy. *Mol Cell Proteomics* **7**(9): 1598-1608

Yan Q, Sun W, Kujala P, Lotfi Y, Vida TA, Bean AJ (2005) CART: an Hrs/actinin-4/BERP/myosin V protein complex required for efficient receptor recycling. *Mol Biol Cell* **16**(5): 2470-2482

Zhang Y, Xiong Y (2001) A p53 amino-terminal nuclear export signal inhibited by DNA damage-induced phosphorylation. *Science* **292**(5523): 1910-1915

Zhou B, Arnett DR, Yu X, Brewster A, Sowd GA, Xie CL, Vila S, Gai D, Fanning E, Chen XS (2012) Structural basis for the interaction of a hexameric replicative helicase with the regulatory subunit of human DNA polymerase alpha-primase. *J Biol Chem* **287**(32): 26854-26866

APPENDIX: TRIM3 Interactome

Hukkelhoven Thesis Appendix: TRIM3 Interactome

Cells: Growing YH/J12 cells
 Antibody: BD 610760
 Elution: 0.1M triethylamine pH 11.5
 Bait

International Protein Index	Protein Name	kDa	Unique Peptide Count	Mascot Score	Sequence Coverage
IPI00123181	Myh9	226.2	51	1902	35.4
IPI00229509	Plec1	517.1	48	1334	16.3
IPI00227299	Vim	53.7	35	2638	75.1
IPI00118899	Actn4	104.9	30	1056	47.6
IPI00208205	Hspa8	70.8	26	975	46.4
IPI00209082	Actn1	102.9	22	666	34.8
IPI00206624	Hspa5	72.3	22	519	40.8
IPI00133903	Hspa9	73.5	19	1038	38.6
IPI00110850	Actb	41.7	18	3243	65.1
IPI00874482	Actg1	41.8	18	3216	65.1
IPI00117352	Tubb5	49.6	15	555	48
IPI00620256	Lmna	74.2	15	420	30.1
IPI00316740	Ddb1	126.8	15	299	17
IPI00169463	Tubb2c	49.8	12	498	39.1
IPI00122928	Tubb6	50.1	12	385	33.6
IPI00468481	Atp5b	56.3	12	351	32.9
IPI00129020	Trim3	80.7	12	311	21.1
IPI00110827	Acta1	42	11	1475	42.7
IPI00109061	Tubb2b	49.9	11	470	41.8
IPI00117348	Tuba1b	50.1	11	364	34.6
IPI00110753	Tuba1a	50.1	11	355	34.6
IPI00798592	Spna2	285.2	11	332	8.7
IPI00119478	Tmod3	39.5	10	216	37.2
IPI00112251	Tubb3	50.4	9	388	21.3
IPI00229080	Hsp90ab1	83.2	8	213	14.1
IPI00393867	Myo1c	119.7	8	140	9.9
IPI00130280	Atp5a1	59.7	7	251	19.2
IPI00109044	2900073G15Rik	19.9	7	251	50.6
IPI00283476	Sh2b1	70.8	7	250	18.5
IPI00126120	Gstz1	24.3	7	189	51.4
IPI00112223	Effhd2	26.8	7	130	34.6
IPI00221528	Actbl2	42	6	989	31.9
IPI00111265	Capza2	32.9	6	193	39.5
IPI00210357	Hnrnpf	45.7	6	188	23.9
IPI00195372	Eef1a1	50.1	6	172	18.4
IPI00553840	Zfp3612	50	6	159	15.1
IPI00131138	Flna	281	5	192	4.4

IPI00226993	Txn1	11.7	1	79	12.4
IPI00372520	Eef1b2l	28	1	79	9.1
IPI00122698	Rbbp7	47.8	1	78	8.2
IPI00138892	Ubb	14.7	1	71	12.5
IPI00556768	Thrap3	108.1	1	69	2.1
IPI00127450	Man2c1	115.6	1	68	1.1
IPI00212969	Hnrnpa2b1	33.9	1	68	10.2
IPI00365852	Erh	12.3	1	68	10.6
IPI00563424	Vdac1	31.3	1	63	9.7
IPI00226275	Wdr26	70.6	1	62	3
IPI00188059	Rpn2	69	1	62	1.9
IPI00117288	Hnrnpab	30.8	1	62	4.9
IPI00407130	Pkm2	57.8	1	60	4.3
IPI00362409	Hnrnpa1	37.4	1	60	5.1
IPI00225312	Msrb3	20.2	1	56	5.9
IPI00568014	Hsph1	96.5	1	56	5.2
IPI00204365	Rpn1	68.4	1	55	1.7
IPI00870042	Tjp1	193.9	1	52	1.1
IPI00117705	Ddost	49	1	51	2.5
IPI00122547	Vdac2	31.7	1	48	7.5
IPI00330649	Myo1e	126.7	1	47	1.7
IPI00130757	Mkln1	84.8	1	46	3.4
IPI00123119	Atr	300.8	1	46	3.2
IPI00223047	Ckap4	63.7	1	45	4.7

Hukkelhoven Thesis
Appendix: TRIM3 Interactome

Cells: Growing YH/J12 cells
 Antibody: BD 610760
 Elution: 0.2M Glycine pH 2.2
 Bait

International Protein Index	Protein Name kDa	Unique Peptide Count	Mascot Score	Sequence Coverage	
IPI00123181	Myh9	226.2	63	2424	38.8
IPI00468273	Plec1	515.2	63	2070	21.7
IPI00227299	Vim	53.7	44	8824	81.1
IPI00118899	Actn4	104.9	30	1125	50
IPI00319830	Spnb2	274.1	23	687	14.5
IPI00110850	Actb	41.7	22	3772	76.3
IPI00208205	Hspa8	70.8	21	802	37.6
IPI00380436	Actn1	103	20	728	33.3
IPI00753793	Spna2	282.2	19	628	12.6
IPI00133903	Hspa9	73.5	18	699	34.9
IPI00117352	Tubb5	49.6	17	561	50.5
IPI00649184	Myo1c	121.9	17	544	21.7
IPI00464223	Fer1f3	233.2	17	319	11.6
IPI00468481	Atp5b	56.3	16	688	53.3
IPI00169463	Tubb2c	49.8	15	579	47.6
IPI00122928	Tubb6	50.1	15	510	47
IPI00114593	Actc1	42	14	2304	58.6
IPI00131138	Flna	281	14	321	8
IPI00110753	Tuba1a	50.1	13	433	41.2
IPI00211813	Myh10	232.5	13	375	9.5
IPI00206624	Hspa5	72.3	12	445	24.2
IPI00169916	Cltc	191.4	11	356	10
IPI00620256	Lmna	74.2	10	353	21.4
IPI00119478	Tmod3	39.5	9	364	33.8
IPI00317794	Ncl	76.7	9	267	19.2
IPI00663627	Flnb	277.6	9	230	6.9
IPI00124700	Tfrc	85.7	9	212	19.5
IPI00129020	Trim3	80.7	8	312	19.9
IPI00311682	Atp1a1	112.9	8	237	13
IPI00130280	Atp5a1	59.7	7	367	23.3
IPI00118120	Myo5a	215.5	7	301	7.8
IPI00230035	Ddx3x	73.1	7	233	19.5
IPI00195372	Eef1a1	50.1	7	164	23.6
IPI00283476	Sh2b1	70.8	6	259	19.3
IPI00453692	Nes	207	6	250	7.3
IPI00229080	Hsp90ab1	83.2	5	241	9.9
IPI00223047	Ckap4	63.7	5	191	14.4

IPI00475154	Rpn2	69	5	177	14.3
IPI00671847	Ppp1r12a	114.9	5	174	8.7
IPI00135971	Tjp1	194.6	5	162	5.2
IPI00109044	2900073G15Rik	19.9	5	150	38.4
IPI00112339	Lima1	84	4	195	8.8
IPI00553840	Zfp3612	50	4	159	11.2
IPI00231925	Gnai2	40.5	4	146	15.2
IPI00205693	Atp1a2	112.1	4	132	8
IPI00153375	Pdlim2	37.7	4	132	16.9
IPI00124287	Pabpc1	70.6	4	127	12.1
IPI00358175	Finc	290.8	4	114	3
IPI00354819	Myl6	17	4	112	34.4
IPI00311344	Cald1	89.3	4	84	14.8
IPI00316623	Ctnnd1	102.5	4	78	8.8
IPI00204365	Rpn1	68.4	4	76	11.9
IPI00420363	Ddx5	69.3	4	71	7.8
IPI00132474	Itgb1	88.2	4	67	6.5
IPI00323349	Tjp2	131.2	4	46	5.5
IPI00565507	Slc25a5	32.2	4	42	24.4
IPI00117689	Ptrf	43.9	3	213	11.7
IPI00231955	Calm1	16.8	3	184	36.9
IPI00121977	Cttn	57.1	3	148	8.3
IPI00210566	Hsp90aa1	84.8	3	132	5.2
IPI00828461	Tmpo	46	3	131	16.5
IPI00170232	Svil	243	3	114	2.5
IPI00119618	Canx	67.2	3	112	6.9
IPI00117705	Ddost	49	3	99	8.4
IPI00210090	Hnrnpu	87.7	3	92	4.3
IPI00112223	Efh2	26.8	3	90	10.8
IPI00191444	Capzb	31.2	3	88	19.6
IPI00111265	Capza2	32.9	3	87	20.6
IPI00330063	Capza1	32.9	3	79	22
IPI00123316	Tpm1	32.7	3	68	9.2
IPI00381563	Specc1	109.8	3	57	7.5
IPI00670247	Srgap1	121.4	3	56	2.6
IPI00378485	Atp1a4	114.7	3	50	4.4
IPI00678133	2610204M08Rik	138.5	2	124	3.5
IPI00210357	Hnrnpf	45.7	2	114	6
IPI00229645	Specc1l	124.4	2	107	5.5
IPI00111416	Stx12	31.2	2	106	10.6
IPI00112963	Ctnna1	100	2	91	4.5
IPI00780608	Hnrnpk	47.5	2	86	8.9
IPI00653624	Pabpc4	65	2	85	5.8
IPI00407425	Myo18a	195.8	2	80	3.6
IPI00122549	Vdac1	32.3	2	76	17.9
IPI00320459	Eppk1	724.2	2	76	1.1
IPI00329913	Pcmt1	24.6	2	73	26.4
IPI00190557	Phb2	33.3	2	71	8.7
IPI00122547	Vdac2	31.7	2	69	11.9

IPI00126090	Itga3	116.7	2	67	2.2
IPI00323134	Cdh2	99.7	2	60	3
IPI00231229	Gstp1	23.4	2	56	14.8
IPI00230133	Hist1h1b	22.6	2	56	9.4
IPI00129276	Eif3a	161.9	2	55	2.4
IPI00115627	Actr3	47.3	2	53	4.5
IPI00123281	Lrrc59	34.9	2	53	10.7
IPI00121378	Alcam	65.1	2	47	4.3
IPI00118101	Raf1	72.9	2	43	3.7
IPI00417227	Synpo	96.7	1	101	2.9
IPI00112460	Nde1	38.5	1	93	6.1
IPI00230394	Lmnb1	66.7	1	89	4.1
IPI00110852	Ssr1	33.7	1	86	5
IPI00138406	Rap1a	21	1	77	6.5
IPI00130118	Rab10	22.5	1	75	5.5
IPI00124771	Slc25a3	39.6	1	71	3.4
IPI00769254	Atp8b2	84.4	1	68	4.9
IPI00126120	Gstz1	24.3	1	67	11.1
IPI00207370	Ppp1r9b	89.6	1	66	2.6
IPI00128904	Pcbp1	37.5	1	65	3.7
IPI00388454	H2ba	14	1	65	20.6
IPI00130343	Hnrnpc	36.9	1	63	7.2
IPI00110487	Bwk1	26.8	1	61	16.2
IPI00129519	Basp1	22.1	1	59	9.7
IPI00114641	Slc3a2	58.8	1	55	5.1
IPI00203390	Ppp1cb	37.2	1	55	9.8
IPI00125267	Vapa	27.8	1	51	4.8
IPI00123199	Nap1l1	45.3	1	48	2.8
IPI00845851	Syne2	782.2	1	47	1.8
IPI00778860	Trim28	36.5	1	47	9.9
IPI00192274	Hnrnpa3	31.1	1	46	14.5
IPI00122696	Rbbp4	47.6	1	45	5.2
IPI00336929	2310014H01Rik	67.1	1	43	1.5

Hukkelhoven Thesis
Appendix: TRIM3 Interactome

Cells: 5uM PTK 48h YH/J12 cells
 Antibody: BD 610760
 Elution: 0.1M triethylamine pH 11.5
 Bait

International Protein Index	Protein Name	Mr kDa	Unique Peptide Count	Mascot Score	Sequence Coverage
IPI00208205	Hspa8	70.8	25	2625	48.9
IPI00133903	Hspa9	73.5	29	3698	47.6
IPI00227299	Vim	53.7	22	728	50.2
IPI00206624	Hspa5	72.3	20	1381	42
IPI00329913	Pcmt1	30.4	13	1107	47.4
IPI00169463	Tubb2c	49.8	11	767	28.5
IPI00117352	Tubb5	49.6	10	751	24.8
IPI00129020	Trim3	80.7	17	831	22.3
IPI00110753	Tuba1a	50.1	9	523	31.5
IPI00130280	Atp5a1	59.7	9	290	18.8
IPI00308213	Ighg1	43.4	10	4243	39.2
IPI00122928	Tubb6	50.1	9	401	23
IPI00110827	Acta1	42	5	203	21.2
IPI00124640	Grn	65	3	72	9.5
IPI00468481	Atp5b	56.3	11	671	34
IPI00117063	Fus	52.6	9	708	15.4
IPI00131224	Tceb2	13.2	6	215	70.3
IPI00785509	Igv	26.6	6	2002	27.1
IPI00553840	Zfp36l2	50	8	523	17.2
IPI00195372	Eef1a1	50.1	7	327	21.2
IPI00283476	Sh2b1	70.8	5	171	14.8
IPI00314950	Rplp0	34.2	4	133	19.6
IPI00221841	Pcmt2	40.7	3	242	8.1
IPI00325146	Anxa2	38.7	1	39	3.2
IPI00269661	Hnrnpa3	39.6	5	276	21.6
IPI00331507	Cul5	90.9	3	35	7.1
IPI00131695	Alb	68.6	3	142	11.5
IPI00231340	Hist4b	11.5	1	39	16.5
IPI00231615	Anxa1	38.8	1	60	8.1
IPI00457467	Igh	12.8	4	615	37.4
IPI00319731	Gapdh	37.4	4	114	16.7
IPI00215229	Pcmt1	42.3	3	128	10.2
IPI00121758	Tardbp	44.5	2	87	9.7
IPI00114052	Snrpb	23.6	1	56	3.5
IPI00229080	Hsp90ab1	83.2	1	64	6.5
IPI00133916	Hnrnp1	49.2	1	34	3.8
IPI00781839	Hnrpc	37.1	9	406	31.3

IPI00138892	Ubb	14.7	2	140	29.7
IPI00458190	Pde4d	85.5	1	32	2.3
IPI00194694	Mett13	50.6	1	37	1.8
IPI00113427	Lyz1	18.4	1	117	7.4
IPI00189519	Hist3	19.4	1	30	12.5
IPI00199865	Farsa	57.7	1	32	2.2
IPI00365852	Erh	12.3	1	112	25
IPI00127071	Ddx41	69.7	11	201	26.8
IPI00134599	Rps3	26.7	5	144	30
IPI00203523	Rpl23a	17.7	5	119	32.7
IPI00317794	Ncl	76.7	5	120	7.2
IPI00911185	Igh	51.2	5	493	17
IPI00670004	Hnrnpa3	36.6	5	301	25.9
IPI00124287	Pabpc1	70.6	4	125	7.7
IPI00213546	Hspa1l	70.5	4	396	13.6
IPI00231693	Rps3a	29.9	3	65	9.5
IPI00324983	Rps17	15.5	3	101	40
IPI00204295	Pabpc4	70.8	3	123	6.2
IPI00117288	Hnrnpab	30.8	3	99	11.9
IPI00119224	Snrpd3	13.9	2	106	15.1
IPI00115992	Rps25	13.7	2	106	15.2
IPI00131357	Rps23	16	2	86	21.4
IPI00112407	Rps14	16.3	2	93	15.9
IPI00110724	Rpl22l1	14.5	2	143	19.7
IPI00626233	Rpl17	26.1	2	34	20.3
IPI00390829	Rpl13	24	2	47	11
IPI00331461	Rpl11	20.2	2	63	21.3
IPI00323800	Nefm	95.9	2	58	3.1
IPI00188524	Nefh	115.3	2	58	2.7
IPI00201060	Lmna	74.3	2	60	5.9
IPI00132443	Hnrnpm	77.6	2	67	4.4
IPI00768214	Hist2a	27.7	2	38	12.5
IPI00108271	Elavl1	36	2	166	7.4
IPI00364910	Cul2	86.9	2	53	8.5
IPI00123617	C330007P06	25.6	2	78	10.8
IPI00120886	Ybx1	35.7	1	145	5.9
IPI00113430	Trim2	81.4	1	51	3.1
IPI00757653	SRp25	24.5	1	74	14.7
IPI00115644	Sar1a	22.3	1	36	5.6
IPI00850220	Rps16	18.4	1	77	11.5
IPI00122421	Rpl27	15.8	1	48	6.6
IPI00849793	Rpl12	17.8	1	60	26.1
IPI00130885	Rbmxt	42.2	1	100	8.8
IPI00130147	Raly	33.1	1	67	3.8
IPI00211116	Pctk1	52.5	1	31	3.9
IPI00229475	Jup	81.7	1	31	2
IPI00112131	Igl-V1	14.2	1	33	6.2
IPI00201032	Hnrpd	38.2	1	69	6.5
IPI00212969	Hnrnpa2b1	33.9	1	46	3.2

IPI00778340	Hnrnpa1	28.5	1	42	7.8
IPI00225294	Guf1	72.4	1	34	1.1
IPI00310646	Gtl3	22.7	1	57	6.2
IPI00117083	Grpel1	24.3	1	42	9.7
IPI00310026	Gal3st1	48.9	1	36	6.6
IPI00368403	Flg2	101.6	1	46	1.8
IPI00355808	Ddef2	106.7	1	34	2.9
IPI00121311	Csda	33.3	1	75	6.2
IPI00123335	Crbn	50.8	1	29	4.7
IPI00284925	Chchd2	15.7	1	45	15.7
IPI00207533	Axl	97.2	1	43	2.2
IPI00129350	Aldh18a1	87.2	1	32	1
IPI00110641	2200002D01	12.1	1	45	12.3

Hukkelhoven Thesis
Appendix: TRIM3 Interactome

Cells: 5uM PTK 48h YH/J12 cells
 Antibody: BD 610760
 Elution: 0.2M Glycine pH 2.2
 Bait

International Protein Index	Protein Nam	kDa	Unique Peptide Count	Mascot Score	Sequence Coverage
IPI00208205	Hspa8	70.8	25	1953	49.1
IPI00133903	Hspa9	73.5	24	2287	38.1
IPI00227299	Vim	53.7	21	1064	50.6
IPI00206624	Hspa5	72.3	16	928	34.9
IPI00329913	Pcmt1	30.4	13	1259	53
IPI00169463	Tubb2c	49.8	13	1177	37.8
IPI00117352	Tubb5	49.6	13	1029	37.8
IPI00129020	Trim3	80.7	10	483	15.3
IPI00110753	Tuba1a	50.1	9	621	33.7
IPI00130280	Atp5a1	59.7	8	314	18.3
IPI00308213	Ighg1	43.4	7	354	27.5
IPI00122928	Tubb6	50.1	7	629	21.5
IPI00110827	Acta1	42	7	294	23.2
IPI00124640	Grn	65	6	76	11
IPI00468481	Atp5b	56.3	5	260	15.7
IPI00117063	Fus	52.6	5	317	11.8
IPI00131224	Tceb2	13.2	5	95	53.4
IPI00785509	Igv	26.6	5	426	28.8
IPI00553840	Zfp36l2	50	4	216	10.2
IPI00195372	Eef1a1	50.1	4	203	13.9
IPI00283476	Sh2b1	70.8	4	104	11.9
IPI00314950	Rplp0	34.2	4	128	19.6
IPI00221841	Pcmt2	40.7	4	186	17.3
IPI00325146	Anxa2	38.7	4	121	13.3
IPI00269661	Hnrnpa3	39.6	3	52	15
IPI00331507	Cul5	90.9	3	66	12.6
IPI00131695	Alb	68.6	3	148	5.8
IPI00231340	Hist4b	11.5	3	97	28.8
IPI00231615	Anxa1	38.8	3	208	15.3
IPI00457467	Igh	12.8	2	438	25.2
IPI00319731	Gapdh	37.4	2	87	14.4
IPI00215229	Pcmt1	42.3	2	84	6.2
IPI00121758	Tardbp	44.5	2	63	5.6
IPI00114052	Snrpb	23.6	2	48	9.5
IPI00229080	Hsp90ab1	83.2	2	134	3.6
IPI00133916	Hnrnp1	49.2	2	187	7.6
IPI00781839	Hnrpc	37.1	1	63	8.4

IPI00138892	Ubb	14.7	1	52	19.5
IPI00458190	Pde4d	85.5	1	54	3.7
IPI00194694	Mett13	50.6	1	42	1.8
IPI00113427	Lyz1	18.4	1	148	7.4
IPI00189519	Hist3	19.4	1	31	9.4
IPI00199865	Farsa	57.7	1	36	2.2
IPI00365852	Erh	12.3	1	93	25
IPI00366081	Dsp	332.2	5	276	5.1
IPI00118286	Sfn	27.7	3	107	14.9
IPI00551802	Hist2b	14	3	93	27.2
IPI00198466	Amy1a	58.8	3	142	9.2
IPI00464776	Tfg	43.1	2	40	9
IPI00462013	Setbp1	173	2	29	3.6
IPI00113127	Rab4a	24.4	2	38	11.5
IPI00123180	Rab37	24.6	2	38	13.9
IPI00880661	Rab15	21.2	2	38	16.4
IPI00114560	Rab1	22.7	2	42	13.2
IPI00204261	Kpnb1	97.1	2	32	2.7
IPI00210566	Hsp90aa1	84.8	2	58	6.3
IPI00210357	Hnrnpf	45.7	2	114	8.2
IPI00153400	H2afj	14	2	83	30.2
IPI00229125	Gsdma2	49.8	2	39	8.8
IPI00764841	Slc25a31	35	1	58	6.6
IPI00153743	Sfrs7	27.4	1	79	9.7
IPI00776959	Rplp2	11	1	48	46.7
IPI00113377	Rplp1	11.5	1	56	14
IPI00658944	Rnf150	33.5	1	31	2.3
IPI00660166	Nlrp1b	133.5	1	32	2.5
IPI00111258	Mvp	96.7	1	55	1.8
IPI00135730	Arf2	20.7	1	38	7.7

Hukkelhoven Thesis
Appendix: TRIM3 Interactome

Cells: Growing YH/J12
 Antibody: Bethyl 209
 Elution: 0.2M Glycine pH 2.2
 Bait

International Protein Index	Protein Name	kDa	Unique Peptide Count	Mascot Score	Sequence Coverage
IPI00468273	Plec1	515.2	66	2565	23.8
IPI00123181	Myh9	226.2	53	1561	32.4
IPI00753793	Spna2	282.2	45	1160	28.7
IPI00319830	Spnb2	274.1	34	839	21.9
IPI00227299	Vim	53.7	33	2676	70.6
IPI00118899	Actn4	104.9	30	1240	46.1
IPI00169916	Cltc	191.4	29	786	23.7
IPI00380436	Actn1	103	28	1026	39.5
IPI00208205	Hspa8	70.8	21	938	42.6
IPI00468481	Atp5b	56.3	19	679	66.2
IPI00649184	Myo1c	121.9	18	389	21.4
IPI00765011	Actg1	58.8	17	2895	47.6
IPI00206624	Hspa5	72.3	17	644	31.2
IPI00620256	Lmna	74.2	17	483	32.2
IPI00131138	Flna	281	17	329	9.7
IPI00339428	Dock7	241	16	468	13.3
IPI00464223	Fer1l3	233.2	16	403	10.1
IPI00874522	Tjp1	194.9	15	410	13.9
IPI00211813	Myh10	232.5	14	466	11.6
IPI00133903	Hspa9	73.5	14	429	26.4
IPI00114593	Actc1	42	13	1272	48.5
IPI00122928	Tubb6	50.1	13	602	39.4
IPI00117352	Tubb5	49.6	13	601	37.6
IPI00117348	Tuba1b	50.1	13	524	39.9
IPI00110753	Tuba1a	50.1	13	489	39.9
IPI00663627	Flnb	277.6	13	278	7
IPI00229080	Hsp90ab1	83.2	12	287	20
IPI00664670	Flnc	292.2	12	250	8.5
IPI00130280	Atp5a1	59.7	11	307	28.8
IPI00323349	Tjp2	131.2	11	98	10.5
IPI00119478	Tmod3	39.5	10	351	38.9
IPI00124700	Tfrc	85.7	10	257	16.9
IPI00119618	Canx	67.2	9	207	19.3
IPI00886393	Cul5	75.9	8	141	17.5
IPI00209148	Hnrpm	73.7	7	276	18
IPI00230035	Ddx3x	73.1	7	243	16.3

IPI00673886	Sorbs2	144.9	7	218	13.3
IPI00129020	Trim3	80.7	7	211	14.2
IPI00119689	Ap2b1	104.5	7	139	12.9
IPI00381563	Specc1	109.8	7	136	12.1
IPI00330649	Myo1e	126.7	7	111	11.5
IPI00117689	Ptrf	43.9	6	276	17.6
IPI00453692	Nes	207	6	274	7.6
IPI00112963	Ctnna1	100	6	234	16.6
IPI00204261	Kpnb1	97.1	6	183	10.4
IPI00132474	Itgb1	88.2	6	168	11.3
IPI00339468	Dhx9	149.6	6	147	7.2
IPI00310131	Ap2a2	104	6	147	11.3
IPI00112223	Efh2	26.8	6	81	22.1
IPI00129276	Eif3a	161.9	6	70	7.4
IPI00129350	Aldh18a1	87.2	5	213	12.5
IPI00467104	Flii	144.7	5	200	6.6
IPI00211695	Ppp1r12a	109.7	5	197	6.9
IPI00195372	Eef1a1	50.1	5	139	14.5
IPI00112339	Lima1	84	5	103	8.1
IPI00311682	Atp1a1	112.9	5	94	6.2
IPI00225609	1600021P15	55.6	4	233	14.5
IPI00194958	Picalm	64.6	4	159	12.6
IPI00229645	Specc1l	124.4	4	150	5.4
IPI00210090	Hnrnpu	87.7	4	147	7.4
IPI00117705	Ddost	49	4	133	10.4
IPI00212014	Vcp	89.5	4	131	7.9
IPI00115627	Actr3	47.3	4	129	12.7
IPI00130185	Ppp1ca	37.5	4	125	16.4
IPI00153375	Pdlim2	37.7	4	120	21.8
IPI00316623	Ctnnd1	102.5	4	117	6.4
IPI00322712	Mfge8	47.2	4	116	11.5
IPI00124287	Pabpc1	70.6	4	111	9.1
IPI00453826	Matr3	94.6	4	105	9.3
IPI00330063	Capza1	32.9	4	96	27.6
IPI00468203	Anxa2	38.7	4	86	20.6
IPI00203214	Eef2	95.2	4	66	8.3
IPI00207989	Myo1d	116	4	63	9.8
IPI00649060	Akap2	126	4	60	5.7
IPI00309035	Rpn1	68.5	4	57	10.5
IPI00678133	Inf2	138.5	3	187	5.2
IPI00224570	Prkar2b	46.1	3	187	11.8
IPI00475154	Rpn2	69	3	139	10.3
IPI00554039	Gapdh	35.8	3	139	17.1
IPI00420363	Ddx5	69.3	3	118	7.2
IPI00330497	Kank2	90.2	3	101	7.6
IPI00781602	Rbm14	62.2	3	101	12.6
IPI00119063	Lrp1	504.4	3	100	1.7
IPI00111265	Capza2	32.9	3	99	21.3
IPI00850112	Synpo	96.2	3	95	9.7

IPI00189723	Tmod1	40.5	3	91	12.5
IPI00114641	Slc3a2	58.8	3	89	7
IPI00123199	Nap1l1	45.3	3	89	9.7
IPI00126090	Itga3	116.7	3	83	5.4
IPI00194974	Hnrnpk	51	3	83	8
IPI00362014	Tln1	270.9	3	81	2.9
IPI00122450	Cald1	60.4	3	69	12.5
IPI00115564	Slc25a4	32.9	3	64	13.8
IPI00779588	Khdrbs1	37.5	3	64	15.5
IPI003331361	Mybbp1a	151.9	3	59	5.2
IPI00125899	Ctnnb1	85.4	3	50	7
IPI00210357	Hnrnpf	45.7	3	38	9.9
IPI00191216	Tardbp	44.5	2	146	9.4
IPI00230394	Lmnb1	66.7	2	136	10.9
IPI00312128	Trim28	88.8	2	130	6.5
IPI00308885	Hspd1	60.9	2	103	8.6
IPI00462445	Nedd4	102.6	2	100	6.5
IPI00515654	Eef1d	31.3	2	97	11.7
IPI00191391	Slc2a1	53.9	2	96	3.7
IPI00407130	Pkm2	57.8	2	93	12.4
IPI00317794	Ncl	76.7	2	91	3.1
IPI00118143	Cttt	61.2	2	89	5.3
IPI00138892	Ubb	14.7	2	86	19.5
IPI00464348	Tmpo	30.5	2	83	25.3
IPI00122547	Vdac2	31.7	2	80	14.6
IPI00231726	Gnai3	40.5	2	77	11.6
IPI00223047	Ckap4	63.7	2	73	8.5
IPI00133374	Sqstm1	48.1	2	72	7
IPI00135475	Dbn1	77.2	2	72	4.5
IPI00323134	Cdh2	99.7	2	72	3
IPI00206325	Afap1	80.7	2	66	5.5
IPI00210635	Nsf	82.6	2	62	6.3
IPI00137331	Cap1	51.5	2	60	10.8
IPI00275539	Rtn4	40.3	2	56	8.5
IPI00118101	Raf1	72.9	2	53	4
IPI00421357	Eprs	170	2	52	4.4
IPI00111258	Mvp	96.7	2	46	5.9
IPI00128818	Dhx15	90.9	2	45	3.4
IPI00330857	Sec63	87.8	2	44	4.5
IPI00121378	Alcam	65.1	2	40	4.3
IPI00661414	Arcp2	34.3	2	40	6.7
IPI00467447	Iqgap1	188.6	2	38	2.2
IPI00124771	Slc25a3	39.6	2	37	10.1
IPI00136883	Ptbp1	56.9	2	42	5.5
IPI00132938	Myadm	35.3	1	107	5.3
IPI00885921	Clk2	88.9	1	100	5.5
IPI00223769	Cd44	40.2	1	99	3.3
IPI00319270	M6prbp1	47.2	1	93	4.3
IPI00129924	9430020K01	144.7	1	88	2

IPI00116281	Cct6a	58	1	78	6.2
IPI00360418	Srgap1	124	1	77	1.8
IPI00170232	Svil	243	1	75	2.9
IPI00126245	Steap3	57.3	1	74	5.8
IPI00111416	Stx12	31.2	1	73	5.1
IPI00377592	Sec31a	144	1	69	3.9
IPI00108844	M6pr	31.2	1	67	10.4
IPI00113895	Actr1a	42.6	1	66	4.3
IPI00368911	Ctnbp2nl	70	1	63	4.2
IPI00121190	Egfr	134.8	1	60	3.6
IPI00331173	Lbr	71.4	1	57	2.4
IPI00130632	Trip6	50.9	1	55	5.4
IPI00118895	Sntb2	56.3	1	55	1.7
IPI00231268	Atp2b1	134.6	1	53	6.1
IPI00885844	Cav1	15.6	1	51	17.3
IPI00119320	Tcirg1	93.4	1	50	1
IPI00229990	Strn3	87.1	1	50	2.1
IPI00400168	Nexn	72.1	1	50	5.9
IPI00314865	Ythdf2	62.8	1	49	1.5
IPI00468924	Sic25a24	52.9	1	49	3.4
IPI00205912	Nono	54.9	1	49	2.9
IPI00137194	Sic16a1	53.2	1	47	1.8
IPI00210187	Pdlim5	63.2	1	46	3
IPI00126253	Lass2	45	1	45	4.2
IPI00117288	Hnrnpab	30.8	1	45	4.9
IPI00421382	Cyld	52	1	45	5.9
IPI00153809	Cd109	161.6	1	45	1.6
IPI00200659	Sdha	71.6	1	44	4
IPI00177038	Actr2	44.7	1	44	5.1
IPI00372146	Rai14	105.9	1	43	3.3
IPI00366292	Eif3d	63.9	1	43	3.1
IPI00330476	Cyflp1	145.1	1	43	3.7
IPI00110852	Ssr1	33.7	1	42	2.7
IPI00130607	Pdlim7	50.1	1	42	5.3
IPI00768466	G3bp1	58.2	1	42	5.5
IPI00315463	Reep5	21.4	1	41	4.8
IPI00115097	Copb2	102.4	1	41	3.2
IPI00781839	Hnrnpc	37.1	1	41	6.3
IPI00468202	Tpbp	46.4	1	40	2.3
IPI00312063	Ldlr	95.1	1	40	4.4
IPI00555301	Ccndbp1	39	1	40	3.9
IPI00123119	Atr	300.8	1	40	1
IPI00137206	Actr10	46.2	1	40	9.6
IPI00281212	Itga10	127.8	1	39	0.7
IPI00396797	Ddx17	72.4	1	38	1.4